VU VRIJE UNIVERSITEIT AMSTERDAM

VU Research Portal

Fluvial and marine sedimentation at a passive continental margin

Vis, G.J.

2009

Link to publication in VU Research Portal

citation for published version (APA)
Vis, G. J. (2009). *Fluvial and marine sedimentation at a passive continental margin: The late Quaternary Tagus depositional system*. [PhD-Thesis - Research and graduation internal, Vrije Universiteit Amsterdam]. Ipskamp Drukkers.

General rights
Copyright and moral rights for the publications made accessible in the public portal are retained by the authors and/or other copyright owners and it is a condition of accessing publications that users recognise and abide by the legal requirements associated with these rights.

- Users may download and print one copy of any publication from the public portal for the purpose of private study or research.
- You may not further distribute the material or use it for any profit-making activity or commercial gain
- You may freely distribute the URL identifying the publication in the public portal

Take down policy
If you believe that this document breaches copyright please contact us providing details, and we will remove access to the work immediately and investigate your claim.

E-mail address:
vuresearchportal.ub@vu.nl

Download date: 13. Mar. 2024

Fluvial and marine sedimentation at a passive continental margin: The late Quaternary Tagus depositional system

Geert-Jan Vis

VRIJE UNIVERSITEIT

FLUVIAL AND MARINE SEDIMENTATION AT A PASSIVE CONTINENTAL MARGIN: THE LATE QUATERNARY TAGUS DEPOSITIONAL SYSTEM

ACADEMISCH PROEFSCHRIFT

ter verkrijging van de graad Doctor aan
de Vrije Universiteit Amsterdam,
op gezag van de rector magnificus
prof.dr. L.M. Bouter,
in het openbaar te verdedigen
ten overstaan van de promotiecommissie
van de faculteit der Aard- en Levenswetenschappen
op vrijdag 20 november 2009 om 13.45 uur
in de aula van de universiteit,
De Boelelaan 1105

door

Geert-Jan Vis

geboren te Reeuwijk

promotoren:	prof.dr. J.F. Vandenberghe
	prof.dr. D. Kroon
copromotoren:	dr. C. Kasse
	dr. S.J.P. Bohncke

reading committee:	prof.dr. F. Abrantes
	prof.dr. R. Mäusbacher
	dr. C. Zielhofer
	dr. S. Jung
	dr. K.M. Cohen

FOKKE & SUKKE

ZIEN HET ALS EEN PROCES VAN *TRIAL AND ERROR*

O Engeitado

(J. Slauerhoff)

Ik voel mij van binnen bederven,
Nu weet ik waaraan ik zal sterven:
Aan de oevers van de Taag.
Aan de gele, afhellende oevers,
Er is niets schooners en droevers,
En 't bestaan verheven en traag.

Ik bewandel 's middags de prado's
En 's avonds hoor ik de fado's
Aanklagen tot diep in den nacht:
"A vida é immenso tristura" –
Ik voel mij al samensnoeren
Met de kwaal die zijn tijd afwacht.

De vrouwen die visch verkoopen
En de wezens die niets meer hopen
Dan een douro meer, voor een keer,
Zij zingen ze even verlaten,
Door de galmgaten der straten,
In een stilte zonder verweer.

Een van hen hoorde ik zingen
En mijn kilte tot droefenis dwingen:
"Ik heb niets tot troost dan mijn klacht.
Het leven kent geen genade,
Niets heb ik dan mijn fado
Om te vullen mijn leege nacht."

Ik voel mij van binnen bederven,
Hier heeft het zin om te sterven,
Waar alles wulpsch zwelgt in smart:
Lisboa, eens stad der steden,
Die 't verleden voortsleept in 't heden,
En ruïnes met roem verwart.

Ik word door dien waan betooverd;
Ook ik heb ontdekt en veroverd,
Die later alles verloor,
Om hier aan den tragen stroom
Bij het graf van den grootsten droom
Te sterven: "tudo é dôr"

O Enjeitado

(J. Slauerhoff)

No fundo, sinto-me apodrecer.
Agora sei onde e de quê irei morrer:
À beira do Tejo, de suas margens
macilentas e inclinadas.
Nada é mais belo e triste
E a existência sublime e lenta.

De tarde vagueio pelos prados
E à noite ouço o queixume dos fados
Até romper a madrugada.
- "A vida é imensa tristura" -
E logo sinto as amarras desse mal
Que no tempo aguarda fatal.

São as varinas quem canta o fado
E os entes que já nada esperam.
-"Mais um copo pra esquecer"-
Deixam-no desamparado,
Ecoando por becos e vielas,
Num silêncio que consente.

Um deles ouvi cantar
E minha frieza tornou-se em pesar:
"Nada me consola além da dor.
A vida não conhece o perdão,
Mais não tenho que este meu fado
P'ra me encher a noite, sem amor."

No fundo, sinto-me apodrecer;
Aqui, de nada serve morrer,
Onde tudo se perde na volúpia da dor:
Lisboa, outrora cidade das cidades,
Arrasta o passado no presente,
E vê nas ruínas uma glória que mente.

Por essa miragem me encantei;
Também eu descobri e conquistei,
Para afinal, de tudo ser perdedor
Morrendo na lentidão da corrente,
Junto à campa do mais nobre
Dos sonhos: "tudo é dor".

PREFACE AND ACKNOWLEDGEMENTS

Het begon allemaal een jaar of twaalf geleden. Ik ging fysische geografie studeren in Utrecht. We werden door de studievereniging ingewijd in de wondere wereld van het grondboren, op een veldje achter het instituut. Een beetje raar was het wel: kijken of er zand in de klei zit door het tussen je tanden te "proeven". Vele kilo's klei later ben ik afgestudeerd als kwartairgeoloog en sta ik in een veld te boren voor mijn toenmalige werkgever. Thijs Oomen, destijds collega, belt me op. Er staat een hele leuke vacature voor een promotieonderzoek op internet bij de Vrije Universiteit in Amsterdam: "echt iets voor jou!". Het is iets met de Taag. De Taag... Wel eens van gehoord, maar het roept vooral associaties met een prutslootje op.

Acht maanden later sta ik in die prutsloot met een vis in de hand (p. 244). Sjoerd Bohncke maakt een foto. Ik was intussen aangenomen aan de VU en Sjoerd en ik waren op verkenning in de Taag. Het was geen prutsloot. Integendeel, het was een bakbeest van een rivier. En er was nog vrijwel geen onderzoek aan gedaan, dat zou ik dan wel even doen. Er moest ook nog gecorreleerd worden met *mariene records*; daar had ik al helemáál geen kaas van gegeten. *Então...*

Terugbeschouwend kan ik zeggen dat ik me geen leuker promotieonderzoek had kunnen voorstellen. Daarvoor moet ik allereerst mijn twee promotoren hartelijk bedanken: Jef Vandenberghe en Dick Kroon. Zij hebben het voorstel in elkaar gezet. Het was een breed opgezet voorstel met daarin veel ruimte voor mij als promovendus om er een eigen invulling aan te geven. En die ruimte kreeg ik. Jef en Dick, vanaf enige afstand hielden jullie altijd mijn vorderingen in de gaten en kwamen jullie met opmerkingen en ideeën. Jef, bedankt voor je constant kritische blik op mijn schrijfsels, de mogelijkheden die je me gaf om me als wetenschapper te ontplooien en de leuke tijden op excursies en congressen. Dick, bedankt voor je niet aflatende enthousiasme en interesse in het project en de altijd weer motiverende gesprekken.

Heel veel dank ben ik ook verschuldigd aan Kees Kasse en Sjoerd Bohncke, mijn copromotoren. Ik heb veel van jullie geleerd, en genoten van alle dingen die we hebben meegemaakt tijdens veldwerken, excursies, congressen, in het lab, achter de computer, boven mijn manuscripten of achter een biertje. Kees, bedankt voor het telkens weer minutieus corrigeren van mijn manuscripten en de oeverloze discussies over de Taag of wat voor ander boeiend onderwerp dan ook. Sjoerd, bedankt voor je hulp met alles wat met pollen en planten te maken heeft. Ik blijf dat maar lastig vinden, zeker met die archaïsche software die nodig is om de resultaten te plotten.

I would like to thank the reading committee for their effort of reading this thesis and providing useful feedback: Fatima Abrantes, Roland Mäusba-

cher, Christoph Zielhofer, Simon Jung and Kim Cohen.

The fieldworks would not have been possible without the help of many people, starting with the students from Amsterdam and Jena. Jos Wit, Esther Bootsma, Thomas Wiatr, Sebastian Wilhelm, Sacha Beetz, Nadine Binder, Julia Baumert, Stephanie Meschner, Stephan Sonntag, Christian Pfeifer, Koen Zuurbier and Jouke Rozema thank you very much for the collection of so much data and for the great times in Portugal! Many thanks also to Thijs Nales and Kim Cohen for your assistance during the 2005 fieldwork. Thijs, core 0501.016 (-23 m) is the deepest manual core of the world! Kim, thanks for the stimulating discussions we had in the field about sedimentology and fluvial and tidal systems, they helped me greatly to understand the large-scale depositional framework of the Tagus River. Many thanks also to the students who did lab analyses on the cores: Alexander Prick, Heerko Zuur and Sander Coenraads-Nederveen. I thank Wim van Leeuwaarden for giving his unpublished pollen data from Vale de Atela to me. Many thanks also to Heike Schneider, Christin Hilbich, Dana Höfer, Carmen Trog and Roland Mäusbacher for the pleasant cooperation and the great times in Jena and Portugal!

Em Portugal, tive ajuda de muitas pessoas. Em primeiro lugar do pessoal dos Serviços Geológicos de Portugal em Lisboa. Em particular agradeço Fatima Abrantes, para organizar tudo que quis. Obrigado também a Susana Lebreiro, Teresa Rodrigues, Antje Voelker, Emília Salgueiro e Helga Bartels-Jónsdóttir para assistência e sociabilidade. Pedro Brito, Luís Rebêlo, Henrique Duarte obrigado para a assistência com DGPS e GIS. Silva Lopes e a tua equipa, muito obrigado para tudo vosso esforço para possibilitar as sondagens na planície fluvial do Tejo, mesmo quando eu fui na Holanda. Carlos Pinto, obrigado para a tua amizade, as visitas de Lisboa, a tua assistência e naturalmente a tradução do resumo! Da Universidade de Lisboa, queria agradecer Teresa Azevêdo, Ana Ramos Pereira e colegas para a introdução no Vale do Tejo. Obrigado também a João Fonseca, Susana Vilanova, Paula Figueiredo e Pedro Costa do grupo de Engenharia Sísmica e Sismologia da Universidade Técnica de Lisboa.

Wim Snippe, muito obrigado para a transporte das amostras de Portugal para Holanda, e para as jantares agradáveis. Este estudo foi impossível sem a ajuda dos agricultores do Vale do Tejo. Nunca foi uma problema de atravessar ou pisar as terras na margem do Rio Tejo; que diferente do que na Holanda! Obrigado! Permanecer em Portugal foi muito agradável na *Casa da Barbara* em Pousos e na *Quinta do Casalinho* em Benfica do Ribatejo. Peter Hahn, João Araújo, Natália, Emídio, Alda e Ana Rita Saldanha, Chocolate e todos outros: muito obrigado para tudo!

Een veldwerk zonder materiaal om monsters te verzamelen en een laboratorium om ze te analyseren is natuurlijk niets. Daarom mijn hartelijke dank

aan Michel Groen, Niek van Harlingen, Jan Veen, Hans Bakker, Frans Backer en de rest van het team van de Instrumentele Dienst. Daarnaast gaat mijn dank uit naar de mensen van het sedimentlab: Martin Konert, Maurice Hooyen, Roel van Elsas, Martine Hagen en Tineke Vogel-Eissens voor hun vakkundige bijstand. Ik spreek hier ook graag mijn dank uit aan Hanneke Bos, Alex Wright, Simon Troelstra, Martine Hagen, Douwe Yntema, Antoine Mientjes en Lisette Kootker voor het analyseren van verschillende monsters variërend van pollen tot potscherven. I thank Antje Voelker, Theresa Rodrigues, Susana Lebreiro and Ulrich Alt-Epping for sampling, preparation and analyses of material for radiocarbon dating. Guus Borger bedankt bij de hulp met het zoeken naar informatie over de landbouwgeschiedenis van het Taag stroomgebied. Klaas Verwer bedankt voor je virtuoze Petrel hulp. Philip Ward, Ane Wiersma, Joachim Rozemeijer, Henk Kombrink en Maarten Pluymaekers bedankt voor jullie constructieve opmerkingen op verschilende stukken tekst. Buurman Piet Vermeent, bedankt voor het lenen van je ladder; die is ideaal om Vanderstaay boren mee naar Portugal te brengen!

Naast het wetenschappelijke werk aan de VU, was er ook een hoop gezelligheid. Iedere ochtend om tien uur koffiepauze; een fenomeen. Alle mogelijke wetenschappelijke en niet-wetenschappelijke onderwerpen passeerden hier de revue. Iedere donderdag was er de Donderdorst van GeoVUsie waar we met veel dorstige promovendi vaak veel langer dan gepland bleven hangen en met andere collega's en studenten vele mooie avonden hadden. Ik wil al mijn collega's hartelijk bedanken voor de goede tijden aan de VU: Jos de Moor, Freek Busschers, Saskia Keesstra, Jochem Jongma, Margot Saher, Martin van Breukelen, Alex Wright, Stefan Engels, Ron Kaandorp, Hubert Vonhof, Jop Brijker, Mirjam Vriend†, Cédric van Meerbeeck, Philip Ward, Hans Renssen, Didier Roche, José Joordens, Emma Versteegh, Aafke Brader, Bert Boekschoten, Frank Peeters, Tjeerd van Weering, John Reimer, Gerald Ganssen, Simon Troelstra, Ronald van Balen, Kay Beets, Maarten Prins, Hanneke Bos, Suzanne Verdegaal, Els Ufkes, Edith van Loon, Ko van Huissteden, Simon Jung, Jan van Dam, Klaas Verwer, Bram van der Kooij, Glenda Garcia-Santos, Bastiaan Notebaert, en Bernd Andeweg. Naast Mirjam overleed helaas ook Orson van de Plassche veel te vroeg. Hij zorgde altijd voor de intellectuele en artistieke noot in de E-3 gang en was altijd beschikbaar voor een leuk gesprek. Ik zal hem missen. Bijzonder goede herinneringen heb ik aan mijn tijd met kamergenoot Ane Wiersma. Wat hebben we geouwehoerd, gelachen, geroddeld, gegoogeld, mandarijnen gegeten, de lucht verziekt, fatsoenlijke auto's bekeken (jij rijdt nu een Volkswagen!?), espresso apparaten gekocht en biertjes gedronken. Het was een gouden tijd!

En dan was er ook nog het eerstejaarsveldwerk in zuidoost Spanje. Heerlijk drie weken studenten de beginselen van de geologie en geomorfologie

bijbrengen en 's avonds de dag doornemen onder het genot van tapas. Bedankt Kees Biermann, Hubert Vonhof, Ronald van Balen, Mirjam Vriend, Karen Leever, Maarten Korver, Andreas Paul, Bram van der Kooij, Maud Meijers, Elco Luijendijk en Ane Wiersma voor de geweldige tijd daar!

Naast de mensen van de VU waren er nog de mensen van de UU en de UvA. Gilles Erkens, Marc Gouw, Marc Hijma, Sanneke van Asselen, Ingwer Bos, Nelleke van Asch, Wim Hoek, Kim Cohen, Esther Stouthamer, Femke Tonneijk en de rest bedankt voor de mooie momenten die we hebben meegemaakt tijdens discussiebijeenkomsten, symposia, congressen, veldwerken, excursies, etentjes, borrels, feestjes etc. Helaas overleed gedurende mijn promotietijd ook Henk Berendsen. Van Henk heb ik veel geleerd over het doen van wetenschappelijk onderzoek zonder *bullshit* en het schrijven van goede teksten. Van hem heb ik ook het enthousiasme voor riviersystemen en kwartairgeologie.

De laatste fase van dit proefschrift viel samen met mijn werk bij TNO. Daar wil ik allereerst mijn teamleider Barthold Schroot hartelijk bedanken voor de ongekende vrijheid en mogelijkheden die ik kreeg om dit proefschrift af te ronden, echt super! Verder is er bij TNO gelukkig ook genoeg gezelligheid met mijn collega's van de EZ Adviesgroep, de *Utah-partycrew* en de koffiehoek.

De toch al niet slechte tijd aan de VU werd aangevuld met vrije tijd, die ik met veel plezier doorbracht in de bergen, in klimhallen, op ski's, op de racefiets, in restaurants en cafés etc. Dank jullie voor de afleiding: Joachim, Hanna, Thijs Nales, Bas, Jeanine, Daniël, Goele, Hans, Jamila, Deon, Dion, Femke, Tim, Jeroen, Rens, Annet, Ane, Ate, Uif, Maud, Reinder, Henk, Thijs Oomen, Arun, Carina, Hugo, Roel, Bastiaan, Annelieke, Mirella, Ashley, Jorn, Guit-Jan, Jenny, Lydia, Fera en Karl.

Als laatste wil ik hier mijn familie bedanken voor de nooit aflatende steun voor dit schijnbaar eeuwig durende project en voor de broodnodige ontspanning, thuis in Reeuwijk, op vakantie of waar dan ook. Pap, Mam, Arnold, Yvette en Jack bedankt!!

Geert-Jan Vis September 2009

CONTENTS

CHAPTER 1

Introduction

Photo: the Tagus River near its source (Sierra de Albarracín, Spain).

1.1 BACKGROUND

Imagine being a grain of sand on a slope, just released from a rock by rain, wind, and temperature swings. Unaware of the journey ahead, you're hit by drops of rain. You're splashed downhill and quickly enter a little stream flowing towards a river. In the river you meet many more grains of sand. Still in the mountains, flow is rapid and while bouncing against other grains at the bottom of the river you move downstream. After some time, the river flow relaxes. So do you, and together with your grainy friends you take a rest at the bottom. You fall asleep. Suddenly you're awoken by something hitting you. The river flow increased and you move further again. This repeats a couple of times. Later, you enter turbid waters that keep moving back and forth. "It's the tide" the other grains tell you. You're not in the river anymore, but in the estuary. Those who are lucky find a place to rest. Others drop in a deep channel and are flushed into the sea. You are one of them. As you move down the water column, the sunlight becomes fainter and fainter. You reach the seafloor, where you think you can finally relax. It's not the end of your journey. When you almost fall asleep, something very noisy and energetic passes by and picks you up again. Bouncing violently, you move down a steep slope. It's your last journey to the dark depths of the deep ocean. There, you settle to relax for eternity.

In a nut shell, the story above represents the depositional system crossing on continental margins. Continental margins are at the confluence of terrestrial and marine processes. This creates a complex mixture of stratigraphic signals in the accumulated sediments (Nittrouer *et al.*, 2007). Globally ~85-95 % of sediment received by oceans is delivered by rivers (Milliman and Meade, 1983; Syvitski *et al.*, 2003). Large fluvial sediment delivery causes high accumulation rates on continental margins, which host the thickest accumulations of sediment in the world (Kennett, 1982). In these accumulations, signals from diverse processes are recorded at high resolution, making deposits on continental margins good archives for sedimentological and environmental studies. The energetic, reworking environment with waves, tides and currents, imposes great challenges on reading these archives. A fundamental understanding of the development of a continental margin is required to translate raw stratigraphic characteristics into a record of sedimentary and environmental processes.

The relevance and importance of studying continental margins becomes clear when considering that a large part of the global population lives along coasts, often on top of continental margin successions. Many people depend on marine resources and important petroleum reservoirs are found in fluvial and marine deposits. However, short-term environmental hazards like landslides, river floods, storm surges and tsunamis and long-term hazards like

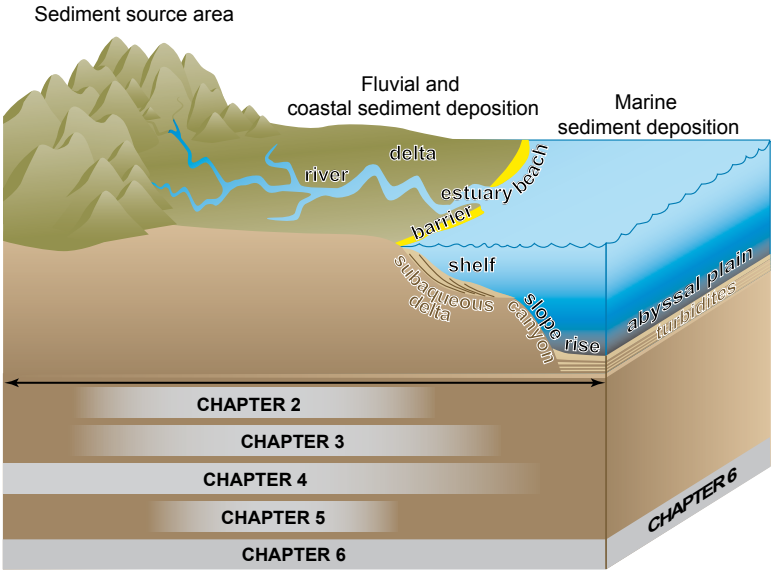

Figure 1.1 | Schematic representation of the main morphological features on a passive continental margin. The lower part of the figure visualizes which chapter covers which part of the passive continental margin.

sea-level rise or fall, tectonic uplift or subsidence and sediment accumulation or erosion threaten people living in these regions.

Two types of continental margins are formed as a result of plate tectonics. Active margins are found along plate boundaries and are shaken by plate movements (Kennett, 1982). They form along convergent plate boundaries where continental lithosphere overrides or subducts oceanic lithosphere and along transform plate boundaries where continental and oceanic lithosphere slide past each other (Pratson *et al.*, 2007). Passive margins ride 'passively' on a lithospheric plate (Kennett, 1982) and result from past/distant spreading (rifting) of continental plate and crust. This results in stretched, strongly attenuated and usually faulted continental crust. Seaward prograding shallow-marine sediment prisms overly, load and suppress continental crust of a passive margin (Allen and Allen, 2005). The presence of sediment prisms and the absence of volcanoes and large earthquakes make passive margins well suited to improve the fundamental understanding of sedimentary processes on continental margins.

Morphologically a passive margin has a typical profile with a subaerial (fluvial, coastal) part and a subaquatic (marine) part (Fig. 1.1). In the subaerial part where rivers reach the ocean, deltas are formed by single-channel or multiple-channel rivers. At the transition from delta to ocean, beaches, barrier islands and estuaries are often present. The subaquatic part consists of the

continental shelf, slope and rise, with an abyssal plain at the foot of the slope. The steep continental slope is often cut by submarine canyons, which usually extend to the abyssal plain (Pratson *et al.*, 2007) and are the source area for turbidity currents. These are currents of rapidly moving sediment-laden water that transport sediment to the abyssal plain.

A plethora of controls and processes operates on passive continental margins. Sedimentary processes are generally forced by a combination of allogenic (climatic, tectonic, eustatic (i.e. sea level) and anthropogenic) and autogenic (intrinsic behaviour and complex response) controls. These controls determine the distribution of depocentres within a depositional system, as well as the larger scale stacking patterns of depositional systems within a sedimentary basin. A strict distinction between allogenic and autogenic controls can not simply be made because complicated interactions among these controls exist (Ethridge *et al.*, 1998; Bridge, 2003; Holbrook *et al.*, 2003; Stouthamer and Berendsen, 2007). Allogenic controls have the largest effect on the balance between sediment supply and energy flux in a depositional environment. This balance leads to processes of sediment accumulation when energy flux decreases, or erosion when energy flux increases (Catuneanu, 2006). Eustacy and tectonics control accumulation directly, while climate controls accumulation indirectly through eustatic change and sediment supply. Climate also affects fluvial discharge, wind, wave and current regimes and sediment supply (weathering, erosion, vegetation, sediment transport) (Catuneanu, 2006).

1.2 AIMS AND OBJECTIVES

The overview given above, illustrates the complexity of a passive continental margin. Sedimentation and stratigraphy on continental margins is a much-studied subject in late Quaternary depositional systems (e.g. Schumm, 1993; Allen and Posamentier, 1993; Christie-Blick and Driscoll, 1995; Blum and Törnqvist, 2000; Blum and Aslan, 2006). However, most studies either focus on the subaerial part or on the subaquatic part of the system. To improve the understanding of sedimentary processes on a passive continental margin and to unravel the controls on terrestrial and marine sedimentation, a synoptic palaeoenvironmental reconstruction of a passive continental margin linking the delta, coastal zone, continental shelf and slope, and the abyssal plain is needed. Special emphasis should be given to the significant influence of transport and sedimentation processes under varying climates in the hinterland and the ocean. For this purpose the collaborative research project SEDPORT was initiated within the European Science Foundation (ESF) EUROCORES EUROMARGINS framework.

The general aims of this project are:

1. To better determine the influence of subaerial and submarine sediment transport mechanisms on the composition and physical properties of the last glacial to Holocene margin sediment cover with respect to modern environmental conditions in general;
2. To investigate how sedimentation processes have changed under varying climate conditions affecting ocean circulation, sea level, continental weathering, vegetation and precipitation since the last glacial into the Holocene.

In order to fulfil these aims, the extensively studied Iberian passive continental margin near the Lower Tagus Valley was chosen as study area (Fig. 1.2) (e.g. Jouanneau *et al.*, 1998; Weaver *et al.*, 2000; Alves *et al.*, 2003; Arzola *et al.*, 2008). During the last ~20,000 years, the Iberian margin experienced pronounced climatic oscillation and although it was glacially influenced as indicated by layers of ice-rafted debris off Portugal, grounding glaciers were absent (Baas *et al.*, 1997; Abrantes *et al.*, 1998; Weaver *et al.*, 2000). Furthermore, large submarine slides and debris flows are less evident and volcanic and tectonic activity are less than along the similarly shaped northwest African margin. The dominant supplier of fluvial sediment to the Portuguese margin is the Tagus River (~$4.5 \cdot 10^5$ t/y, Rocha *et al.*, 2005). Due to the narrow exit of the Lower Tagus Valley west of Lisbon (Fig. 1.2), the Tagus River acts as a point source of sediment which, in combination with the absence of large rivers to the north and south of the study area, makes this region well suited for the study of sediment fluxes. Most of the sediments supplied by the Tagus River are deposited in the Lower Tagus Valley or on the narrow shelf off Lisbon and a small part is transported towards the abyssal plain through the Cascais and Lisbon Canyons (Jouanneau *et al.*, 1998). Boundary conditions are well constrained. The narrow and deep bedrock-confined Lower Tagus Valley is an efficient trap for fluvial, tidal and marine deposits and enables robust sediment pathway and volumetric reconstructions. During low relative sea level the narrow continental shelf caused efficient sediment bypassing to the Tagus Abyssal Plain while during relative sea-level highstand sediments were efficiently trapped in the Lower Tagus Valley and on the narrow shelf (Jouanneau *et al.*, 1998).

Local studies of the late Quaternary sedimentary valley fill of the Lower Tagus Valley have been published recently (Azevêdo, 2001; Ramos *et al.*, 2002; Ramos Pereira *et al.*, 2002; Azevêdo *et al.*, 2004; Azevêdo *et al.*, 2007; Van der Schriek *et al.*, 2007a). However, a valley-wide 3D reconstruction of the complete Lower Tagus Valley fill was still missing. Additionally, time control of the valley-fill development was poor and a sequence stratigraphic

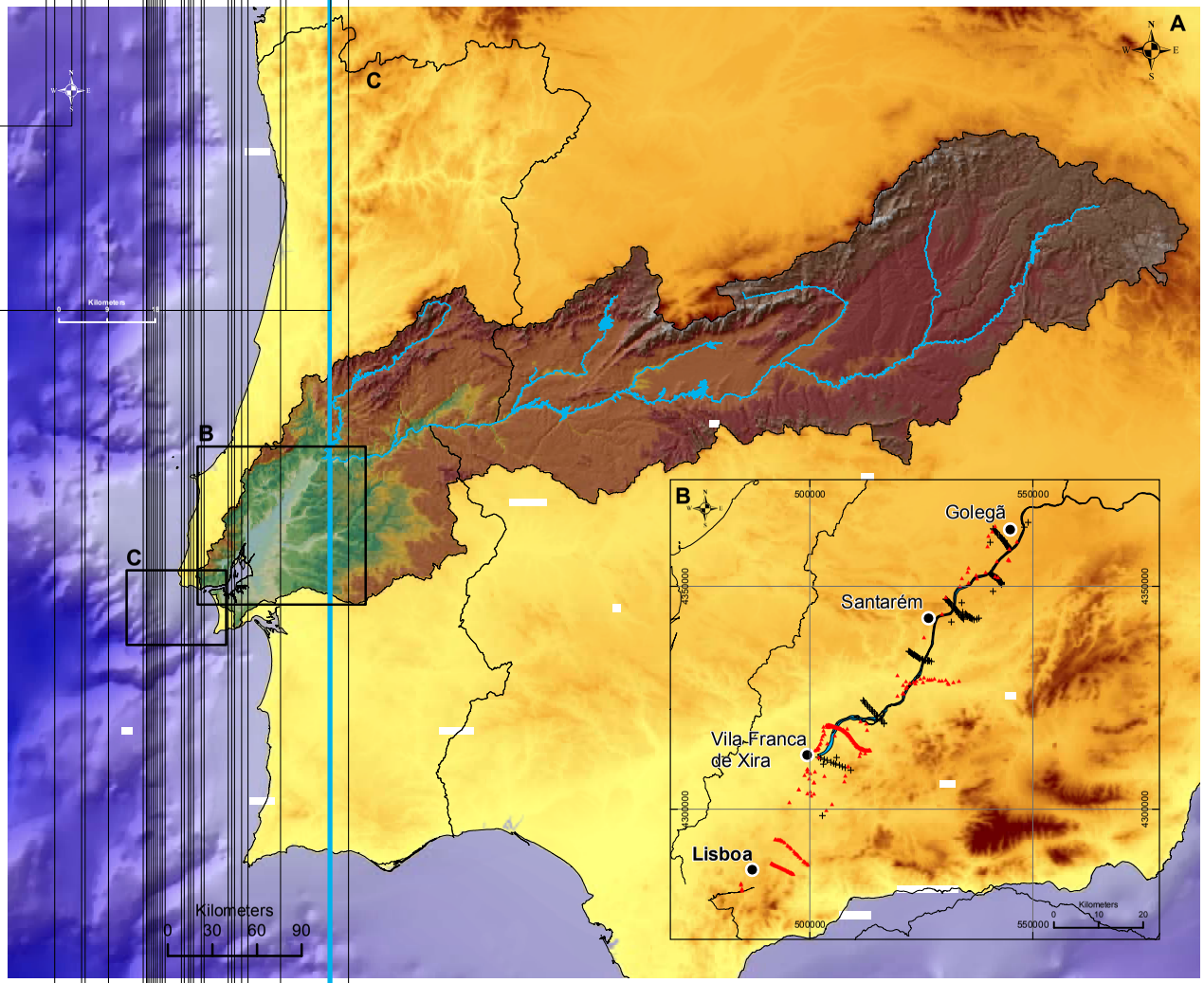

LEGEND

Elevation (SRTM, v3)

+ 2000 m
(500 m in inset maps)

0 m

Bathymetry
(main map: GEBCO;
inset map: INETI/DGM)

0 m

-5000 m
(-2000 m in inset map)

Elevation catchment in m
(SRTM, v3)

- 2250 - 2500
- 2000 - 2250
- 1750 - 2000
- 1500 - 1750
- 1000 - 1500
- 750 - 1000
- 500 - 750
- 250 - 500
- 200 - 250
- 150 - 200
- 100 - 150
- 50 - 100
- 25 - 50
- 10 - 25
- 0 - 10

Cores

- marine cores (this study)
- marine cores (previous studies)
- terrestrial cores (this study)
- terrestrial cores (previuous studies)

European Datum 1950/UTM Zone 29N

framework has not been established. A palaeogeographic reconstruction and relative sea-level curve of the Lower Tagus Valley since the last glacial period are also missing. Since the above mentioned subjects have not yet been studied in detail, a study of depocenter migration in the late Quaternary Tagus fluvial and marine depositional system is also lacking. An integrated approach with a sediment budget based on land-sea correlation would provide detailed insight in sea level, tectonic and climatic control on passive margin deposition (Blum and Törnqvist, 2000; Sommerfield and Lee, 2004).

On a smaller spatial and temporal scale, sedimentation on the Iberian passive margin was likely also controlled by human impact. Many studies of depositional systems on the Iberian Peninsula reveal indications of human impact on sedimentation during the last two millennia (Chester and James, 1991; Allen *et al.*, 1996; Bao *et al.*, 1999; Dabrio *et al.*, 1999; Dias *et al.*, 2000; Dinis *et al.*, 2006; Thorndycraft and Benito, 2006a; Fletcher *et al.*, 2007; Van der Schriek *et al.*, 2007a; Van der Schriek *et al.*, 2007b).

Periods of increased fluvial activity have been recognised in the middle Spanish reach of the Tagus River using slackwater deposits and palaeo-stage indicators (Benito *et al.*, 2003b; Benito *et al.*, 2003c). However, a hiatus is present in the flood record due to erosion, as testified by a lack of data between 7000 and 1000 cal BP (Benito *et al.*, 2003b). In addition, the middle-reach sites represent floods triggered in the upstream portion of the catchment only and data including large downstream tributaries are missing. On the Tagus continental shelf, marine records have been studied regarding climatic changes and Tagus palaeo discharge, especially for the last 2000 years (Abrantes *et al.*, 2005; Bartels-Jónsdóttir *et al.*, 2006; Gil *et al.*, 2006, 2007; Lebreiro *et al.*, 2006). Nonetheless, the Holocene Tagus flood record is still fragmentary. Continuous records from the aggrading Holocene floodplain in the Lower Tagus Valley have not been studied in terms of flooding history. A single study on past Tagus fluvial activity only covers the period 1855-1998 AD (Azevêdo *et al.*, 2004).

With respect to the general aims of the SEDPORT project, the specific objectives related with the sedimentary development of the Iberian passive continental margin are:

1. To determine the influence of sediment transport mechanisms on the composition and physical properties of fluvial-marine sediments in the

Figure 1.2 | Location of the study areas on the Iberian passive continental margin near the Lower Tagus Valley. The main map (A) shows the Tagus catchment and study areas on the Iberian Peninsula and the location of marine core MD03-2698. Digital Elevation Data from Jarvis *et al.* (2006), bathymetry from IOC, IHO and BODC (2003). Inset map (B) shows the location of terrestrial cores. Inset map (C) shows the location of marine cores on the shelf and the location of the mudbelt, detailed bathymetry from INETI/DGM.

Lower Tagus Valley and on the adjacent shelf and abyssal plain since the Last Glacial Maximum (~20,000 cal BP) and to investigate how fluvial and marine sedimentation processes have varied due to changed external control by climate, tectonics, sea level, vegetation and human impact;

2. To study the facies and their distribution, sedimentary architecture and timing of the sedimentary fill of the Lower Tagus Valley since the Last lacial Maximum, and based on that, to construct a sequence-stratigraphic framework and discuss the controls on the nature and architecture of the incised-valley succession;
3. To reconstruct the palaeogeographic evolution of the Lower Tagus Valley since the Last Glacial Maximum and to evaluate the relative importance of external controls on the infill of the palaeo-valley and on the spatial and temporal changes of the sedimentary environments;
4. To demonstrate the sedimentary response of the Tagus fluvial-marine depositional system to human impact in the Tagus catchment;
5. To decipher depocenter migration of the Tagus fluvial-marine sediment dispersal system since the Last Glacial Maximum and to identify the relative importance of eustatic, climatic and anthropogenic controls;
6. To present a sediment budget based on quantitative sediment volume reconstructions and to relate changed sediment fluxes to changes in climate and erosion intensity.

To achieve these objectives, a large dataset was created for the Lower Tagus Valley. It consists of 144 hand cores from the Lower Tagus Valley floodplain (maximum depth 23 m). Four mechanical deep cores (maximum depth 52 m) were recovered with a rotary drilling rig. Additionally, lithological and sedimentological information from 284 cone penetration tests, and continuous and discontinuous geological cores used for geotechnical studies for the construction of bridges, dikes, and buildings, were used (De Mendonça, 1933; LUSOPONTE, 1995; BRISA, 2005; INETI, 2007;). The terrestrial sediments were dated using radiocarbon dates from 54 sites. In the marine realm, three piston cores were used; two from the continental shelf (D13882 and GeoB-8903-1) and one from the Tagus Abyssal Plain (MD03-2698). From these cores 34 radiocarbon dates were obtained. Samples were analyzed from these terrestrial and marine cores for grainsize, heavy mineral, organic matter, carbonate, floral and faunal content. Finally, volumes of deposited sediment were quantified using spatial models generated in Petrel 2008 software (Schlumberger Ltd.).

1.3 OUTLINE

This thesis contains five journal papers (Chapters 2 to 6), a Synthesis (Chapter 7), and summaries in English, Portuguese and Dutch. The journal papers are presented in their original form, except for some lay-out changes. Consequently, some repetition in the text with respect to regional setting, methods and references is inevitable.

Chapters 2 and 3 deal with sedimentological and palaeogeographical aspects of the last 20,000 years of the Lower Tagus Valley fill history. They concentrate primarily on the definition of facies units, their 3D arrangement, the temporal and spatial development of environments, the reconstruction of relative sea-level rise, the establishment of a sequence-stratigraphic framework, the identification of controls and the comparison of the Tagus valley-fill with other systems.

Chapter 4 presents a correlation of terrestrial and marine deposits for the last ~2500 years based on sediment cores from the Lower Tagus Valley floodplain and the mudbelt on the Tagus continental shelf. This chapter mainly focuses on synchronous depositional events in the terrestrial and marine sediments. Chapter 5 presents the flooding history of the Tagus River for the last ~6500 years. It uses two sediment cores from distal low-energy backswamps at opposite sides of the Tagus river floodplain. Their synchronous development and changes in sedimentation rates and local vegetation are attributed to allogenic forcing factors.

In Chapter 6 the data gathered in the previous chapters are used to present depocenter migration and to quantify volumes of sediment deposited in the Lower Tagus Valley and on the Tagus continental shelf for the periods 12,000-7000 cal BP and 7000-0 cal BP. Changes in sediment flux are confronted with past large-scale regional climate changes and future implications of global warming and enhanced erosion in the Tagus catchment are discussed. Chapter 7 provides a synthesis of the results presented in Chapters 2 to 6 with respect to the aims of the SEDPORT project and offers directions for future research.

CHAPTER 2

The Lower Tagus Valley in Portugal contains a well-developed valley-fill succession covering the complete Late Pleistocene and Holocene periods. As large-scale stratigraphic and chronologic frameworks of the Lower Tagus Valley are not yet available, this paper describes facies, facies distribution, and sedimentary architecture of the late Quaternary valley fill. Twenty four radiocarbon ages provide a detailed chronological framework. Local factors affected the nature and architecture of the incised valley-fill succession. The valley is confined by pre-Holocene deposits and is connected with a narrow continental shelf. This configuration facilitated deep incision, which prevented large-scale marine flooding and erosion. Consequently a thick lowstand systems tract has been preserved. The unusually thick lowstand systems tract was probably formed in a previously (30,000-20,000 cal BP) incised narrow valley, when relative sea-level fall was maximal. The lowstand deposits were preserved due to subsequent rapid early Holocene relative sea-level rise and transgression, when tidal and marine environments migrated inland (transgressive systems tract). A constant sea level in the middle to late Holocene, and continuous fluvial sediment supply, caused rapid bayhead delta progradation (highstand systems tract). This study shows that the late Quaternary evolution of the Lower Tagus Valley is determined by a narrow continental shelf and deep glacial incision, rapid post-glacial relative sea-level rise, a wave-protected setting, and large fluvial sediment supply.

Based on: Vis, G.-J. and Kasse, C., Late Quaternary valley-fill succession of the Lower Tagus Valley, Portugal. *Sedimentary Geology* (2009), **doi:**10.1016/j.sedgeo.2009.07.010 (http://www.sciencedirect.com/science/journal/02773791)

Late Quaternary valley-fill succession of the Lower Tagus Valley, Portugal

Photo: the Tagus River seen from Portas do Sol (Santarém).

2.1 INTRODUCTION

Numerous studies have focused on facies and sequence stratigraphy of incised-valley fills over the past 15 years (e.g. Allen and Posamentier, 1993; Dalrymple *et al.*, 1994; Emery and Myers, 1996; Talling, 1998; Amorosi *et al.*, 1999; Dabrio *et al.*, 1999; Blum and Aslan, 2006; Boyd *et al.*, 2006; Dalrymple, 2006; Sakai *et al.*, 2006; Mattheus *et al.*, 2007). The filling of incised valleys

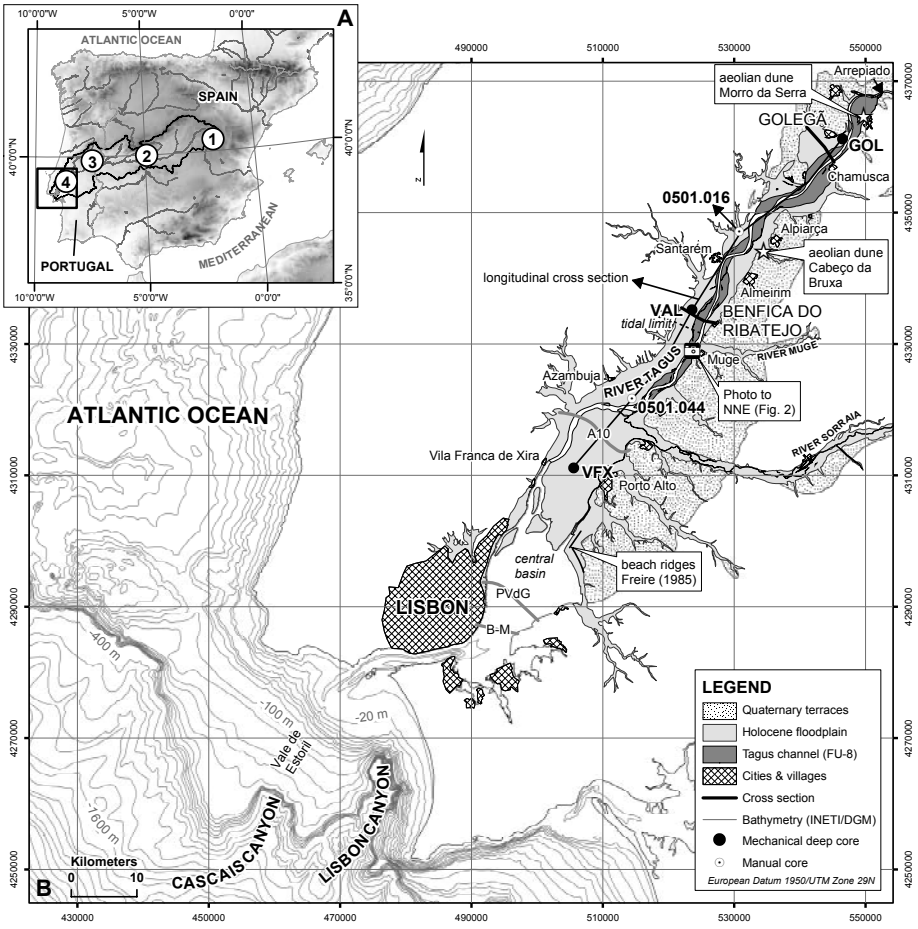

Figure 2.1 | Location map of the Lower Tagus Valley. The inset map (A) shows the Tagus catchment and study area on the Iberian Peninsula, Digital Elevation Data from Jarvis *et al.* (2006). 1: Mesozoic Spanish Cordillera; 2: Spanish Tertiary Sedimentary Tagus Basin; 3: Palaeozoic Hesperian Massif; 4: Lower Tagus Basin (LTB). The main map (B) shows the location of the Golegã and Benfica do Ribatejo cross sections, the longitudinal cross section and the deep cores. Deep cores from north to south: GOL, 0501.016, VAL, 0501.044 and VFX. A10: A10 bridge, geotechnical data (BRISA, 2005), PVdG: Ponte Vasco da Gama bridge, geotechnical data (LUSOPONTE, 1995), B-M: Beato-Montijo bridge, geotechnical data (De Mendonça, 1933). Quaternary terraces after Zbyszewski (1969).

is largely controlled by the balance between accommodation space, which is often governed by the rate of relative sea-level (RSL) rise, the input of fluvially and marine derived sediment, and the slope of the incised valley bottom (Dalrymple, 2006). Further, the facies distribution in the valley fill results from the interplay between waves, tides and rivers. Well developed and preserved lowstand systems tracts (LST) are rare in the incised-valley literature, with most examples showing absent or considerably condensed sections (Nichol *et al.*, 1996; Heap and Nichol, 1997; Nichol *et al.*, 1997).

Many rivers flowing from the Iberian Peninsula into the Atlantic Ocean have Holocene valley fills with coastal successions up to 40 m thick: Odiel-Tinto Rivers (Borrego *et al.*, 1999; Dabrio *et al.*, 1999; Dabrio *et al.*, 2000; Lario *et al.*, 2002), Guadiana River (Boski *et al.*, 2002; Lobo *et al.*, 2003), Mira River (Alday *et al.*, 2006), and Douro River (Naughton *et al.*, 2007a). However, since these rivers are relatively small, fluvial progradation is limited, although some systems show coastal progradation (e.g. Goy *et al.*, 1996). The Lower Tagus Valley (LTV) is located on the Iberian west coast, where submarine canyons reach the narrow (~30 km) continental shelf break (Lastras *et al.*, 2008) (Fig. 2.1). The narrow shelf and submarine canyons, combined with a large catchment, provide ideal circumstances for deep incision during low RSL and thus possible formation of a well developed late Quaternary lowstand systems tract (LST). Local studies of the late Quaternary valley fill of the LTV have been published recently (Azevêdo, 2001; Ramos *et al.*, 2002; Ramos Pereira *et al.*, 2002; Azevêdo *et al.*, 2004; Azevêdo *et al.*, 2007; Van der Schriek *et al.*, 2007a). However, a valley-wide 3D reconstruction of the complete LTV fill is still missing. Additionally, the chronological control of the valley-fill development is poor.

This chapter aims to study the facies and their distribution, sedimentary architecture, and chronology of the sedimentary fill of the LTV covering roughly the period since the Last Glacial Maximum (LGM). Subsequently, a sequence-stratigraphic framework is constructed, and the effects of local factors affecting the nature and architecture of the incised-valley succession are discussed. To achieve this, three valley cross sections are constructed, using 122 manually and 3 mechanically derived cores to a maximum depth of 52 m, oriented in both longitudinal and transverse directions relative to the valley axis. Facies units are defined using grainsize and floral and faunal content. Twenty-four radiocarbon ages provide the absolute chronology for the valley-fill history of the LTV since the LGM.

Figure 2.2 | Northward oblique aerial photo of the Tagus channel near Benfica do Ribatejo (location on Fig. 2.1). Channel width ~350 m.

2.2 REGIONAL SETTING

The Tagus River originates at an elevation of about 1600 m in eastern Spain (Fig. 2.1) and has a length of ~1000 km with a catchment area of 80,630 km^2 (Bettencourt and Ramos, 2003; Le Pera and Arribas, 2004). It enters the Atlantic Ocean near Lisbon in a passive continental margin setting with a narrow continental shelf (<30 km). The average discharge near its mouth is 400 m^3/s, but the river is characterised by extreme seasonal and annual variability with peak discharges more than 30 times the average discharge (Benito *et al.*, 2003; Bettencourt and Ramos, 2003). The present-day Lower Tagus Valley floodplain (Figs. 2.1 and 2.2) is 5-10 km wide and ~85 km long, has an elevation of ~22 m near Golegã in the north and ~2 m near Vila Franca de Xira in the south, and an average gradient of ~24 cm/km.

The central basin south of Vila Franca de Xira (Fig. 2.1) is characterised by an ebb-dominated semi-diurnal mesotidal regime with a mean tidal amplitude of 1.5 m at neap tide and 4 m at spring tide (Portela and Neves, 1994; Bettencourt and Ramos, 2003). The effect of the tides is noticed upstream to Muge (about 50 km north of Lisbon), in a nearly freshwater environment. The deep (≤40 m) and narrow bedrock-constrained tidal inlet provides a morphologically unique situation, where the LTV is sheltered against the high-energy wave regime on the Atlantic Ocean where winter wave heights up to 10 m occur (Instituto Hidrográfico Portugal, 2008). Therefore, waves play a very minor role within the central basin (Fortunato *et al.*, 1999) and tides and fluvial discharge are the dominant energy suppliers.

The shallow central basin is dominated by mud and muddy sand at the bottom (Fig. 2.3A); sand is only present in the narrow channels near Vila Franca de Xira and offshore Lisbon (Portela and Neves, 1994; Jouanneau *et al.*, 1998). The turbidity maximum is located in the central basin between Vila Franca de Xira and Lisbon, and inland migration of offshore sands occurs only occasionally (Vale and Sundby, 1987; Barros, 1996), as corroborated by the sediment distribution on the central basin floor (Fig. 2.3A). Only a small fraction of the tidal energy reaches the fluvial part of the basin (Fig. 2.3B) (Fortunato *et al.*, 1999). Generally, since the LGM, RSL in south and west Iberia rose rapidly to approximately the present-day level by around 7000 cal BP and has remained more or less constant since then (Boski *et al.*, 2002; Waelbroeck *et al.*, 2002; Fernández-Salas *et al.*, 2003).

The LTV forms part of the Lusitanian Basin, which is an inverted Mesozoic trough, resulting from aborted Triassic rifting (Masson and Miles, 1984; Rasmussen *et al.*, 1998; Carvalho *et al.*, 2005). Inversion tectonics during the Tertiary resulted in the formation of a compressional foredeep—the Lower Tagus Basin—in which up to 2000 m of sediment accumulated

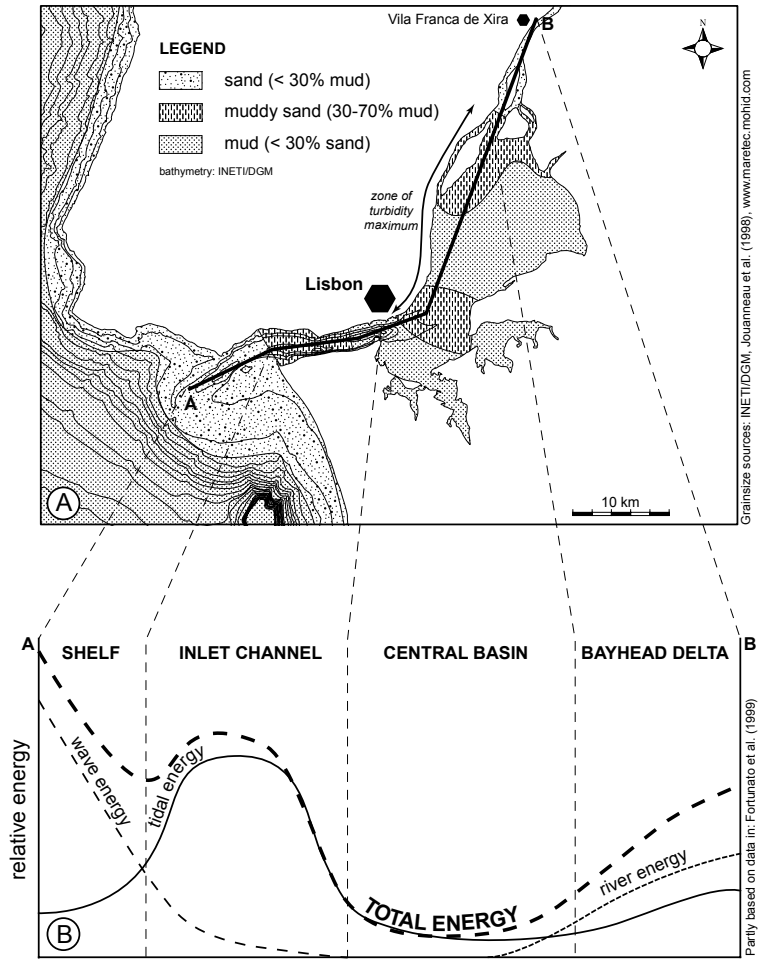

Figure 2.3 | (A) Generalised sediment distribution in the Lower Tagus Valley central basin and offshore area. Note the absence of sand in the central basin. (B) Schematic relative energy levels and sources in the bayhead delta, central basin, inlet channel and shelf regions.

(Barbosa, 1995; Rasmussen *et al.*, 1998). Several studies have focussed on the location and activity of faults in the LTV (e.g. Cabral and Ribeiro, 1989; Barbosa, 1995; Rasmussen *et al.*, 1998; Curtis, 1999; Vilanova and Fonseca, 2004). However, the presence and activity of faults along and underneath the Holocene valley-fill sediments remains the subject of debate (e.g. Fonseca *et al.*, 2000; Cabral, 2001; Fonseca and Vilanova, 2001). The region is known to be tectonically active, as illustrated by large historic earthquakes in 1531, 1755 and 1909 AD (Chester, 2001).

Since the Pliocene-Early Pleistocene the area was lifted up to 200 m above present sea level and at present continues to be uplifted at 0.05-0.10

mm/y (Cabral, 1995). The uplift resulted in a staircase of Pleistocene fluvial terraces, mainly located east of the river up to ~100 m above the Holocene floodplain (Fig. 2.1). For an overview of the published work on the Pleistocene terraces, the reader is referred to Van der Schriek *et al.* (2007a).

2.3 METHODS

To understand the distribution of LTV facies units, two cross sections perpendicular to the valley axis and one longitudinal cross section covering the entire present-day floodplain (as mapped on the Carta Geológica de Portugal (IGM/INETI, 2008) were designed (Fig. 2.1). Cores were taken with an average spacing of 300 m and their location was measured using a Garmin GPS-12 receiver (horizontal resolution ~5 m). The elevation of core sites relative to mean sea level (m.s.l.) was measured using Trimble DGPS equipment (vertical resolution ~5 mm). The hand cores were recovered using Edelman augers for sediment above the groundwater table, and the gauge and the Van der Staay suction-corer for sediment below the groundwater table (Van de Meene *et al.*, 1979). Sediments were described in the field at 10 cm intervals following the method explained in Berendsen & Stouthamer (2001). For the present paper, lithological classifications were converted to USDA terminology.

Three mechanical deep cores (maximum depth 52 m) were recovered with a rotary drilling rig, with protection against borehole collapse by steel casing. The cores have diameters of 121 mm and 105 mm; recovery was poorest in sand (20 %) and best in clay sediments (100 %). Additionally, lithological and sedimentological information from 284 cone penetration tests, and continuous and discontinuous geological cores used for geotechnical studies for the construction of bridges, dikes, and buildings, were used (De Mendonça, 1933; LUSOPONTE, 1995; BRISA, 2005; INETI, 2007).

Grainsize samples (451) from 1 cm thick sediment slices in lithologically uniform intervals were spaced ~50 cm apart. Measurements were done using a Fritsch A22 Laser Particle Sizer following the methods described by Konert and Vandenberghe (1997). About 1-2 g of bulk sediment was pretreated with H_2O_2 and HCl to remove organic matter and carbonates respectively. Median grainsize (D50) and standard deviation were calculated using GRADISTAT software (Blott and Pye, 2001).

Botanical macrofossil samples (from generally 1 cm thick sediment slices) were boiled with sodium pyrophosphate and sieved. Macrofossils were picked from the residue and determined at VU University Amsterdam. Pollen samples (34) were prepared following the description by Faegri and Iversen (1975); the material was sieved through a 7-8 mm nylon mesh and clastic ma-

terial was removed using a sodium polytungstate heavy liquid separation. The samples were embedded in glycerine jelly and sealed with paraffin wax. Shells, foraminifera, ostracods, and diatoms were sieved from the sediment using a 63 μm sieve.

A set of twenty four radiocarbon ages was used to construct the chronological framework. The material for radiocarbon dating consisted as far as possible of terrestrial botanical macrofossils that were manually selected from generally 1 cm thick sediment slices, and otherwise bulk samples were used. Most botanical macro remains were most likely not in-situ, but their good quality suggests they were probably not transported very far. The radiocarbon ages were calibrated using the program OxCal v3.10 (Bronk Ramsey, 1995, 2001, 2005), using the atmospheric data from Reimer *et al.* (2004). Radiocarbon ages are expressed as calibrated calendar ages (cal BP) with age spans at the 2σ range.

2.4 RESULTS

The detailed environmental reconstruction is based on all of the available data combined into the facies description and interpretation following Doyle and Bennet (1998, p. 397). This resulted in the identification of nine Pleistocene and Holocene facies units (FU) within the LTV. They are described from base to top, using two transverse cross sections (Figs. 2.4 and 2.5 and *Addendum 1*) and one longitudinal cross section, relative to the valley axis (Fig. 2.6). Facies units are described in detail in Tables 2.1 and 2.2 with characteristic grainsize distributions per facies unit given in Fig. 2.7 and photographs in Fig. 2.8.

Facies Unit 1A (fluvial terrace deposits)

The poorly sorted, mainly coarse-grained, sand and gravel of FU-1A (Table 2.1, Fig. 2.7) indicate deposition in a high-energy environment with sufficient stream power to transport coarse gravel. The absence of a fining-upwards succession in the top of FU-1A and the flat morphology are attributed to sand and gravel bars being deposited in channels of a fluvial braided system, analogous to the Pleistocene Tagus terraces.

No absolute time control is available for this unit, but based on its stratigraphic position and previous studies, deposition within the Pleistocene is assumed (Ribeiro *et al.*, 1977; Rosina, 2004; Cunha *et al.*, 2005; Cunha *et al.*, 2008).

Facies Unit 1B (high-gradient fluvial channels)

This unit consists of poorly sorted, coarse-grained gravely sand, in a short

fining-upward succession (Table 2.1, Figs. 2.7 and 2.8A), indicating a high-energy fluvial environment with sufficient stream power to transport coarse gravel. In combination with the steep slope (60 m/100 km = ~60 cm/km), this unit represents channel bars of a coarse-grained braided river.

Radiocarbon dating suggests formation of this unit before the Late Glacial period (14,700-11,500 cal BP), as indicated by a radiocarbon age of 14,260-13,780 cal BP (UtC-14908) (Table 2.3) in the top of this unit in core VFX (Fig. 2.6).

Facies Unit 2 (aggrading fluvial overbank)

This unit consists of fine sandy and clayey silts, in a generally fining-upward succession (Table 2.1). The presence of many large (≤ 3 cm) carbonate concretions in the basal 6 m in core VFX (Fig. 2.6) suggests that evaporation exceeded precipitation (i.e. seasonally dry climates). The large thickness of this basal interval, with many carbonate concretions, implies a long period of deposition in the order of 10^3 years. In the upper 6 m of FU-2 in core VFX, the intercalated fine sand layers, the decreasing amount and size of carbonate concretions, and the increase of humic levels, all suggest an increased sedimentation rate and a wetter and more dynamic sedimentary environment. FU-2 was most likely intermittently deposited under subaerial conditions in a low-energy environment. Sedimentation started in a proximal floodbasin which gradually transformed into a levee, all belonging to a single-channel fluvial system. This is supported by the grainsize characteristics of poorly sorted mixtures of fine sand, silt, and clay that resemble those of the Holocene levee and crevasse deposits of FU-7 (Fig. 2.7).

Radiocarbon ages of 14,260-13,780 cal BP (UtC-14908) for the base of this unit, and of 11,800-11,200 cal BP (UtC-14907) in the top of this unit in core VFX (Fig. 2.6) imply deposition within the Late Glacial (Table 2.3).

Facies Unit 3A (brackish water marshes and tidal flats)

This mainly mud (clay + silt)-dominated locally bioturbated unit with indications for both brackish (shells, agglutinated foraminifera, pyrite, Chenopodiaceae pollen) and freshwater (seeds) conditions (Tables 2.1 and 2.2, Figs. 2.7 and 2.8B) is interpreted as a (low) brackish water marsh or tidal flat environment with occasional freshwater input from the river. Freitas *et al.* (1999), Ruiz *et al.* (2005) and Van der Schriek *et al.* (2007b) found the same foraminifera in similar settings in Portugal. Except for the top, this unit has a soft consistency, indicating little exposure during deposition. The substantial thickness of the low marsh and tidal flat deposits suggests vertical aggradation rather than progradation due to the rapid RSL rise before ~7000 cal BP (Boski *et al.*, 2002; Waelbroeck *et al.*, 2002; Fernández-Salas *et al.*, 2003). Since

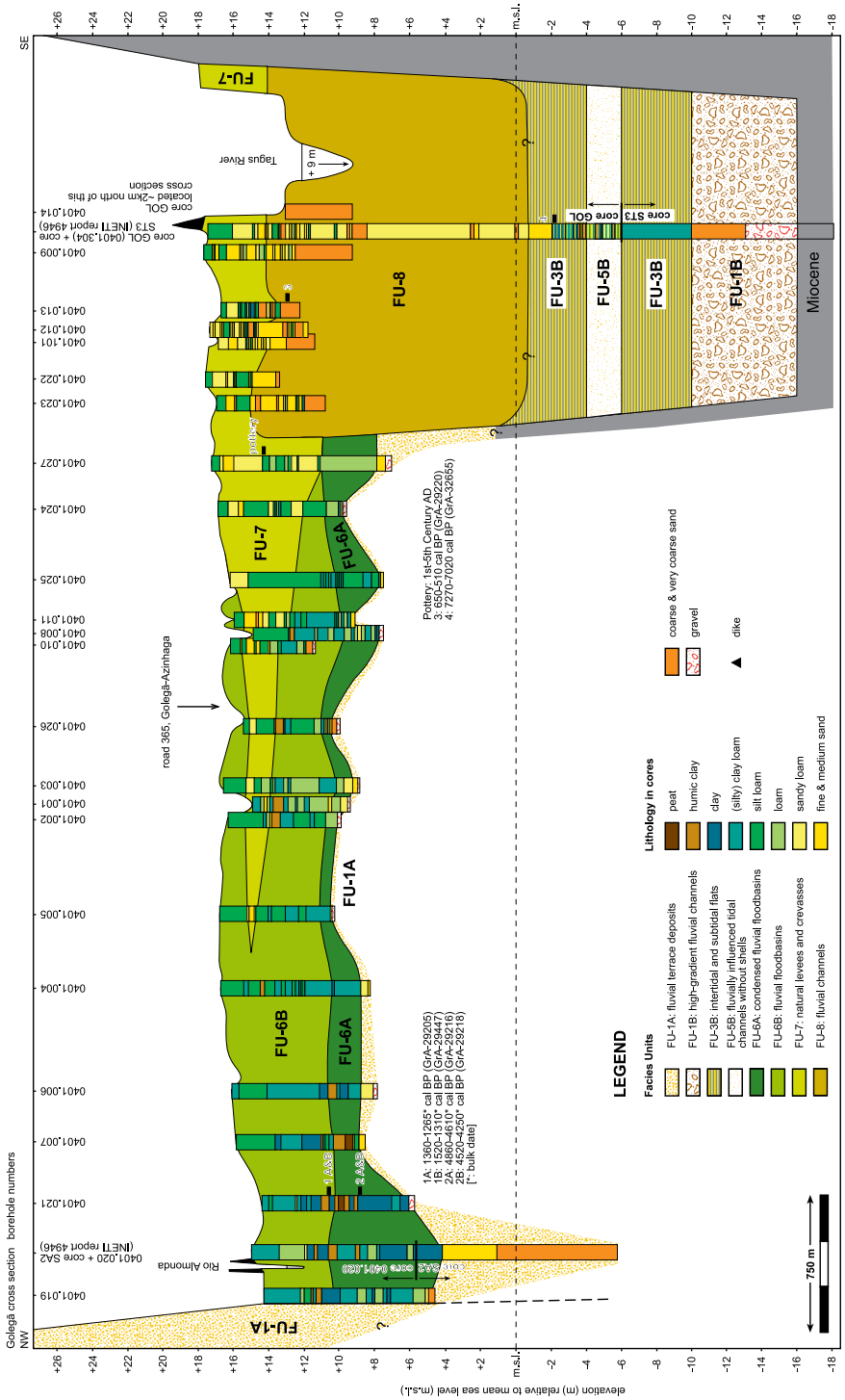

Figure 2.4 | Golegã cross section. Lithology and distribution of facies units are based on manual corings and mechanical corings GOL and SA2 and ST3 (INETI, 2007). Coring GOL was projected from its original location east of Golegã (Fig. 2.1). A full-colour version of this cross section can be found in *Addendum 1*.

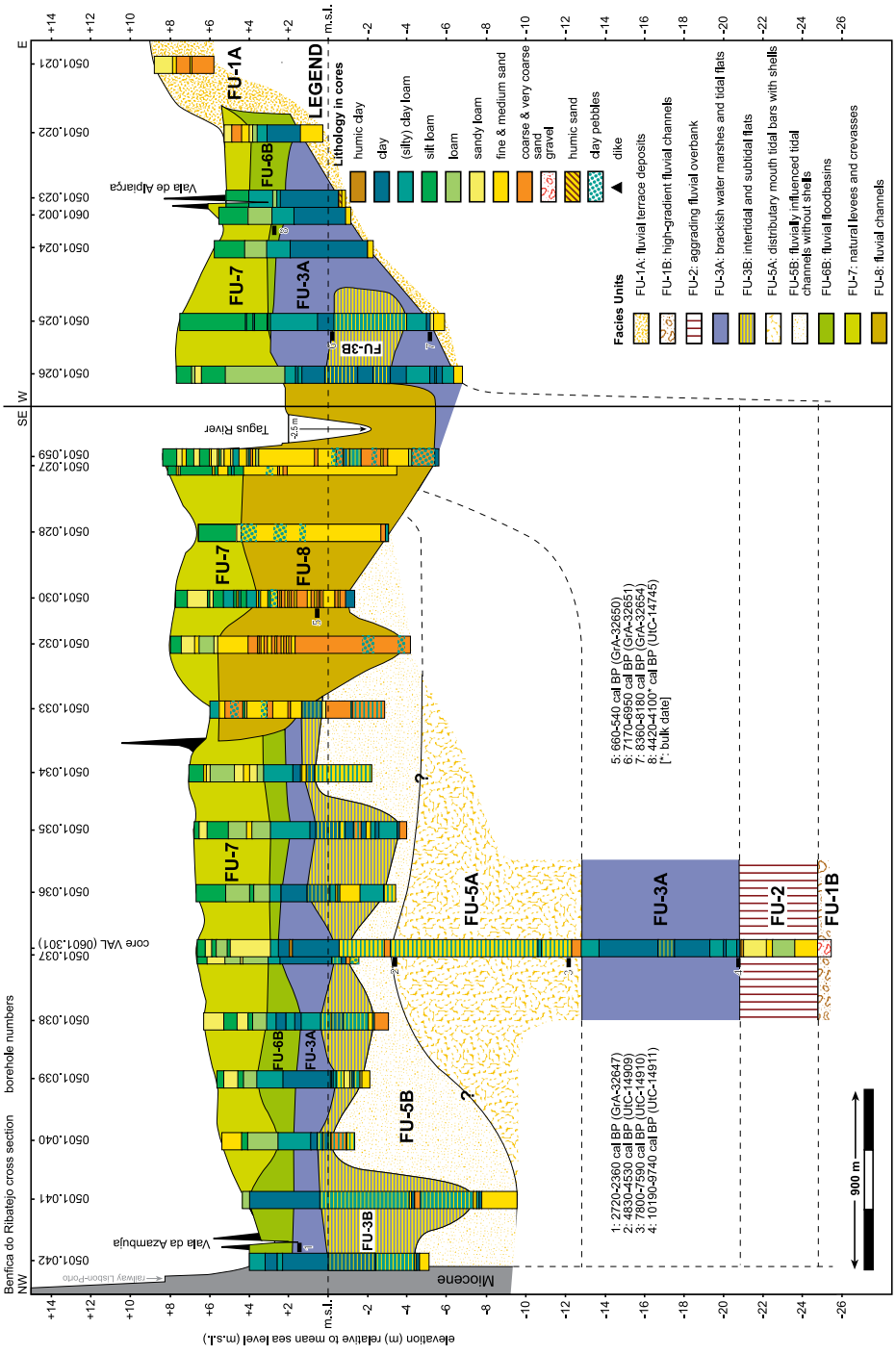

Figure 2.5 | Benfica do Ribatejo cross section. Lithology and distribution of facies units are based on manual corings and mechanical coring VAL. A full-colour version of this cross section can be found in *Addendum 1*.

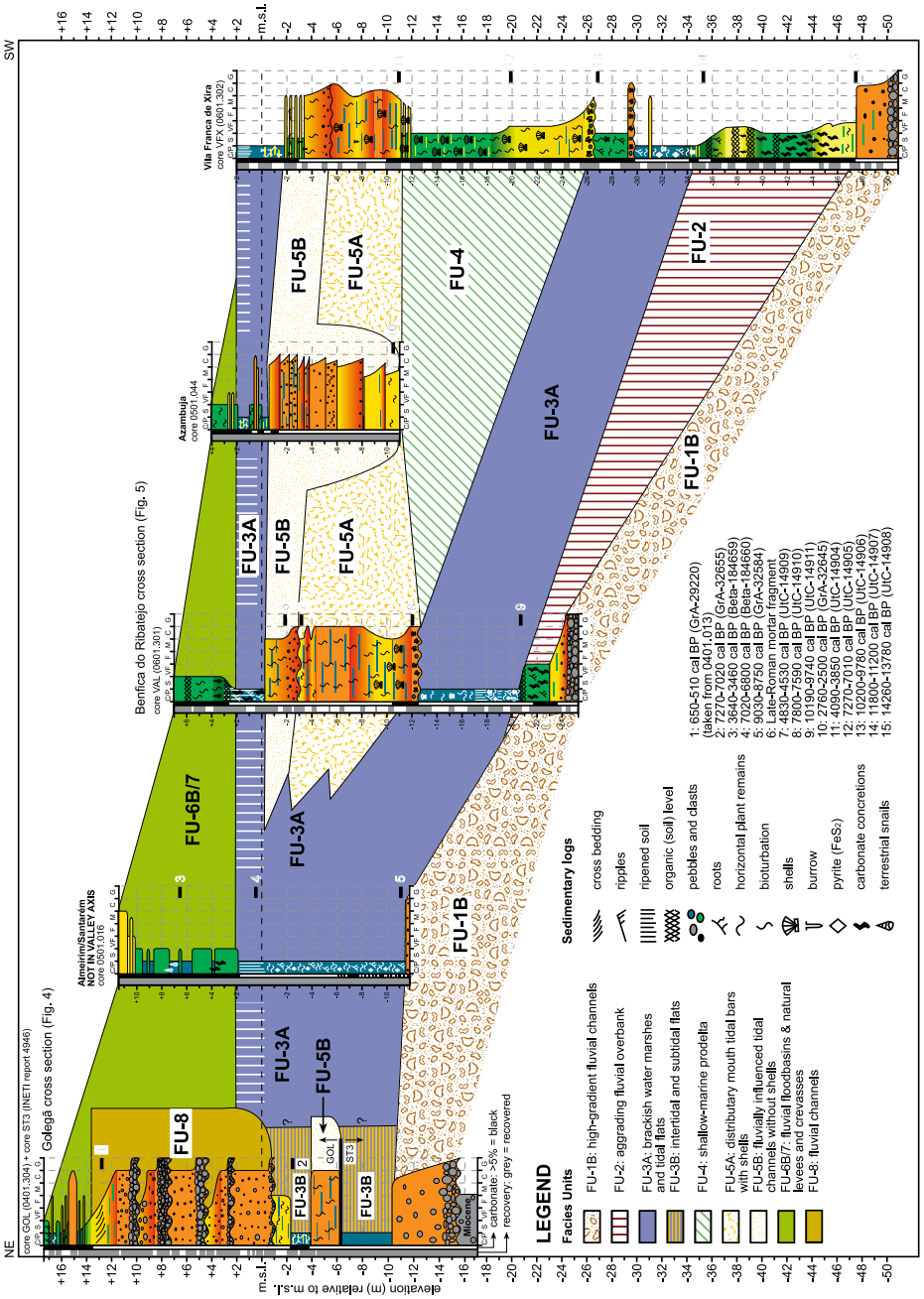

Figure 2.6 | Longitudinal NE-SW cross section through the Lower Tagus Valley. Lithology and distribution of facies units are based on manual corings 0501.016 and 0501.044 and mechanical corings GOL, VAL and VFX. Distance between corings is not to scale. Note that only coring GOL penetrates Tagus channel belt deposits (FU-8), the other corings are located some distance away from the channel belt (Fig. 2.1). Lithology: C/P = clay or peat, S = silt, VF = very fine sand, F = fine sand, M = medium sand, C = coarse sand and G = gravel. A full-colour version of this cross section can be found in *Addendum 1*.

~7000 cal BP, RSL rise has been negligible and therefore vertical aggradation was strongly limited, resulting in pedogenesis in the upper 1.5-2 m due to subaerial exposure and soil ripening. This level is generally situated ~2 m above present-day sea level and reflects a high marsh, developed between mean high water (MHW) and highest astronomical tide (HAT). The upper part of FU-3A is completely decalcified, whereas in the basal part, formed during rapid RSL rise, some carbonate containing intervals as well as (partly dissolved) shell remains are still present. The lack of carbonate foraminifera, shells, and sedimentary carbonate in the upper part of FU-3A probably results from decalcification by organic acids originating from decomposing plant remains during and after deposition. South of Benfica do Ribatejo, decalcification of the upper part is limited because of more recent deposition.

Within this unit, Freire (1985) found beach ridge and dune deposits created by longshore currents (Fig. 2.1). They are located south of Porto Alto, on the eastern side of the valley, and consist of elongated sand ridges up to 8 m high, containing well-sorted, medium-grained sand (350-500 μm).

Radiocarbon dating and stratigraphic position reveal continuous deposition of this unit since its first occurrence in core VFX (11,800-11,200 cal BP (UtC-14907), Table 2.3, Fig. 2.6). Basal deposition of FU-3A occurred progressively later northwards due to early Holocene RSL rise and transgression. In core VAL, sedimentation of FU-3A started around 10,190-9740 cal BP (UtC-14911), and in core 0501.016 at 9030-8750 cal BP (GrA-32584) (Fig. 2.6). In contrast, the upper part of FU-3A and its associated soil formation is progressively younger southwards. In core 0501.016 the top is dated at about 7020-6800 cal BP (Beta-184660) (Fig. 2.6). In the Benfica do Ribatejo cross section (Fig. 2.5), two radiocarbon ages indicate an age between 4420-4100 cal BP (UtC-14745) in core 0601.002, and 2720-2360 cal BP (GrA-32647) in core 0501.042. South of Benfica do Ribatejo, FU-3A is present just below the surface, and at the fringes of the present day central basin it is still being formed.

Facies Unit 3B (intertidal and subtidal flats)

This laminated unit with shells and foraminifera consists predominantly of clay with well-defined sand laminae (Table 2.1, Figs. 2.7 and 2.8C-E), and is interpreted to be a tidal deposit. The thickness and lateral extent of the laminae is highly variable, so it is difficult to determine whether lenticular bedding or thinly interlayered sand/mud bedding was found. Using the study of Reineck and Wunderlich (1968) it is concluded that deposition took place in intertidal and subtidal zones.

Radiocarbon ages indicate deposition shortly after 8360-8180 cal BP (GrA-32654) in core 0501.025 (Table 2.3, Fig. 2.5). In core GOL (Fig. 2.4),

Table 2.1 | Description of facies units from the Lower Tagus Valley. [1]: Geotechnical studies for the Ponte Vasco da Gama (LUSOPONTE, 1995), A10 bridge (BRISA, 2005) and data from INETI archives (INETI, 2007).

Facies Unit	Lithology	Colour	Carbonate	Basal bounding surface	Geometry	Location	Organics	Flora & fauna	Details
1A	very fine to coarse-grained sand, usually poorly sorted, 1-10 % rounded gravel up to ~30 mm Ø	grey, yellow, orange, brown	≤ 5%	not reached	↕ unknown top: +17- -7 m m.s.l.	Golegã & Benfica do Ribatejo, base (Figs. 2.4 & 2.5)	plant roots in top	barren	compact sediment, unit has flat top and slopes seaward, incised into Miocene-Pliocene deposits
1B	fine to coarse-grained, angular sand, poorly sorted, with increasing gravel to base (≤ 20 %), mainly rounded quartz & quartzite pebbles & cobbles ≤ 9 cm Ø	grey, yellow-grey, brown-grey	0%	erosive	↕ ~10 m[1] top: 0- -48 m m.s.l. slope: 0.001-0.0005 m/m	Bottom of all cross sections (Figs. 2.4, 2.5 & 2.6)	barren	barren	fining-upwards, unit has rather flat top morphology[1] and slopes seaward, incised into Miocene-Pliocene deposits
2	clay, (silty) clay loam, loam and very fine to fine sand with parallel lamination	grey, bluish grey, green-grey, brown-grey	base ≥ 5%, top ≤ 5%	sharp-gradual	↕ ~12 m top: -21- -41 m m.s.l.	Downstream part of valley in cores VAL & VFX (Figs. 2.5 & 2.6)	plant roots & plant remains, wood frags. fine black organics	*Scirpus lacustris,* Polygonaceae sp., *Mentha sp., Alnus sp.* unrecognisable seeds	fining-upwards, dark-brown soil A-horizon in top with plant remains, roots and black/brown mottling. Many carbonate concretions (≤ 3cm), decreasing to top. In core VAL in top of unit: marble-like appearance. Most likely only locally present. Directly overlies FU-1B and thins landward
3A	generally structureless clay and silty clay with locally very fine sand lamination. In core VFX at -29 and -31 m m.s.l. sand layers	dark grey	usually 0%, some deeper parts ≥ 5%	sharp	↕ ~13 m top: ≤ +2 m m.s.l.	Widespread and continuous across study area (Figs. 2.5 & 2.6)	plant roots, horizontal plant remains	Chenopodiaceae sp. pollen, *Isoetes sp.* spores, freshwater plant seeds, diatoms, dinoflaggelates, (Spiniferites type), foraminifera (mainly agglutinated)	pyrite crystals and pyrite in diatoms, foraminifera and plant remains, bioturbation. Top 1.5-2 m + m.s.l.: very firm consistency, angular blocky structure, carbonised plant material, coarse many carbonate concretions = pedogenesis. Underneath: soft, shell-like breaking = no ripening bioturbation. Pedogenesis decreases southward,
3B	plastic, soft clay and (silty) clay loam with laminae and lenses of very fine to coarse-grained sand with gravel up to 2 cm Ø. Clay-sand contacts sharp, sand laminae 0.1-10 cm. Thin laminae: well sorted very fine to fine sand, thicker laminae: medium to poorly sorted medium to coarse-grained sand. Clay layers: 0.1-3 cm. In general, rhythmic clay-sand alternations. Some sand layers disturbed and preserved as sand nests or spots = bioturbation	grey, dark grey	clay: 0% sand: > 5%	erosive or gradual	↕ ~8 m top: ≤ +1 m m.s.l.	Widespread across study area (Figs. 2.4 & 2.5). Found within incised valley near Golegã (Fig. 2.4)	horizontally layered, freshwater detrital plant remains	Chenopodiaceae sp. pollen *Isoetes sp.* spores freshwater plant seeds (well preserved), diatoms, dinoflaggelates (Spiniferites type), foraminifera (calcareous & agglutinated)	shells, shell fragments and carbonate foraminifera are only present South of Azambuja. This unit often contains methane gas
4	plastic, soft slightly sandy, (silty) clay loam and silty clay with rare sand laminae, many sand spots = (strong) bioturbation and burrowing. Many shell fragments and shells in living position	dark grey	> 5%	erosive, lag deposit with clay pebbles & shell fragments	↕ ~16 m ↔ 7.5-9 km top: ~-10 m m.s.l.	Only recovered in core VFX (Fig. 2.6)	freshwater detrital plant remains (well preserved)	Characeae sp. spores *Gloeotrichia sp.* spores *Isoetes sp.* spores freshwater plant seeds (well preserved), diatoms, ostracods, foraminifera (calcareous)	base of unit is fining-upwards series of ~6 m with shell-rich lag deposit overlain by medium sand, fining to very fine sand. Top has gradual but rapid transition to FU-5A. Valley-wide presence from Azambuja southwards[1]. Directly overlies FU-3A
5A	medium to poorly sorted medium to coarse-grained sand. Coarse-grained intervals with ≤ 10% gravel. Within sand: clay laminae ≤ 3 cm, often disturbed = bioturbation	grey, dark grey	> 5% when shells present	gradual in core VFX, further sharp erosive, lag deposit with clay pebbles &	↕ ~9 m ↔ 2.7-9 km (eroded) top: ~-3 m m.s.l.	Nearly valley-wide near Benfica do Ribatejo (Fig. 2.5)	freshwater detrital plant remains (well preserved)	freshwater plant seeds (well preserved), foraminifera (calcareous)	coarsening-upwards, within unit: small, sharp erosive bounding surfaces with gravel, clay pebbles & shell fragments. Not present in Ponte Vasco da Gama (LUSOPONTE, 1995) transect. Shells abundantly present. Directly overlies

Table 2.1 (*continued*)

Facies Unit	Lithology	Colour	Carbonate	Basal bounding surface	Geometry	Location	Organics	Flora & fauna	Details
				shells and shell fragments					FU-3A and FU-4 (Fig. 6)
5B	poorly sorted very fine to coarse-grained sand, gravel ≤ 3% (≤ 1 cm), disturbed clay drapes/laminae = bioturbation	grey, dark grey	0%	erosive, lag deposit with gravel, clay pebbles and rare shell fragments	↕ ≥ 10 m ↔ 1-9 km top: ~+1 m m.s.l.	Associated with FU-3B near Golegã (Fig. 2.4), overlies FU-5A in south (Figs. 2.5 & 2.6)	horizontally layered freshwater plant remains (well preserved)	Chenopodiaceae sp. pollen freshwater plant seeds	generally fining-upwards (coarsening-upwards in core 0501.044). Shells & foraminifera are extremely rare. Covered by FU-3A/B in south
6A	sandy loam, loam, silt loam and (silty) clay loam and humic clay, peaty clay and peat intervals. General grainsize decrease away from river channel	black-grey, grey, orange-grey, green-grey, blue-grey	≤ 5%	sharp	↕ 1-2 m (locally ~6 m) ↔ ~4 km top: ~+10 m	Only found near Golegã (Fig. 2.4) covering FU-1A	unrecognisable plant remains	barren	tough consistency, small carbonate concretions, root traces, white & green spots, animal bioturbation, admixture of sand grains. Locally greenish, bluish colours. Generally: alternating wet and dry conditions
6B	silt loam, (silty) clay loam and clay, very local occurrence of poorly sorted (loamy) coarse-grained sand with up to 10% gravel deposited by small brook channels from uplands. General grainsize decrease away from river channel. Distal areas: gyttja, peat, peaty clay and humic clay layers	brown, grey, dark brown, grey-brown, dark grey	proximal areas: ≥ 5%, distal areas: 0%	sharp	↕ ~10 m top: +4- +21 m m.s.l.	Golegã & Benfica do Ribatejo (Figs. 2.4 & 2.5)	proximal: very rare; distal: some plant remains	proximal: very rare; distal: seeds and pollen better preserved	unit forms southwards thinning wedge. Ongoing sedimentation on active floodplain with shallow (ephemeral) flood-channels at surface. Contains iron-oxides, iron-concretions, manganese spots, carbonate concretions and is well oxygenated. More charcoal to top. A-horizons: ≤ 50 cm, dark brown-grey to dark brown, sometimes hard, dry and crumbly with white lines (no carbonate)
7	sandy loam, loam, silt loam and usually well sorted very fine to fine-grained sand in laminae. Grainsize fines away from channel. Locally medium to coarse-grained sands, some in channels or splays	brown, grey, yellow-brown, dark brown, grey-brown, dark grey	≥ 5%	sharp, at channel bases: sharp erosive	↕ ~10 m ↔ ~4 km top: ≤ 5 m relative to floodbasins	At surface between Golegã and Azambuja (Fig. 2.6)	very rare, only local plant roots	barren	present on both sides along Tagus channel (FU-8), not present near Vila Franca de Xira. Shallow (ephemeral) flood-channels at surface. Often much charcoal present
8	medium to coarse-grained sand, up to 100% gravel (in core GOL) with pebbles and cobbles with long axis ≤ 12 cm in channel lags. No large stones downstream of core GOL. No significant downstream grainsize change. Several channel lag deposits	grey, yellow, brown-grey, orange-grey, dark grey, brown-yellow	0- < 5%	erosive, lag deposit with gravel, limestone & clay pebbles, pottery & brick fragments, wood, plant remains, seeds	↕ ~13 m (Golegã) ↕ ~8 m (Azambuja) ↔ 3-1 km top: +12- +1 m m.s.l.	Between Arrepiado and Azambuja (Fig. 2.1)	plant remains well preserved in lag deposits & channel fills	seeds well preserved in lag deposits & channel fills	fining-upwards, pebbles & cobbles dominated by quartz & quartzite (≥ 93%), up to 5% granite, sand has colourful, "clean" appearance, charcoal present. In core GOL: several stacked fining-upwards sequences. Near Vila Franca de Xira no sandy channel belt present
9	well sorted, angular medium sand (210-420 μm) with large scale, low-angle cross-bedding. Also organic mica-rich laminae present at base of low-angle cross-bedded sets	grey-yellow, brown-grey	0%	sharp	Morro da Serra: 2.5 km^2, ↕ ~10 m top: +30 m m.s.l. Goucharia: 7,200 m^2, ↕ ~5.5 m top: +16 m m.s.l.	Found near Golegã (*Morro da Serra*) and Almeirim (*Cabeço da Bruxa*) (Fig. 2.1)	some buried plant roots	barren	*Morro da Serra*: strongly bioturbated organic horizons often cut-off by erosion and present at base of cross-bedded slip faces. Finger-shaped bioturbation tracks by beetles. Concentrations of large mica's and charcoal within organic horizons. Situated on FU-6B. Low angle cross-bedding points to dominance of NW winds. *Cabeço da Bruxa*: no palaeosols or charcoal found, situated on FU-1

sedimentation continued at least until 7270-7020 cal BP (GrA-32655), and until 7170-6950 cal BP (GrA-32651) in core 0501.025 (Fig. 2.5). Deposition of this unit continues to the present-day in the central basin, south of Vila Franca de Xira.

Facies Unit 4 (shallow-marine prodelta)

The lower part of this unit shows a fining-upward tendency. FU-4 consists of sand, (silty) clay loam, and silty clay (Table 2.1, Figs. 2.7 and 2.8F), and contains a variety of marine fauna (Table 2.2) and a lack of sedimentary structures due to strong bioturbation; it is therefore interpreted as a fully marine prodelta-type deposit. The erosive base with coarse shell-rich sand is interpreted as the transgressive invasion of an open marine environment. This was followed by rapid drowning of the site, creating a quiet, deep water environment below the wave base, where fine sediment was deposited from suspension. The strong bioturbation corroborates with the interpretation of a quiet environment.

This unit was deposited after 10,200-9780 cal BP (UtC-14906) (Table 2.3), as indicated by a radiocarbon age just below the erosive basal bounding surface in core VFX (Fig. 2.6). Around -20 m m.s.l. the fining-upward trend ends and the unit has a uniform clayey appearance. This change took place around 7270-7010 cal BP (UtC-14905) and probably indicates deep water deposition as RSL had nearly reached its present-day value at that time (Boski *et al.*, 2002; Fernández-Salas *et al.*, 2003). The quiet depositional environment resulted from a palaeo-water depth of ~20 m, which is below wave base in this sheltered environment. Deposition of this unit in core VFX gradually ended around 4090-3850 cal BP (UtC-14904).

Facies Unit 5A (distributary mouth tidal bars with shells)

This is a coarsening-upward unit consisting of medium to coarse-grained sand with clay laminae (Table 2.1, Figs. 2.7 and 2.8G); it is interpreted as coalesced distributary mouth tidal bars (Dalrymple and Choi, 2007). Flow expansion in the standing water of the brackish to saltwater central basin, and a rapid decrease in shear stress, resulted in shallowing at the river mouth and coarsening-upward distributary mouth tidal bars. The gradual transition at the base of FU-5A in core VFX (Fig. 2.6) is explained as the progressive deposition of sand onto the prodelta deposits of FU-4. Locally FU-5A has an erosive base (e.g. core VAL), implying that the progradational mouth bar succession gradually turned into a system of mixed fluvial and tidal channels with erosive bases (Meckel, 1975; Dalrymple *et al.*, 1990; Dalrymple *et al.*, 1992). The shell content indicates that brackish water conditions prevailed (Table 2.2).

From Benfica do Ribatejo southwards this unit becomes progressively younger. In core VAL, the base of the unit was dated at 7800-7590 cal BP

(UtC-14910); the final deposition in core VAL occurred shortly after 4830-4530 cal BP (UtC-14909), a date just below the sharp basal boundary of the overlying FU-5B (Fig. 2.6). In core VFX, deposition starts later, around 4090-3850 cal BP (UtC-14904) (Table 2.3, Fig. 2.6).

Facies Unit 5B (fluvially influenced tidal channels without shells)

This widespread unit is generally fining-upwards, and sand-dominated with occasional clay drapes and an absence of shells, which may be explained by strong salinity variations or freshwater conditions (Table 2.1, Fig. 2.7). The unit is interpreted as pointbar-type sedimentation in a fluvially influenced tidal channel (Reading, 1998; Dalrymple and Choi, 2007).

From Golegã southwards, this unit is younger (Fig. 2.6). In core GOL, the unit was already deposited before 7270-7020 cal BP (GrA-32655) (Table 2.3). In core 0501.044 the base was dated at 2760-2500 cal BP (GrA-32645), and in core VAL a Late-Roman mortar fragment indicates deposition after ~1600 cal BP.

Facies Unit 6A (condensed fluvial floodbasins)

This is a unit consisting of (peaty) clay and loam which is deposited in a fluvial floodbasin setting (Table 2.1, Figs. 2.7 and 2.8H). The firm consistency, dark colour, small carbonate concretions, root traces, bioturbation, and the admixture of coarse sand grains at the base of FU-6A, imply slow sedimentation and simultaneous soil formation. In the Golegã cross section (Fig. 2.4), a lateral grainsize-fining away from the Tagus channel implies that both natural levee-type deposition and floodbasin deposition took place in this unit.

In the Golegã cross section (Fig. 2.4), radiocarbon ages within the upper part of this unit indicate that deposition started before 4860-4610 cal BP (GrA-29216) and 4520-4240 cal BP (GrA-29218) (Table 2.3). In the top of FU-6A a hiatus is present, indicated by radiocarbon ages of 1520-1310 cal BP (GrA-29447) and 1360-1265 cal BP (GrA-29205) for the base of the overlying FU-6B.

Facies Unit 6B (fluvial floodbasins)

This fine-grained and locally organic unit, containing several soil A-horizons, is deposited in a fluvial floodbasin setting (Table 2.1, Figs. 2.7 and 2.8I). In comparison to FU-6A, FU-6B contains less organic material and less soil formation. These deposits result from the prograding fluvial Tagus system, which forms a southward thinning wedge over the underlying deposits.

The oldest deposits of FU-6B were found in core 0501.016 (Fig. 2.6), where this unit reaches its maximum thickness. Here, the underlying top of

Facies Unit	Description	Shells (with tidal reference/ water depth)		Foraminifera (with tidal reference)	
3A	tidal salt marsh and tidal flats	*Cerastoderma edule*	intertidal to -15 m	*Jadammina macrescens* (varying concentrations)	≥ MHW
		Crassostrea angulata	intertidal to -60 m	*Trochammina inflata* (varying concentrations)	≥ MHW
		Hydrobia ulvae	upper intertidal	*Ammonia becarii* (rare)	≤ MHW
		*Scrobicularia plana**	intertidal/estuarine	*Elphidium sp.* (rare)	≤ MHW
		(n=11)		(n=18)	
3B	intertidal and subtidal channels and flats	*Cerastoderma edule*	intertidal to -15 m	*Jadammina macrescens* (rare)	≥ MHW
		Crassostrea angulata	intertidal to -60 m	*Trochammina inflata* (rare)	≥ MHW
		Hydrobia ulvae	upper intertidal	*Ammonia becarii* (rare)	≤ MHW
		Mya sp.	intertidal to -20 m	*Elphidium sp.* (rare)	≤ MHW
		Nassarius sp.	low tide to -15 m	*Nonionella sp.* (rare)	≤ MHW
		*Scrobicularia plana**	intertidal/estuarine	(n=9)	
		(n=11)			
4	shallow marine prodelta	*Chlamys sp.**	low shore to >-100 m	*Ammonia becarii* (many)	≤ MHW
		Crassostrea angulata	intertidal to -60 m	*Elphidium sp.* (many)	≤ MHW
		Ensis sp.	sublittoral	(n=10)	
		Laevicardium sp.	sublittoral		
		Mysella sp.	?		
		Nassarius sp.	low tide to -15 m		
		Nucula sp.	sublittoral		
		Spisula sp.	-10 to -70 m		
		Venus sp.	sublittoral to -100 m		
		brittle star-fragments (*Echinoderm*)	sublittoral to -100 m		
		(n=17)			
5A	distributary mouth tidal bars with shells	*Cerastoderma edule*	intertidal to -15 m	*Ammonia becarii* (rare)	≤ MHW
		*Chlamys cf. varia**	low shore to >-100 m	*Elphidium sp.* (rare)	≤ MHW
		Crassostrea angulata	intertidal to -60 m	(n=2)	
		Hydrobia ulvae	upper intertidal		
		Mysella sp.	?		
		Nassarius sp.	low tide to -15 m		
		Scrobicularia plana	intertidal/estuarine		
		Spisula sp.	-10 to -70 m		
		(n=5)			
6B	aggrading fluvial floodbasins	*Cecilioides acicula* = terrestrial snail,	0-40 cm in soil	barren	--
		freshwater shells (*undiff.*)			
		(n=10)			

Table 2.2 | Shell and foraminiferal content of 6 facies units from the Lower Tagus Valley. *: some in living position. Determinations by S. Troelstra and A. Wright, VU University Amsterdam.

Table 2.3 | Radiocarbon ages from Lower Tagus Valley sediments. Radiocarbon "Lab. Nr.": GrA = Centre for Isotope Research, University of Groningen; UtC = R.J. van de Graaff Laboratory, Utrecht University. Coordinates in European Datum 1950/UTM Zone 29N.

Lab. Nr.	Figure	Facies Unit	14C age yrs BP ± 1σ	Age cal. BP 2σ	Coordinates (x-y/z) (m)	Sample depth (cm)	Borehole nr.	Material	Significance	Remarks
GrA-29205	2.4	6B	1390 ± 35	1360-1265	541.501-4362.494/+14.3	366-370	0401.021	bulk humic clay	start sed.	caustic extract
GrA-29216	2.4	6A	4215 ± 40	4860-4610	541.501-4362.494/+14.3	554-556	0401.021	bulk humic clay	end sed.	caustic extract
GrA-29218	2.4	6A	3945 ± 40	4520-4240	541.501-4362.494/+14.3	554-556	0401.021	bulk humic clay	end sed.	residue
GrA-29220	2.4 & 2.6	8	545 ± 35	650-510	544.533-4358.745/+16.63	370-380	0401.013	charcoal	Tagus activity	charcoal
GrA-29447	2.4	6B	1510 ± 40	1520-1310	541.501-4362.494/+14.3	366-370	0401.021	bulk humic clay	start sed.	residue
GrA-30860	-	9	325 ± 30	480-300	548.938-4364.435/+25	110-120	--	charcoal	dune activity	charcoal
GrA-32584	2.6	3A	8030 ± 40	9030-8750	531.088-4346.563/+11.38	2230-2240	0501.016	*Iris pseudacorus* seed	drowning	sieved at 63µm
GrA-32645	2.6	5B	2555 ± 30	2760-2500	514.940-4321.160/+4	1440-1450	0501.044	terrestrial botanical macrofossils	mouth bar	sieved at 125 µm
GrA-32647	2.5	3A	2480 ± 30	2720-2360	522.094-4335.448/+3.94	240-250	0501.042	non-rounded wood pieces	soil formation	sieved at 125 µm
GrA-32650	2.5	8	600 ± 25	660-540	524.799-4333.804/+7.60	690-700	0501.030	twig with bud	Tagus activity	sieved at 125 µm
GrA-32651	2.5	3B	6165 ± 35	7170-6950	526.038-4333.421/+7.42	770-780	0501.025	oxidized organic plant remains	marsh sed.	sieved at 63 µm
GrA-32654	2.5	3A	7440 ± 40	8360-8180	526.038-4333.421/+7.42	1260-1270	0501.025	terrestrial botanical macrofossils	start sed.	sieved at 63 µm
GrA-32655	2.4 & 2.6	3B	6265 ± 35	7270-7020	544.750-4358.375/+17.40	1967-1974	0401.304	undifferentiated plant remains	clay layer	sieved at 63 µm
UtC-14745	2.5	6B	3849 ± 47	4420-4100	526.420-4333.197/+5	280-290	0601.002	bulk humic clay	soil formation	--
UtC-14904	2.6	5A	3647 ± 41	4090-3850	505.439-4310.324/+2	1281	0601.302	terrestrial botanical macrofossils	start sed.	sieved at 63 µm
UtC-14905	2.6	4	6247 ± 46	7270-7010	505.439-4310.324/+2	2192-2196	0601.302	terrestrial botanical macrofossils	start sed.	sieved at 63 µm
UtC-14906	2.6	3A	8900 ± 50	10200-9780	505.439-4310.324/+2	2842-2848	0601.302	terrestrial botanical macrofossils + roots	marsh sed.	sieved at 63 µm
UtC-14907	2.6	2	9990 ± 70	11800-11200	505.439-4310.324/+2	3710-3716	0601.302	terrestrial botanical macrofossils	start marsh sed.	sieved at 63 µm
UtC-14908	2.6	1B	12160 ± 90	14260-13780	505.439-4310.324/+2	4919-4925	0601.302	root + small branch-like pieces	start floodplain	sieved at 63 µm
UtC-14909	2.5 & 2.6	5A	4145 ± 42	4830-4530	523.321-4334.600/+7	1004-1010	0601.301	terrestrial botanical macrofossils	sedimentation	sieved at 63 µm
UtC-14910	2.5 & 2.6	5A	6860 ± 50	7800-7590	523.321-4334.600/+7	1898	0601.301	terrestrial botanical macrofossils	start sed.	sieved at 63 µm
UtC-14911	2.5 & 2.6	3A	8880 ± 60	10190-9740	523.321-4334.600/+7	2748-2753	0601.301	terrestrial botanical macrofossils	start sed.	sieved at 63 µm
Beta-184659	2.6	FU-6B	3320 ± 40	3640-3460	530.589-4347.131/+11.15	649-650	SEV	peat/wood	tidal marsh sed.	Azevêdo et al. (2007)
Beta-184660	2.6	FU-3A	6090 ± 40	7020-6800	530.589-4347.131/+11.15	1074-1075	SEV	peat/wood	floodbasin sed.	Azevêdo et al. (2007)

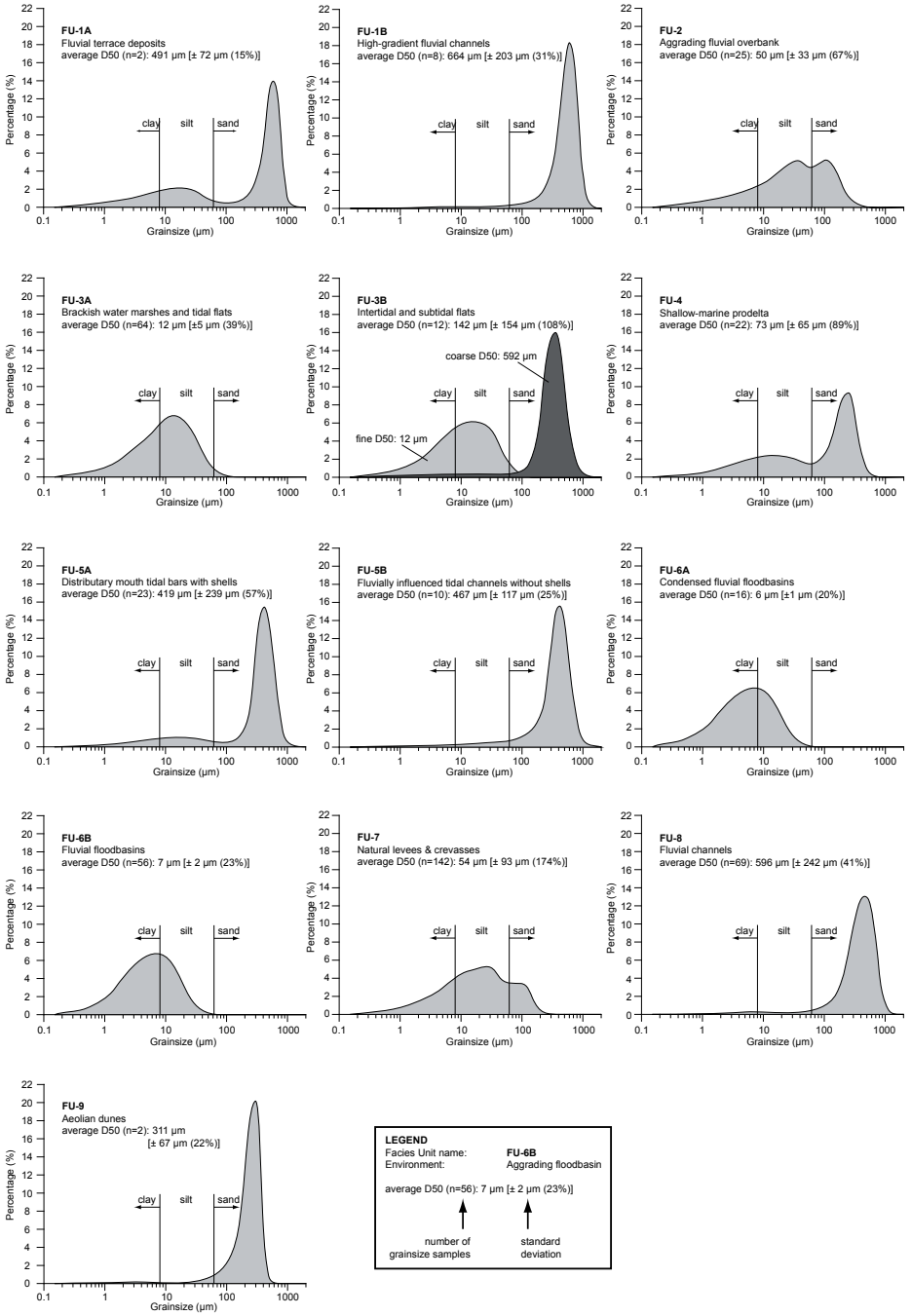

Figure 2.7 | Characteristic grainsize distributions per facies unit for the Lower Tagus Valley. From the total number of samples per facies unit, the most characteristic distribution is shown. Note that due to the grainsize measurement technique (see Methods) the upper limit of the clay fraction is at 8 µm. The dark grey distribution in FU-3B represents samples taken from sand laminae; the light grey distribution represents samples from clay laminae.

FU-3A is dated at 7020-6800 cal BP (Beta-184660), and the overlying floodbasin deposits of FU-6B at 3640-3460 cal BP (Beta-184659) at ~2 m from the base. The transition from FU-3A to FU-6B occurred between these dates and, taking the slower accumulation rate and soil formation in the upper part of FU-3A into account, is estimated at 4500 cal BP. Deposition of the floodbasin deposits of FU-6B started somewhat later in the north, due to the high position of the terraces of FU-1A (Fig. 2.4). In the Benfica do Ribatejo cross section in the south, deposition started after 4420-4100 cal BP (UtC-14745) at the eastern side, and after 2720-2360 cal BP (GrA-32647) at the western side (Table 2.3, Fig. 2.5).

Facies Unit 7 (natural levees and crevasses)

The deposits in this laminated unit, consisting of loam, silt, and well-sorted fine sand are interpreted as fluvial levee deposits (Table 2.1, Figs. 2.7 and 2.8K). Within this unit, the coarse-grained small channels and splays are interpreted as crevasse-splay deposits (not visible in the presented data). Since the finer grainsize limits of crevasse deposits are very similar to levee deposits, these two facies are grouped. It is striking that the levee tops were found up to 5 m above the floodbasin (Fig. 2.5), indicating that floodbasin sedimentation rates were much lower than levee sedimentation rates. The lateral extent of the younger levees is much larger than before and they overlie floodbasin deposits of FU-6B (Fig. 2.4), implying rather recent (<1000 y) accelerated sedimentation of the levees.

The age of this unit is similar to the floodbasin deposits of FU-6B due to their genetic relationship.

Facies Unit 8 (fluvial channels)

The gravel-rich medium to coarse-grained sand in a fining-upward succession (Table 2.1, Figs 7 and 8J, L, M) indicates deposition in a high-energy environment with sufficient stream power to transport coarse sand and gravel. Analogous to the present-day channel bed situation (Fig. 2.2), deposition in the past probably took place in alternate bars, unit bars, braid bars, and point bars. In core GOL (Fig. 2.6) several fining-upwards successions were observed and the channel belt has the largest thickness (~14.5 m), implying stacked channel deposits. No change was found in gravel petrography in this stacked series (Table 2.1), implying limited geological time in this succession. The only indication of downstream fining in the channel belt is a lack of large pebbles and cobbles south of Golegã.

The channel belt is progressively younger downstream. The oldest occurrence of this unit is in core GOL (Fig. 2.4), where the channel belt prograded over the tidal deposits of FU-3B, after 7270-7020 cal BP (GrA-32655)

(Table 2.3). Higher in the channel belt, young dates were obtained: 650-510 cal BP (GrA-29220) in core 0401.013 (Fig. 2.4) and 660-540 cal BP (GrA-32650) in core 0501.030 (Fig. 2.5). Furthermore, Roman pottery (Fig. 2.8M), brick fragments, and charcoal indicate deposition during and after the Roman Era (lasting until ~1650 cal BP). The absence of older dates is interpreted as the result of channel reworking through time.

Facies Unit 9 (aeolian dunes)

The deposits of this unit consist of well-sorted medium-grained sand with low-angle cross-bedding (Table 2.1, Figs. 2.7 and 2.8N), which is interpreted as being deposited in an aeolian environment. The morphology, which consists of local hills rising up to 11 m above the surrounding plain, indicates deposition as dunes. The Morro da Serra dune is most likely the result of the man-made deviation of the Tagus channel during the 16th century and the associated rapid westward shift of the channel as described by Azevêdo (2001). The rapid lateral migration of the Tagus channel provided the source material for the dunes that were formed by northwesterly winds.

Radiocarbon dated charcoal in the Morro da Serra dune gives an age of 480-300 cal BP (GrA-30860), implying deposition during medieval times. The Cabeço da Bruxa dune was not radiocarbon dated, but because these deposits are located directly on top of FU-1A sandy terrace deposits with no floodbasin fines of FU-6B in between, an age older than FU-6B is assumed.

2.5 DISCUSSION

Valley-fill history

Late Pleistocene fluvial phase (Fig. 2.9A)

The progressive, stepwise lowering of RSL during the Late Pleistocene, reaching the lowest level of -120 m m.s.l. at around 20,000 cal BP (Waelbroeck *et al.*, 2002), caused deep incision in Tertiary and Pleistocene LTV deposits. The incised LTV passes to the Atlantic Ocean through a narrow (<2 km) and deep (~70 m) valley south of Lisbon (Fig. 2.1). The narrowness of the valley results from bedrock control (basalt at -70 m m.s.l.), ~200 m of Quaternary uplift

Figure 2.8 | Photographs of typical sediments for facies units in the Lower Tagus Valley. Ruler scale is in centimetres. A = high-gradient fluvial channel, B = brackish water marshes and tidal flats, C, D & E = intertidal and subtidal flats, F = shallow-marine prodelta, G = distributary mouth tidal bars with shells, H = condensed fluvial floodbasins, I = fluvial floodbasins, J = brackish water marshes and tidal flats eroded by Tagus fluvial channel, K = levee, L = Tagus fluvial channel in core GOL, M = Tagus fluvial channel in core 0501.012 with Roman amphora fragment, N = Morro da Serra aeolian dune.

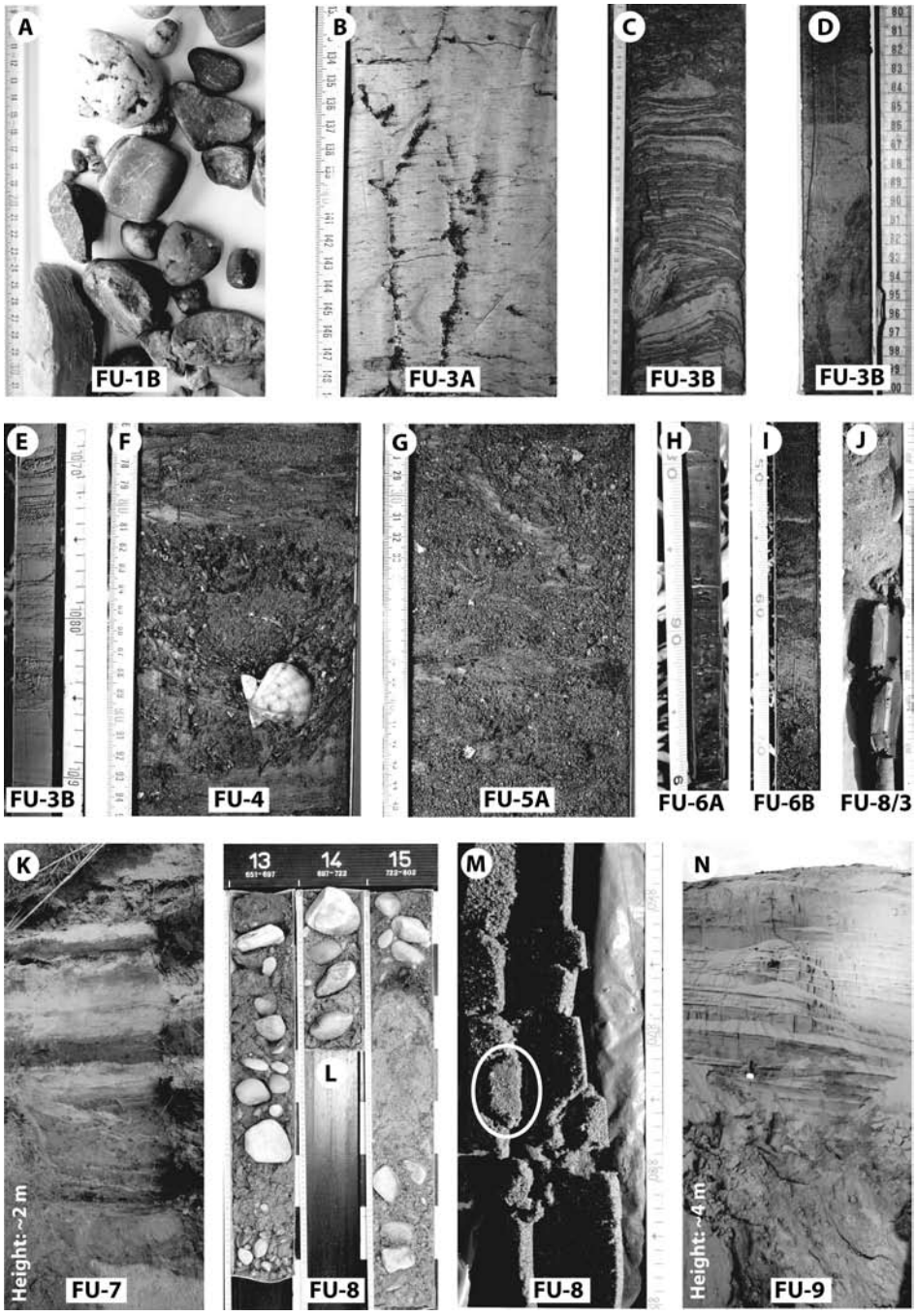
A
FU-1B
B
FU-3A
C
FU-3B
D
FU-3B
E
FU-3B
F
FU-4
G
FU-5A
H
FU-6A
I
FU-6B
J
FU-8/3
K
Height: ~2 m
FU-7
13
14
15
L
FU-8
M
FU-8
N
Height: ~4 m
FU-9

(Carta Geológica do Concelho de Lisboa, 1985; Cabral, 1995), and repeated fluvial incision during Pleistocene low RSL periods. The narrow valley and the Vale de Estoril and Cascais Canyon (Fig. 2.1) connected the LTV via a more or less undisturbed longitudinal river gradient across the 30 km narrow shelf to the continental slope and deep marine environment (Vanney and Mougenot, 1981). This connection led to a—in the Quaternary fluvial record—rarely observed efficient offshore sediment bypass (Blum and Törnqvist, 2000), causing optimal sediment discharge.

Incision and lateral erosion created a ~9 km wide valley near Azambuja where amalgamated braided channel belt deposits accumulated. The braided river was probably a sediment conveyor belt fluvial system, rather than an aggrading system, as testified by the relatively small thickness (10-15 m) and large width of FU-1B (BRISA, 2005).

After ~14,000 cal BP the braided river transformed into a single-channel river with fine-grained overbank sedimentation in the deepest incised axis of the lowstand valley (Figs. 2.6 and 2.9B, core VFX; FU-2). This change is interpreted as resulting from increased temperatures and precipitation after ~14,000 cal BP, causing a dramatic spread of woodland (Roucoux *et al.*, 2005), which led to less extreme discharge peaks and higher production of finer sediment. Around 12,000 cal BP, RSL had risen to about -60 m m.s.l. (Waelbroeck *et al.*, 2002) causing upstream migration of fluvial onlap coupled with a rise of the channel base elevation and floodplain surface (Blum and Törnqvist, 2000; Cohen, 2005). This resulted in the upstream migration of the long-profile crossover (cf. Blum and Törnqvist, 2000), causing fluvial sedimentation downstream of this point and incision upstream of the onlap point.

The large thickness (~12 m) of FU-2 is remarkable and unparalleled in Quaternary incised valleys. It may be related to the fast RSL fall from -90 to -120 m m.s.l. during the period 30,000-20,000 cal BP (Waelbroeck *et al.*, 2002) (Fig. 2.9A). Because the LTV was directly connected with the offshore region, the Tagus River responded immediately by strong incision along the valley axis, creating a narrow incised valley within the broad Late Pleistocene braided river floodplain (Fig. 2.9A, FU-1B). Rapid deglacial RSL rise subsequently drowned the incised valley, causing accumulation and preservation

Figure 2.9 | Schematic block diagrams illustrating the valley-fill history since the Late Pleistocene and a graph showing eustatic sea-level since 120,000 cal BP (Waelbroeck *et al.*, 2002). GOL/VFX = approximate locations of Golegã and Vila Franca de Xira respectively. (A) From 30,000-20,000 cal BP rapidly falling RSL caused local incision within the high-gradient Tagus braided river floodplain. (B) Around 7000 cal BP maximum transgression occurred and RSL had reached approximately the present-day level. Fluvial environments were pushed far inland and replaced by tidal and marine (prodelta) environments. (C) Around 4000 cal BP a fluvial wedge and bayhead delta prograded downstream across fluvial terraces and tidal deposits, progressively filling the central basin.

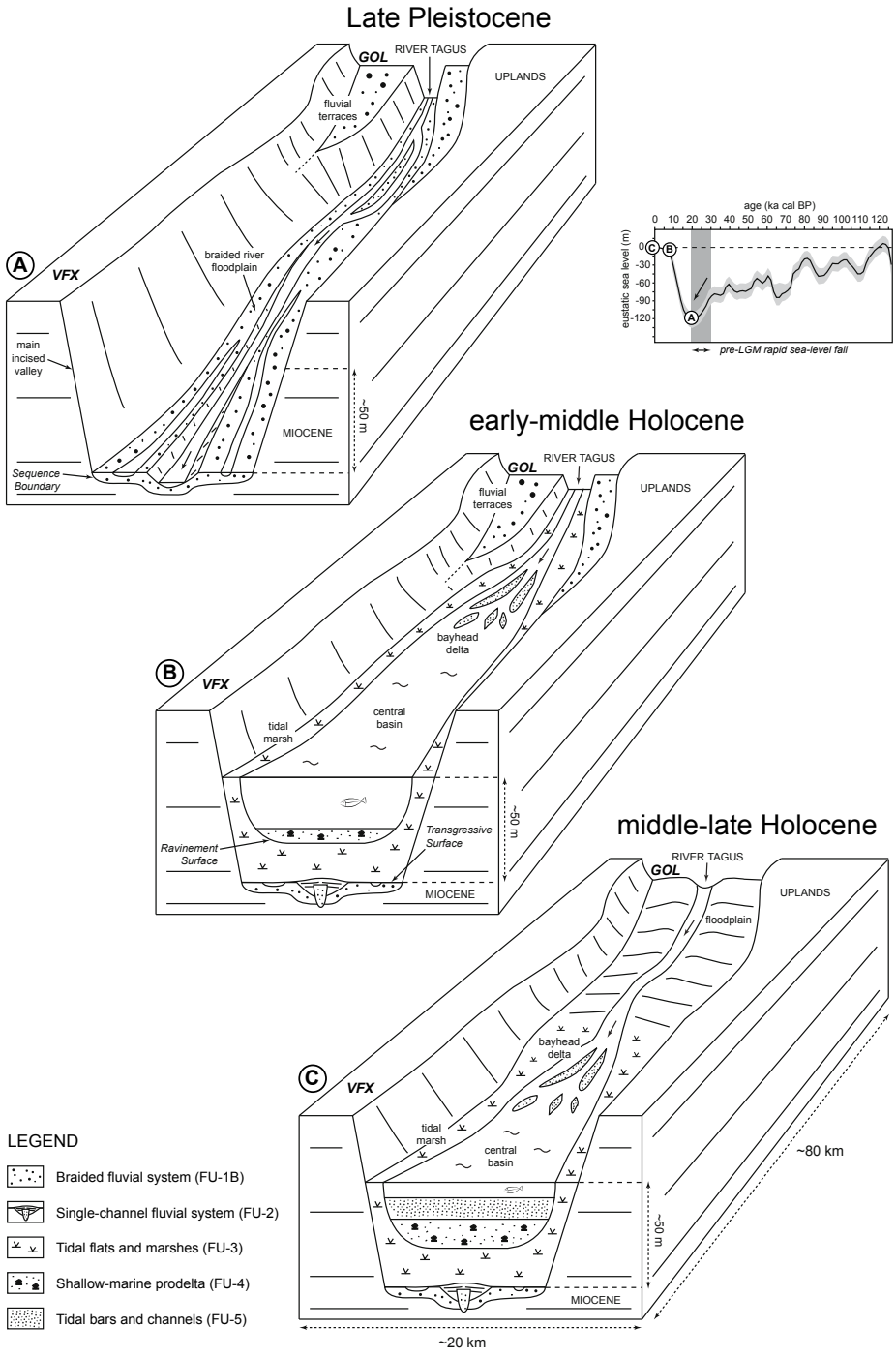
Late Pleistocene
GOL
RIVER TAGUS
UPLANDS
fluvial terraces
braided river floodplain
A
VFX
main incised valley
MIOCENE
Sequence Boundary
~50 m
age (ka cal BP)
0 10 20 30 40 50 60 70 80 90 100 110 120
eustatic sea level (m)
0
-30
-60
-90
-120
C
B
A
pre-LGM rapid sea-level fall
early-middle Holocene
GOL
RIVER TAGUS
UPLANDS
fluvial terraces
bayhead delta
B
VFX
tidal marsh
central basin
~50 m
Ravinement Surface
Transgressive Surface
MIOCENE
middle-late Holocene
RIVER TAGUS
GOL
UPLANDS
floodplain
bayhead delta
C
VFX
tidal marsh
central basin
~80 km
~50 m
MIOCENE
~20 km
LEGEND
Braided fluvial system (FU-1B)
Single-channel fluvial system (FU-2)
Tidal flats and marshes (FU-3)
Shallow-marine prodelta (FU-4)
Tidal bars and channels (FU-5)

of fine-grained lowstand deposits (FU-2). The higher elevated parts of the braided river floodplain were flooded later (see below), and brackish water marsh and tidal flat deposits (FU-3A) directly overly fluvial gravel (FU-1B), as illustrated by core 0501.016 (Figs. 2.6 and 2.9B).

Early to middle Holocene transgression (Fig. 2.9B)

Rapid RSL rise and fast upstream migration of the coastal onlap point pushed the fluvial system inland. The accommodation space could not be filled with freshwater deposits, and consequently LTV back-filling was dominated by mainly fine-grained brackish water marshes and tidal flats (FU-3A) (Figs. 2.6 and 2.9B). Back-filling started around 11,500 cal BP near Vila Franca de Xira, and had reached Santarém about 2500 years later (Figs. 2.1 and 2.6).

The deposits of the low brackish water marshes and tidal flats (FU-3A) are soft and rich in organics and pyrite (FeS_2), indicating formation around or below mean sea level, which limited pedogenesis. Similar deposits have been described on the Dutch coastal plain (Pons and Van Oosten, 1974; Van Staalduinen, 1979). Their large extent and sedimentary characteristics are most likely the result of rapid RSL rise, prohibiting silting-up of the low brackish water marshes and tidal flats to higher levels.

The tidal environments continuously migrated inland and reached the narrow valley near Golegã well before 7000 cal BP (Figs. 2.4 and 2.9B). The funnel shape of the valley probably promoted amplification of the tides and currents, similar to the Scheldt estuary in the Netherlands and Belgium (Van der Spek, 1997), resulting in intertidal and subtidal flats and tidal channels up to ~100 km inland (FU-3B and 5B).

Since 10,000 cal BP the environment represented by FU-3A was replaced by a transgressive open-marine environment near Vila Franca de Xira (Fig. 2.6; core VFX: -26 m m.s.l.; FU-4). When RSL rise had ended around 7000 cal BP (Boski *et al.*, 2002; Fernández-Salas *et al.*, 2003), a wide and deep marine basin was created (Fig. 2.9B). Simultaneously, north of Santarém pedogenesis started in the brackish water marshes (Fig. 2.6, core 0501.016; FU-3A), and near Benfica do Ribatejo the first distributary mouth tidal bars were formed (Fig. 2.6, core VAL; FU-5A), indicating the start of bayhead delta progradation into the central basin (Fig. 2.9B).

Middle to late Holocene regression and delta progradation (Fig. 2.9C)

The end of RSL rise around 7000 cal BP, and continued fluvial sediment input, resulted in the change from a transgressive to a regressive system with down-stream migration of the distributary mouth tidal bars (Fig. 2.5; FU-5A) and bayhead delta (FU-6/7/8). The prograding bayhead delta migrated southward over brackish water marshes, tidal channels, and flats into the shallowing cen-

tral basin (Fig. 2.9C). The regression resulted in considerable silting-up of the brackish water marshes (FU-3A) above mean high water (MHW) and diminishing tidal influence, which facilitated pedogenesis (Fig. 2.6; ripened soil).

The narrow tidal inlet south of Lisbon and the wide central basin efficiently dissipated the tidal energy by friction. This hampered inland transport of marine-sourced sediment and resulted in a muddy central basin (Fig. 2.3) into which the bayhead delta prograded. This means that regression was mainly upstream-controlled by sediment input from the hinterland. The upstream sediment source, the position of the tidal sand bars landward of the muddy central basin, and the relatively straight channels, imply a tide-dominated nature for the bayhead delta, comparable to the Gironde estuary (Allen, 1991; Dalrymple *et al.*, 1992). Simultaneously with downstream progradation, the Holocene onlap point migrated upstream into the small basins east of Arrepiado which currently have flat valley-fill topographies, a mechanism also discussed by Blum and Törnqvist (2000) and Cohen (2005).

Sequence-stratigraphic interpretation

The LTV comprises a classic example of a valley-fill succession with an incised lowstand fluvial system at its base, filled with a transgressive-regressive sediment wedge (type 1 depositional sequence (cf. Van Wagoner *et al.*, 1988; Emery and Myers, 1996)). The basal sequence boundary (SB) is expressed as an erosive contact at the base of the lowstand fluvial deposits overlying Tertiary deposits (Fig. 2.10). The facies units described above can be attributed to a fourth-order depositional sequence (0.01-0.5 Ma) deposited as a result of Late Pleistocene to Holocene eustatic sea-level changes. Due to a lacking upper bounding unconformity the sequence is not yet complete. The LTV sequence stratigraphy, consisting of a lowstand systems tract (LST), transgressive systems tract (TST), and highstand systems tract (HST), is illustrated in Fig. 2.10.

The LGM and Late Glacial fluvial units FU-1B and FU-2 (Fig. 2.6) correspond with the LST (cf. Posamentier and Allen, 1999) (Fig. 2.10). The large thickness of FU-2, and the LST in general, is remarkable since LST's are commonly condensed (e.g. Van Wagoner *et al.*, 1988; Allen and Posamentier, 1993). The narrow incised valley, related to the 30,000-20,000 cal BP RSL drop, within the broad lowstand braided river floodplain (FU-1B) and the rapid deglacial drowning of the incised valley, facilitated accumulation and *preservation* of fine-grained lowstand deposits. The limited extent of the deepest incision may explain the rarity of thick LST sequences observed in other late Quaternary incised valleys (e.g. Amorosi *et al.*, 1999; Dabrio *et al.*, 1999).

The top of FU-1B and FU-2 corresponds with the transgressive surface (TS) (Figs. 2.9B and 2.10), since it is overlain by tidal and marine deposits

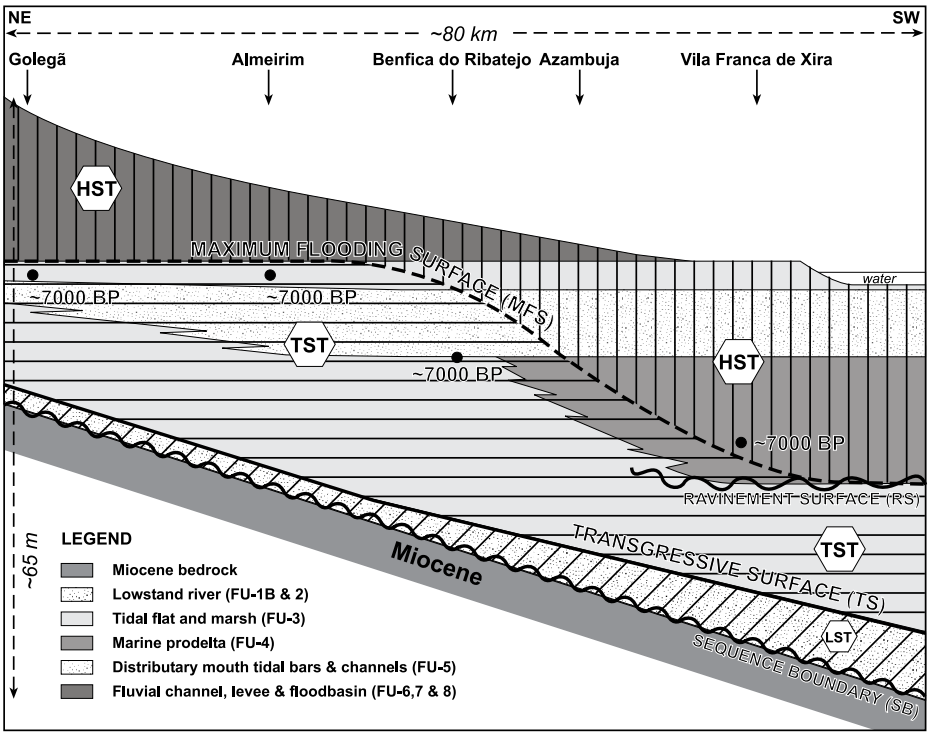

Figure 2.10 | Schematic representation of Lower Tagus Valley sequence stratigraphy. Note that the fine-grained upper part of the LST is present locally and thins northward, whereas the coarse-grained lower part is widely distributed.

of FU-3 and basal parts of FU-4 and 5. These deposits form a large landward thinning sediment wedge, belonging to the TST (Fig. 2.10). This systems tract indicates drowning of the system, since the rate of accommodation space creation by RSL rise outpaced sediment supply. In the south, a diachronous ravinement surface (RS) lies at the top of the TST (Figs. 2.9C and 2.10), and becomes younger in age moving landwards. It is marked by the abrupt shift of tidal flat and marsh environments (FU-3) to fully marine conditions (FU-4). Landward of the maximum marine transgression, tidally influenced channels and bars (FU-5), and extensive tidal flat and marsh environments (FU-3), persisted during the entire TST sequence (Fig. 2.10). More seaward of the maximum transgression, these tidal flat and marsh deposits were partly removed by incision of the RS. No fluvial environments were encountered in the TST. This results from the deeply incised, high-gradient Late Pleistocene valley and rapid RSL rise which pushed the fluvial system far inland.

The maximum flooding surface (MFS) represents the top of the TST (Fig. 2.10) and reflects the point when the rate of accommodation-space creation decreased and just matched sediment supply. In the study area, the MFS represents a line of subaerial and subaqueous "palaeo topography" around

7000 cal BP (the time of maximum marine transgression) making it difficult to locate solely based on sedimentary characteristics. Therefore, its location is mainly based on radiocarbon chronology (Fig. 2.10). Around 7000 cal BP, tidal environments (FU-3 and FU-5B) had reached the upstream valley near Golegã, distributary mouth tidal bars and channels (FU-5) formed near Benfica do Ribatejo, and the infilling of the marine basin with prodelta sediments (FU-4) started near Vila Franca de Xira (Fig. 2.6).

The landward part of the MFS is represented by strong pedogenesis around +2 m m.s.l. in the top of the tidal flat and marsh deposits (Fig. 2.10). The pedogenesis results from silting to a high level during relatively constant RSL when the prograding fluvial wedge had not yet formed, thus representing the turnover from transgressive to regressive conditions.

The final phase of the sequence is the HST (Fig. 2.10), formed since ~7000 cal BP by an aggrading and prograding bayhead delta (FU-6/7/8) and distributary mouth tidal bars, channels, and prodelta deposits (FU-4 and 5) which were pushed basinward. The absence of marine sand in the HST (FU-4) can be attributed to the specific morphology of the LTV. The valley has always been sheltered against the high-energy wave regime on the Atlantic Ocean by the narrow inlet south of Lisbon (Fig. 2.1). Thus, waves have played a very minor role in the LTV infill history. Marine sand entering the LTV did not migrate far upstream because the wide muddy central basin east of Lisbon efficiently dissipated tidal energy by friction (Fig. 2.3).

2.6 CONCLUSIONS

The Lower Tagus Valley sedimentary record covers the period since ~20,000 cal BP and consists of up to ~50 m of fluvial, tidal, and marine deposits. The valley-fill history was strongly dominated by RSL control and sediment supply. The sedimentary succession provides a classic sequence-stratigraphic example with a remarkably well developed and preserved lowstand systems tract (LST). The thick LST probably resulted from local deep incision within the broad fluvial plain during the period 30,000-20,000 cal BP, when RSL dropped to -120 m. Lowstand deposits were preserved due to subsequent rapid RSL rise and transgression, preventing marine erosion. The top of the lowstand fluvial system is marked by the transgressive surface covered by tidal marsh and mudflat deposits.

The transgressive systems tract (TST) is represented by deposits from the early to middle Holocene transgression. Extensive marshes and a large estuarine-marine central basin were formed in the drowned Lower Tagus Valley. The abrupt shift of tidal flat and marsh environments to fully marine

conditions marks the diachronous ravinement surface. The maximum flooding surface was formed around 7000 cal BP.

The middle to late Holocene regression formed the highstand systems tract (HST). Rapid progradation of the bayhead delta occurred and the muddy central basin was filled since ~7000 cal BP. A constant RSL and continuous fluvial sediment supply caused formation of a fluvial sediment wedge. The regression was mainly upstream-controlled, while the tidal energy was dissipated quickly in the narrow tidal inlet and wide central basin.

This study shows that the late Quaternary evolution of the Lower Tagus Valley is determined by a narrow continental shelf and deep glacial incision, rapid post-glacial RSL rise, a wave-protected setting, and large fluvial sediment supply. This makes the Lower Tagus Valley a unique sedimentary archive which provides detailed understanding of the development and preservation of lowstand systems tracts. Furthermore, it can act as a key for recognising lowstand systems tracts in the geological record.

CHAPTER 3

Because of the deep glacial incision, the Lower Tagus Valley hosts a sedimentary record since ~20,000 cal BP, making this a unique site along the European Atlantic margin with respect to palaeogeographic and sea-level changes. Based on nine cross sections and 55 radiocarbon dates together with a newly created relative sea-level curve, we constructed five palaeogeographic maps of the infill of the Lower Tagus Valley since ~20,000 cal BP. We illustrate that relative sea-level rise and fluvial sediment supply were the prime forcing factors determining the depositional history and palaeogeographic changes. Around 20,000 cal BP a deeply incised braided river existed, which was directly connected to the ocean across the narrow continental shelf. After that (~12,000 cal BP) the gradually moister and warmer climate caused a change to a single-channel river. During the following period (12,000-7000 cal BP) relative sea-level rise resulted in a transgression in the Lower Tagus Valley and the establishment of extensive tidal environments. After relative sea-level rise had ended (~7000 cal BP) the valley was progressively filled by a fluvial wedge and tidally influenced bayhead delta. Since ~1000 cal BP the valley-fill history was dominated by increased sediment input due to human-induced degradation of catchment slopes. Generally, climate was of subordinate importance during the entire studied period, merely causing a single-channel river resulting from the change from the cold Heinrich event 1 to the temperate Bölling-Allerød interstadial. Despite the tectonic activity in the region, neotectonic uplift or subsidence were limited, as supported by the horizontal relative sea-level curve since ~7000 cal BP. Neotectonics played a minor role due to the large distance from the Fennoscandian ice sheet and the narrow continental shelf, which prohibited strong glacio- and hydro-isostatic movements.

Late Pleistocene and Holocene palaeogeography of the Lower Tagus Valley (Portugal): effects of relative sea level, valley morphology and sediment supply

Based on: Vis, G.-J., Kasse, C. and Vandenberghe, J., Late Pleistocene and Holocene palaeogeography of the Lower Tagus Valley (Portugal): effects of relative sea level, valley morphology and sediment supply. *Quaternary Science Reviews* (2008), **doi:** 10.1016/j.quascirev.2008.07.003 (http://www.sciencedirect.com/science/journal/00370738)

Photo: coring of Tagus sediments by Sebastian Wilhelm and Thomas Wiatr (Benfica do Ribatejo).

3.1 INTRODUCTION

Incised-valley fills in various settings around the globe and with different complexities have been studied intensively (e.g. Allen, 1990; Allen and Posamentier, 1993; Dalrymple *et al.*, 1994; Dalrymple and Zaitlin, 1994; Zaitlin *et al.*, 1994; Lesueur *et al.*, 2003). Moreover, long-term Quaternary fluvial records of major European river systems have been studied in detail (e.g. Van den Berg, 1996; Antoine, 1997; Bridgland *et al.*, 2001; Amorosi *et al.*, 2004). However, detailed postglacial palaeogeographic reconstructions of fluvial systems in an

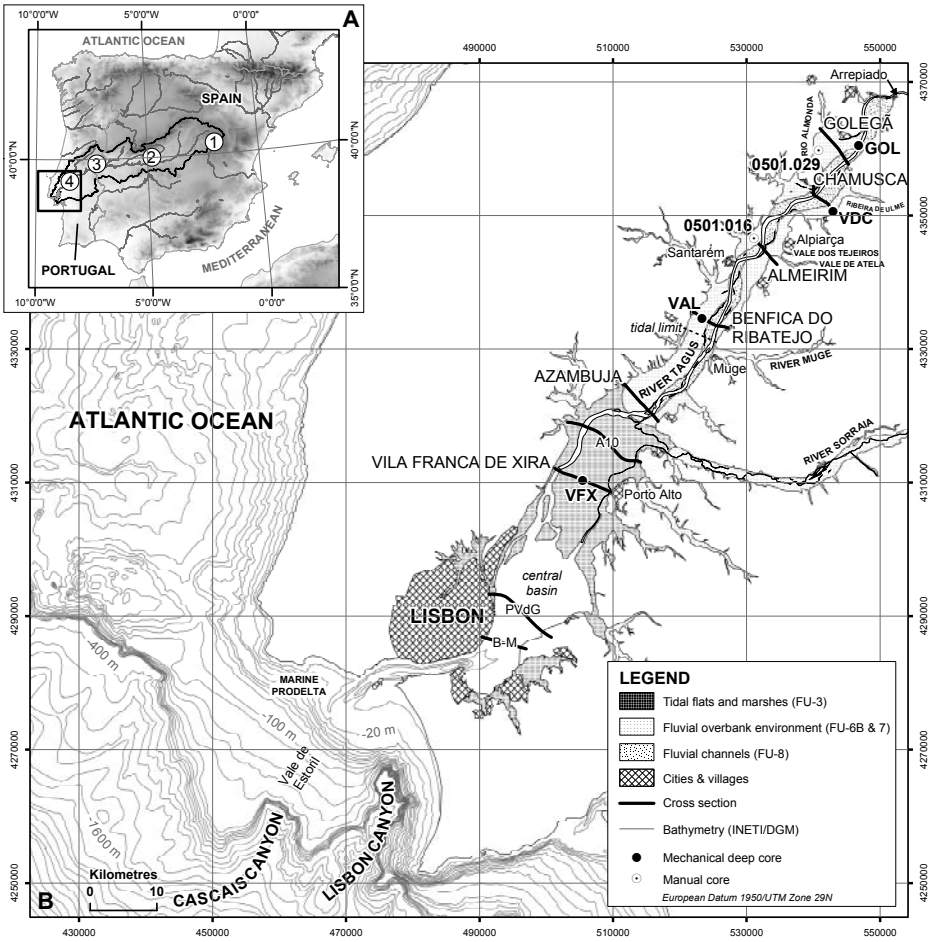

Figure 3.1 | Location map of the Lower Tagus Valley. The inset map (A) shows the Tagus catchment and study area on the Iberian Peninsula, Digital Elevation Data from Jarvis *et al.* (2006). 1: Mesozoic Spanish Cordillera; 2: Spanish Tertiary Sedimentary Tagus Basin; 3: Palaeozoic Hesperian Massif; 4: Lower Tagus Basin (LTB). The main map (B) shows the location of the cross sections and cores. A10: A10 bridge, geotechnical data (BRISA, 2005); PVdG: Ponte Vasco da Gama bridge, geotechnical data (LUSOPONTE, 1995); B-M: Beato-Montijo bridge, geotechnical data (De Mendonça, 1933).

incised setting are scarce. An example of a detailed palaeogeographic reconstruction is provided by the Rhine-Meuse delta in The Netherlands (Weerts and Berendsen, 1995; Berendsen and Stouthamer, 2000; Busschers *et al.*, 2007). The extensive continental shelf buffered sea-level fall-induced incision during the Late Pleistocene period, resulting in a relatively low-gradient glacial lowstand surface (~24 cm/km) underneath the Holocene Rhine-Meuse delta (Berendsen and Stouthamer, 2001). Consequently, marine inundation as a result of late Quaternary sea-level rise only started after ~9000 cal BP and the sediment sequences of the previous phases are possibly preserved in present-day offshore regions.

To better understand the palaeogeographic evolution of incised-valley fills during the Late Glacial (14,700-11,500 cal BP) and Holocene periods, locations with a large terrestrial accommodation space are needed. Narrow continental shelves facilitated rapid headward erosion and incised valley formation during sea-level fall and lowstand. Such conditions occurred along the Atlantic west coast of Europe, south of Bordeaux. However, most rivers along this coast have relatively small catchments and low sediment discharges resulting—in combination with narrow valleys—in the development of estuaries (Borrego *et al.*, 1995; Rodríguez-Ramírez *et al.*, 1996; Borrego *et al.*, 1999; Dabrio *et al.*, 2000; Psuty and Moreira, 2000; Boski *et al.*, 2002; Bao *et al.*, 2007; Naughton *et al.*, 2007a).

On the Iberian Peninsula, the palaeogeographic evolution has been studied for the Odiel, Tinto and Guadalete rivers in south Spain (Borrego *et al.*, 1999; Dabrio *et al.*, 2000) and the Muge and Douro rivers in middle and north Portugal (Naughton *et al.*, 2007a; Van der Schriek *et al.*, 2007b). In the Guadalete valley the Late Pleistocene lowstand surface was found at a maximum depth of 30-35 m (Dabrio *et al.*, 2000). As a result, the Guadalete sedimentary sequence starts around 10,500 cal BP with muddy tidal deposits on top of fluvial sand and gravel. In the Douro valley, the sedimentary sequence starts at about 10,720 cal BP at -13.9 m m.s.l. (Naughton *et al.*, 2007a), which is too shallow regarding the concurrent sea level of -30 m (Toscano and Macintyre, 2003), and a sediment hiatus is assumed.

The Lower Tagus Valley in Portugal, has an exceptionally long sedimentary record since ~14,000 cal BP (Chapter 2). The steep gradient of the lowstand fluvial system (~60 cm/km) at the base of the valley-fill favoured early transgression and good preservation of early Holocene sediments. The facies distribution demonstrates that fluvial aggradation started shortly after 14,000 cal BP, followed by brackish water marsh and tidal flat sedimentation since ~11,500 cal BP. During the middle and late Holocene, drowning of the incised valley ended due to the deceleration of relative sea-level rise and a system with a bayhead delta, deep central basin and narrow tidal inlet originated.

The well-established chronology for the Lower Tagus Valley is based on 55 radiocarbon dates. Such a continuous sedimentary record since the Late Glacial period is unprecedented in Europe. Furthermore, the Tagus catchment is the tenth largest river system in Europe. Because of the large sediment discharge and the minor effect of waves, the 100 km long and 10 km wide Lower Tagus Valley has been filled with fluvial and tidal deposits. During the last millennia of the Holocene, sediment input was at least partly influenced by human activities like deforestation in the catchment (e.g. Van Leeuwaarden and Janssen, 1985; Van der Knaap and Van Leeuwen, 1995; Benito *et al.*, 2003c).

This chapter aims to reconstruct the palaeogeography of the Lower Tagus Valley covering the period since ~20,000 cal BP. Nine valley cross sections and a sea-level curve for the study area were constructed. The palaeogeography of the Lower Tagus Valley will be presented in five palaeogeographic maps. The Lower Tagus Valley sedimentary record hosts a unique archive of the effect of sea-level rise, fluvial dynamics and human impact. The importance of the forcing factors on the infill of the palaeo-valley and on the spatial and temporal changes of the sedimentary environments will be evaluated.

Regional setting

The Tagus River has a length of ~1000 km and a catchment area of 80,630 km^2 (Bettencourt and Ramos, 2003; Le Pera and Arribas, 2004). It enters the Atlantic Ocean near Lisbon in a passive continental margin setting with a narrow continental shelf (<30 km) (Fig. 3.1). The average discharge near its mouth is 400 m^3/s, but the river is characterised by extreme seasonal and annual variability with peak discharges more than 30 times the average discharge (Benito *et al.*, 2003b; Bettencourt and Ramos, 2003). The present-day Lower Tagus floodplain (Fig. 3.1) is 5-10 km wide and ~85 km long, has an elevation of ~22 m near Golegã in the north and ~2 m near Vila Franca de Xira in the south, with an average gradient of ~24 cm/km.

The central basin south of Vila Franca de Xira (Fig. 3.1) is characterised by an ebb-dominated semi-diurnal mesotidal regime with a mean tidal amplitude of 1.5 m at neap tide and 4 m at spring tide (Portela and Neves, 1994; Bettencourt and Ramos, 2003). Changes in tidal amplitude and energy during the Holocene are unknown. However, the narrow bedrock-constrained tidal inlet provides a morphologically unique situation, where the Lower Tagus Valley is sheltered against the high-energy wave regime on the Atlantic Ocean where winter wave heights up to 10 m can occur (Instituto Hidrográfico, Portugal). Therefore waves play a very minor role within the central basin (Fortunato *et al.*, 1999) and tides and fluvial discharge are the dominant energy suppliers.

Geology, tectonics and geomorphology

The Tagus originates at an elevation of about 1600 m in eastern Spain (Fig. 3.1) and flows westwards to the NNE-SSW oriented Lower Tagus Basin (LTB). This basin forms part of the Lusitanian Basin, which is an inverted Mesozoic trough, resulting from aborted Triassic rifting (Masson and Miles, 1984; Rasmussen *et al.*, 1998; Carvalho *et al.*, 2005). Inversion tectonics during the Tertiary resulted in the formation of a compressional foredeep—the Lower Tagus Basin—in which up to 2000 m of sediment accumulated (Barbosa, 1995; Rasmussen *et al.*, 1998). Despite the work on the location and activity of faults in the Lower Tagus Valley (e.g. Cabral and Ribeiro, 1989; Barbosa, 1995; Rasmussen *et al.*, 1998; Curtis, 1999; Vilanova and Fonseca, 2004), their presence and activity remain subject of debate, especially the ones along and underneath the Holocene valley-fill sediments (e.g. Fonseca *et al.*, 2000; Cabral, 2001; Fonseca and Vilanova, 2001). However, the region is tectonically active, as illustrated by a large earthquake in 1531, the well-known 1755 earthquake and tsunami and the 1909 Lisbon region earthquake (Chester, 2001).

Since the Pliocene-Early Pleistocene the Tertiary deposits were uplifted to the present maximum elevation of ~200 m above sea level and presently continue to be uplifted at 0.05-0.10 mm/y (Cabral, 1995). The uplift resulted in a staircase of Pleistocene fluvial terraces which are mainly located east of the river up to ~100 m above the Holocene floodplain. For an overview of the published work on the Pleistocene terraces, the reader is referred to Van der Schriek *et al.* (2007a).

3.2 METHODS

Core data

To understand the distribution of facies units in the Lower Tagus Valley, six cross sections perpendicular to the valley axis were designed. The cross sections cover the entire present-day floodplain (Fig. 3.1) like it has been mapped on the Carta Geológica de Portugal (1:50.000). Corings were spaced on average 300 m (Figs. 3.2, 3.3, 3.4 and 3.5), 500 m (Fig. 3.6) and 1000 m apart (Fig. 3.7) and their location was measured using a Garmin GPS-12 receiver (horizontal resolution ~5 m). The elevation of the corings relative to sea level was measured using Trimble DGPS equipment (vertical resolution ~5 mm). A set of 122 hand-corings (maximum depth 23 m) were used for this study, together with 4 mechanical deep corings. The hand corings were done using Edelman augers for sediment above the groundwater table and the gauge and the Van der Staay suction-corer for sediment below the groundwater table (Van de

Meene *et al.*, 1979). The sediments were described in the field following the method explained in Berendsen and Stouthamer (2001). For this paper, lithological classifications were converted to USDA terminology.

Four mechanical deep corings provide undisturbed cores to a maximum depth of 52 m. They were carried out with a rotary drilling rig and protected by steel casing. Recovery ranged from 20 % to 100 % with poorest recovery in sand and best recovery in clay sediments. In addition, lithological and sedimentological information resulting from cone penetration tests and continuous and discontinuous geological cores used for geotechnical studies for the construction of bridges, dikes and buildings were used to construct three cross sections in the south (Figs. 3.1 and 3.8) (De Mendonça, 1933; LUSOPONTE, 1995; BRISA, 2005; INETI, 2007).

Sample treatment

Grainsize was measured using a Fritsch A22 Laser Particle Sizer which resulted in grainsize distributions in the range of 0.15-2000 μm. Prior to grainsize measurement, the samples were prepared following the methods described by Konert and Vandenberghe (1997). About 1-2 g of bulk sediment was pre-treated with H_2O_2 and HCl to remove organic matter and carbonates, respectively.

Radiocarbon and archaeological dating

A set of 55 radiocarbon dates were used to construct the chronological framework. The material for radiocarbon dating consisted as much as possible of terrestrial botanical macrofossils that were manually selected from generally 1 cm thick sediment slices, otherwise bulk samples were used. Most botanical macro remains were most likely not in-situ, but because they were of good quality they were probably not transported very far. The radiocarbon ages were calibrated using the program OxCal v3.10 (Bronk Ramsey, 1995, 2001, 2005) using the atmospheric data from Reimer *et al.* (2004). The 14C age of fragments of a *Scrobicularia plana* shell from Van der Schriek *et al.* (2007b) was calibrated using the program CALIB v5.0 (Stuiver and Reimer, 1993; Stuiver *et al.*, 2005) and the Marine04 age calibration data from Hughen *et al.* (2004). For the marine samples, a Delta R of 262 years with a standard deviation of 164 years was used. All mentioned radiocarbon dates are expressed as calibrated calendar ages (cal BP) with age spans at the 2σ range (Table 3.1).

Palaeogeographic reconstruction

The palaeogeographic reconstruction of the Lower Tagus Valley since the Late Pleistocene sea-level lowstand is based on the spatial and temporal changes of various sedimentary environments in nine cross sections. The sedimentary

environments were defined using facies units (FU) which were identified using lithological and sedimentological data, combined with floral (pollen, terrestrial botanical macro remains, diatoms) and faunal (shells, foraminifera, dinoflagellates) indicators (Table 3.2) (Chapter 2). The three-dimensional distribution and configuration of facies units was established using a fence diagram (Fig. 3.8). The chronology of environmental change is based on 55 radiocarbon dates and archaeological artefacts presented in this study (Tables 3.1 and 3.3) and radiocarbon dates published by Van Leeuwaarden and Janssen (1985), Ramos *et al.* (2002), Ramos Pereira *et al.* (2002), Azevêdo *et al.* (2006a) and Van der Schriek *et al.* (2007b). Furthermore, published archaeological and historical data were used (Kalb and Höck, 1979; Delgado, 1981; Kalb and Höck, 1984; Freire, 1985; Carvalho and Almeida, 1996; Azevêdo, 2001; Van der Schriek *et al.*, 2007b). The sea-level reconstructions by Hanebuth *et al.* (2000) for the period before ~11,500 cal BP and the one presented in this study (Fig. 3.9B) for the period after ~11,500 cal BP, were used to reconstruct palaeowater depths and coastlines. Based on the data described above and general concepts on the behaviour of deltas, estuaries and coasts (e.g. Reading, 1998; Bridge, 2003), the palaeogeography per time interval was reconstructed. The time intervals were chosen according to data availability and major changes in valley-fill history. The palaeogeographic maps were drawn using ArcGIS 9.2 software.

3.3 RESULTS

Geometry and chronology of the facies units

For the description of the facies units (FU) see Table 3.2 and Fig. 3.8 for the general geometry. *Addendum 1* contains full-colour versions of the cross sections.

FU-1A

The poorly sorted, mainly coarse-grained sand and gravel of FU-1A, indicate deposition in a high-energy environment. Due to the absence of a fining-upward sequence in the top of FU-1A and the flat surface morphology, these terrace sediments are interpreted as deposited as sand and gravel bars in channels of a fluvial braided system. The terraces were mainly found along the eastern margin of the valley; north of Alpiarça they are present at the western side.

FU-1B

At the base of most cross sections, poorly sorted, coarse-grained gravely sand was found in short fining-upward sequences (FU-1B) overlying Miocene

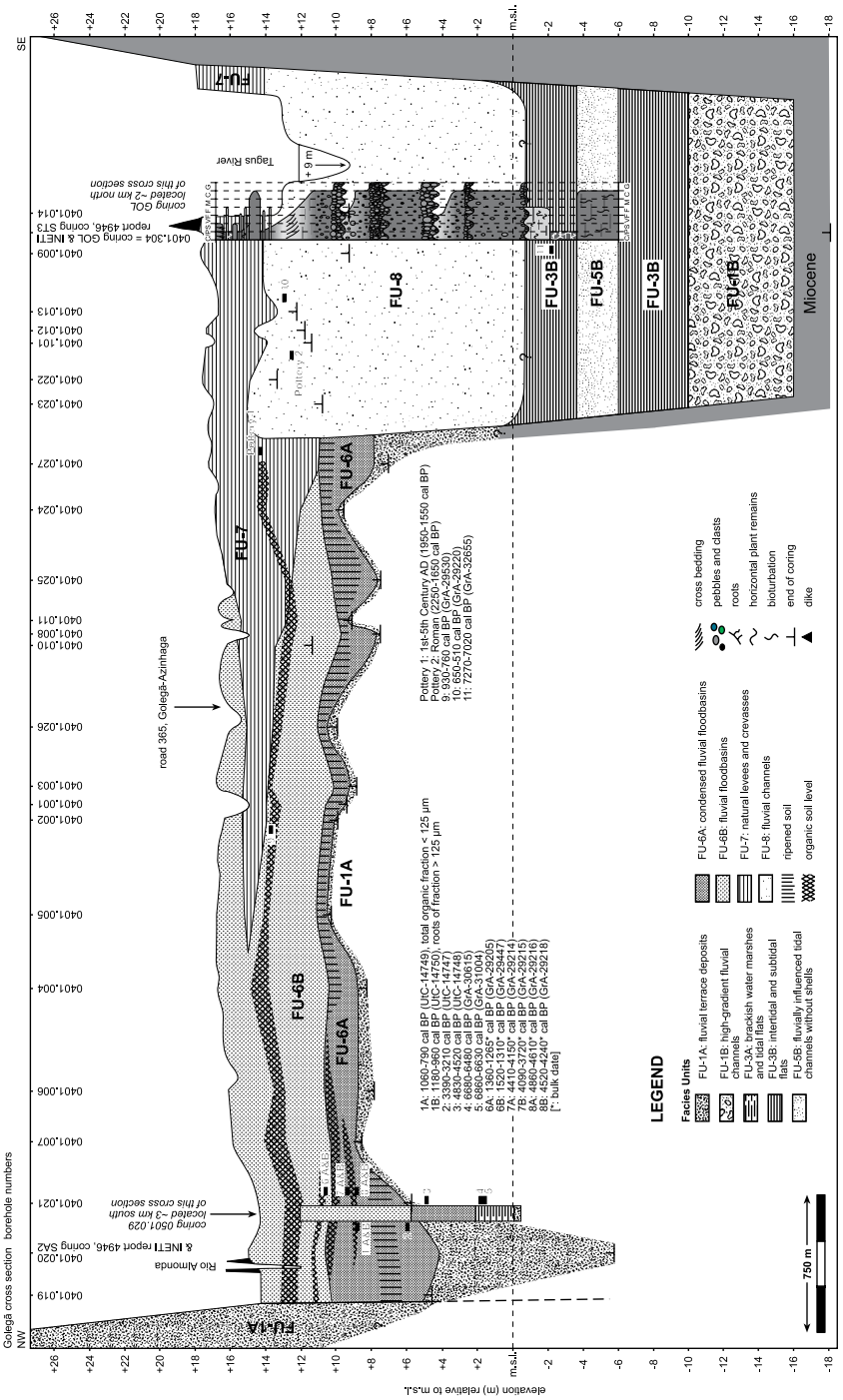

Figure 3.2 | Golegã cross section. Lithology and distribution of facies units are based on manual corings and mechanical corings GOL and SA2 and ST3 (INETI, 2007). Coring GOL was projected from its original location east of Golegã (Fig. 3.1). Lithology: C/P: clay or peat; S: silt; VF: very fine sand; F: fine sand; M: medium sand; C: coarse sand and G: gravel. A full-colour version of this cross section can be found in *Addendum 1*.

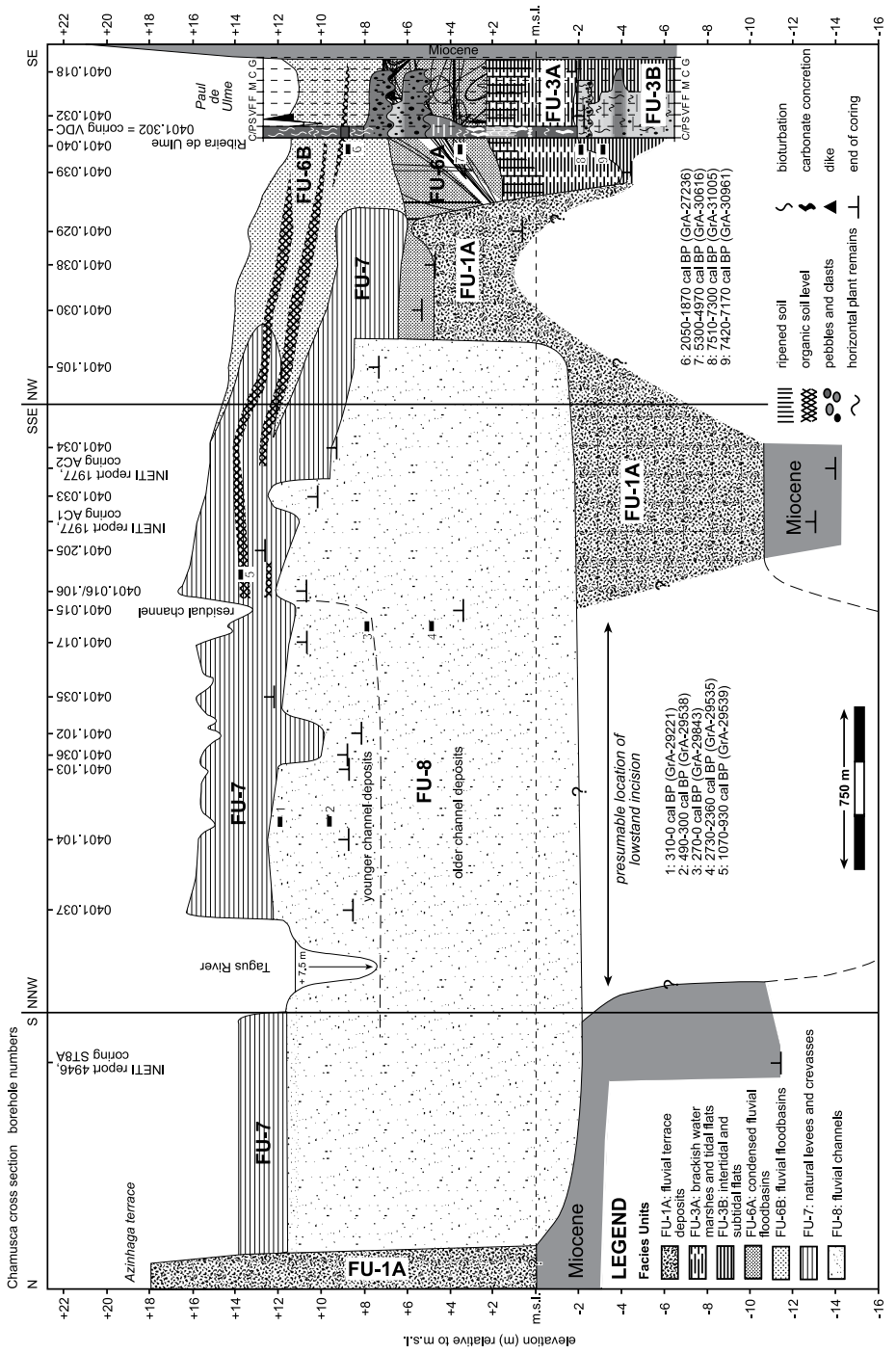

Figure 3.3 | Chamusca cross section. Lithology and distribution of facies units are based on manual corings and mechanical corings VDC, ST8A, AC1 and AC2 (INETI, 2007). Lithology: C/P: clay or peat; S: silt; VF: very fine sand; F: fine sand; M: medium sand; C: coarse sand and G: gravel. Coring 0401.204 with date GrA-27236, is located approximately at site 0401.302 but was not plotted here. A full-colour version of this cross section can be found in *Addendum 1*.

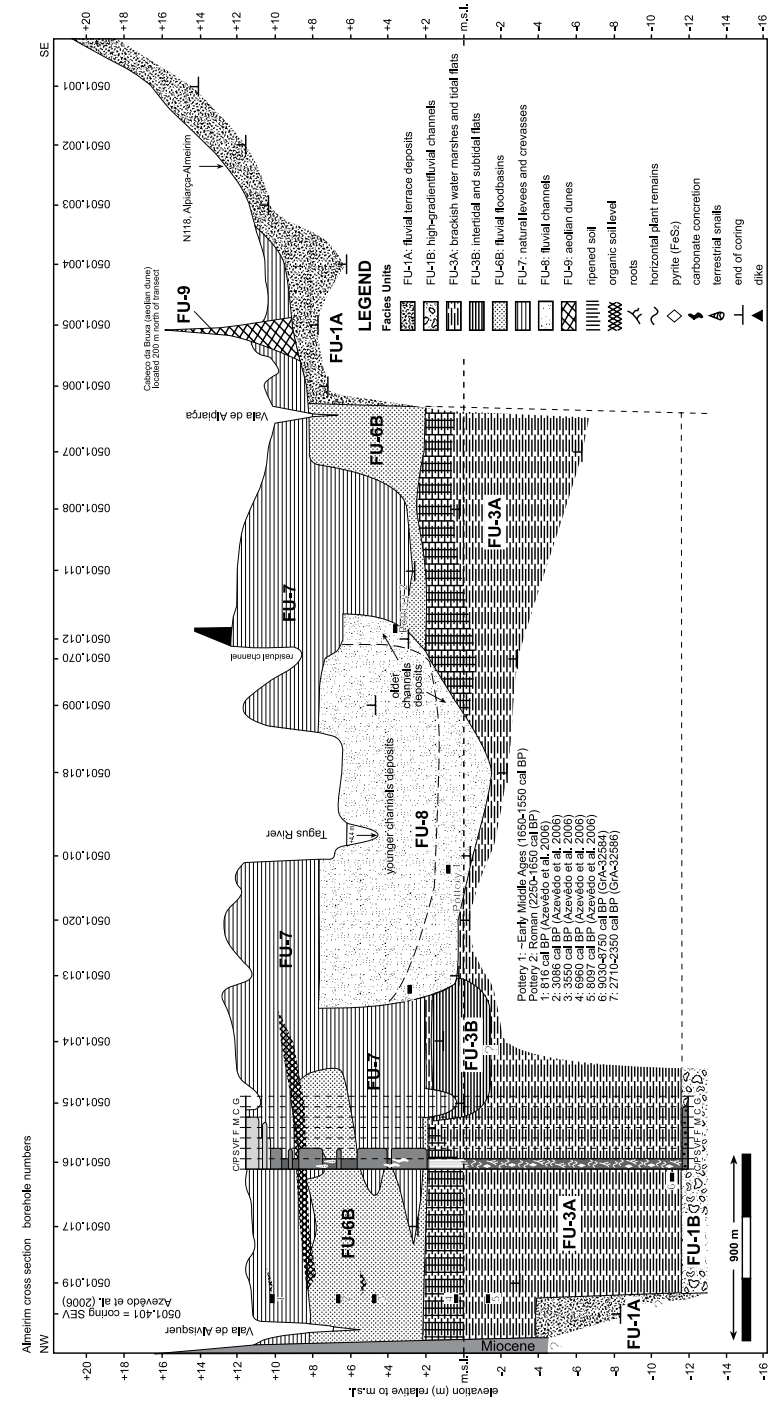

Figure 3.4 | Almeirim cross section. Lithology and distribution of facies units are based on manual corings and mechanical coring SEV (Azevêdo *et al.*, 2006a). Lithology: C/P: clay or peat; S: silt; VF: very fine sand; F: fine sand; M: medium sand; C: coarse sand and G: gravel. On aeolian dune "Cabeço da Bruxa" traces of Late Bronze age (~2700 cal BP) graves were found (Kalb and Höck, 1979). A full-colour version of this cross section can be found in *Addendum 1*.

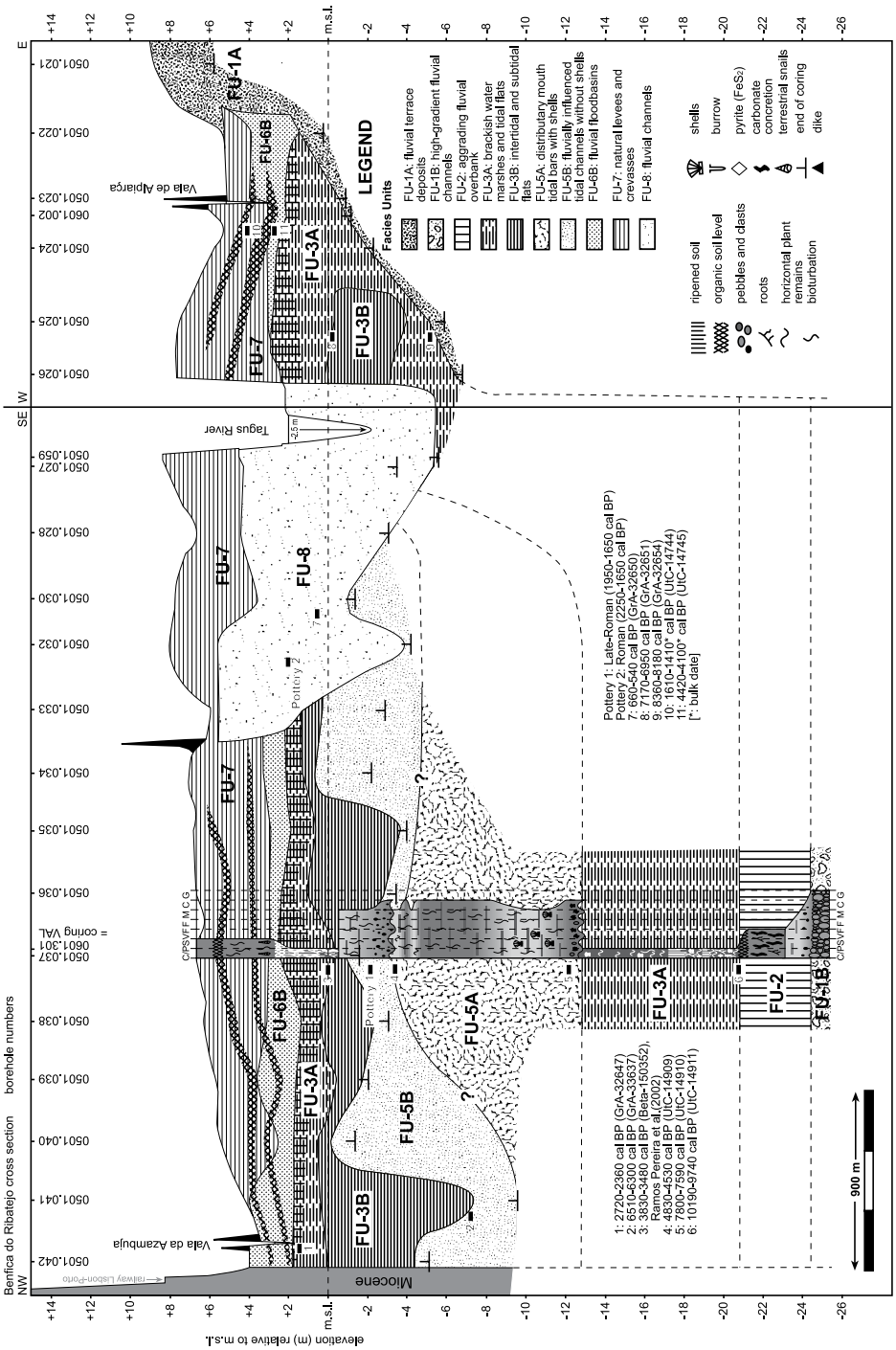

Figure 3.5 | Benfica do Ribatejo cross section. Lithology and distribution of facies units are based on manual corings and mechanical coring VAL. Lithology: C/P: clay or peat; S: silt; VF: very fine sand; F: fine sand; M: medium sand; C: coarse sand and G: gravel. A full-colour version of this cross section can be found in *Addendum 1*.

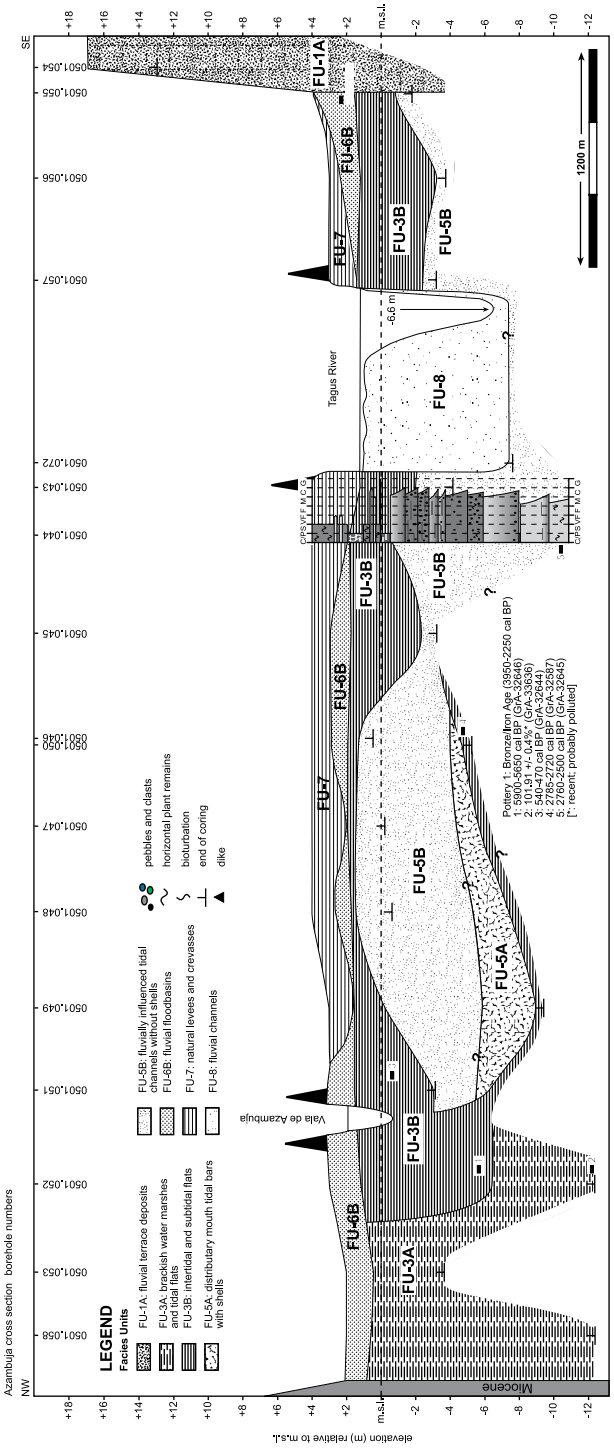

Figure 3.6 | Azambuja cross section. Lithology and distribution of facies units are based on manual corings. Lithology: C/P: clay or peat; S: silt; VF: very fine sand; F: fine sand; M: medium sand; C: coarse sand and G: gravel. A full-colour version of this cross section can be found in *Addendum 1*.

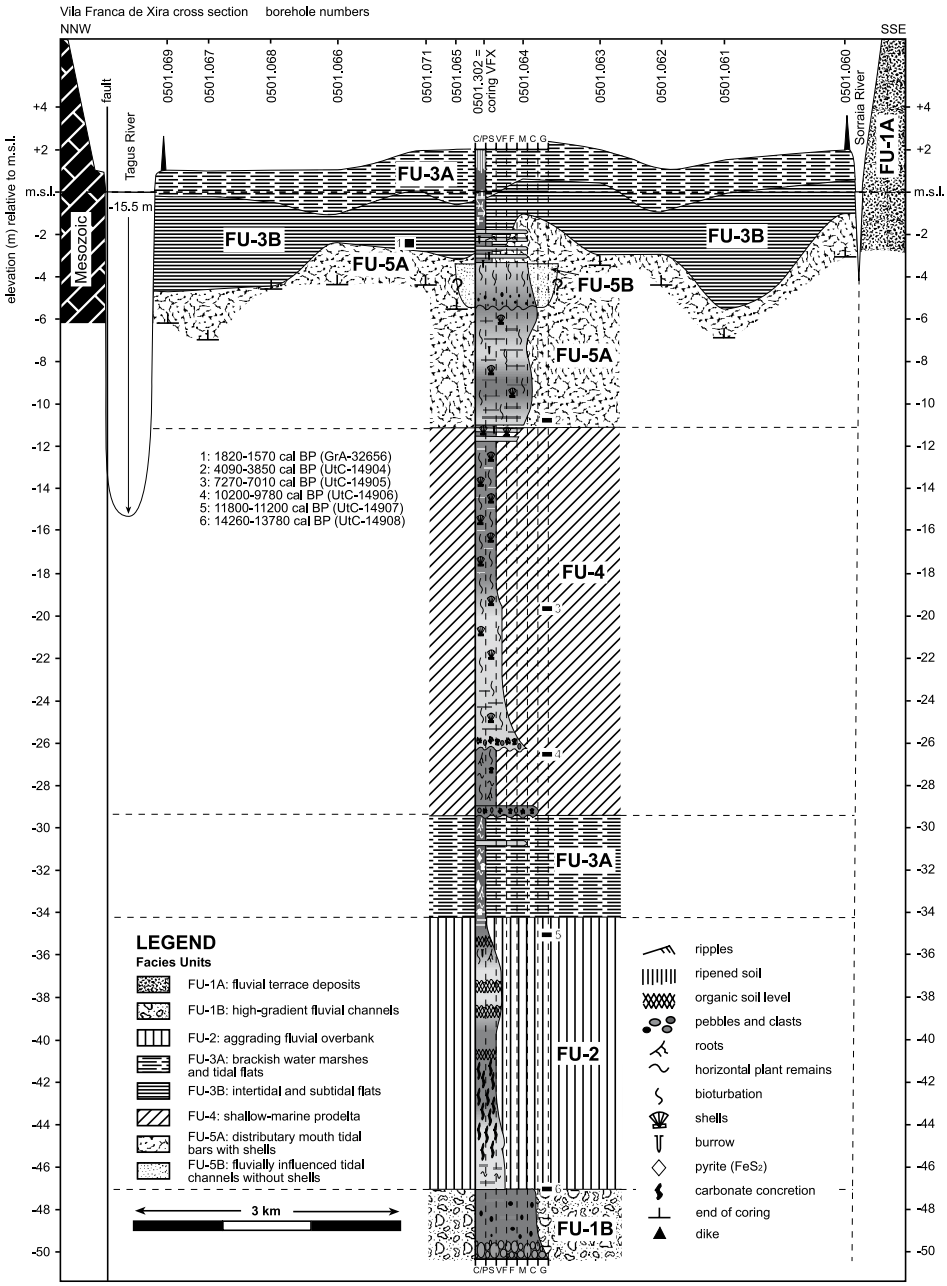

Figure 3.7 | Vila Franca de Xira cross section. Lithology and distribution of facies units are based on manual corings and mechanical coring VFX. Lithology: C/P: clay or peat; S: silt; VF: very fine sand; F: fine sand; M: medium sand; C: coarse sand and G: gravel. A full-colour version of this cross section can be found in *Addendum 1*.

Table 3.1 | Radiocarbon dates from the Lower Tagus Valley fill. Coordinates in European Datum 1950/UTM Zone 29N.

Lab. Nr.	Figure	14C age yrs BP ± 1σ	Age cal. BP 2σ	Coordinates (x-y/z) (m)	Sample depth (cm)	Borehole nr.	Material	Significance	14C type	Remarks
GrA-27234	3.10	5530 ± 45	6410-6210	531.812-4342.025/+8	740-741	0401.203	peat	GW-level	bulk AMS	-
GrA-27236	3.3	2005 ± 35	2050-1870	543.112-4350.825/+9	300-310	0401.204	peat/bark	res. channel	AMS	-
GrA-29205	3.2	1390 ± 35	1360-1265	541.501-4362.494/+14.3	366-370	0401.021	humic clay	start sed.	AMS	caustic extract
GrA-29214	3.2	3850 ± 40	4410-4150	541.501-4362.494/+14.3	506-508	0401.021	humic clay	end sed.	AMS	caustic extract
GrA-29215	3.2	3610 ± 60	4090-3720	541.501-4362.494/+14.3	506-508	0401.021	humic clay	end sed.	AMS	residue
GrA-29216	3.2	4215 ± 40	4860-4610	541.501-4362.494/+14.3	554-556	0401.021	humic clay	end sed.	AMS	caustic extract
GrA-29218	3.2	3945 ± 40	4520-4240	541.501-4362.494/+14.3	554-556	0401.021	humic clay	end sed.	AMS	residue
GrA-29220	3.2	545 ± 35	650-510	544.533-4358.745/+16.63	370-380	0401.013	charcoal	active Tagus	AMS	charcoal
GrA-29221	3.3	200 ± 35	310-0	540.649-4352.679/+15.68	370-380	0401.104	charcoal	active Tagus	AMS	charcoal
GrA-29447	3.2	1510 ± 40	1520-1310	541.501-4362.494/+14.3	366-370	0401.021	humic clay	start sed.	AMS	residue
GrA-29530	3.2	930 ± 35	930-760	542.899-4360.935/+16.23	260-270	0401.002	terrestrial botanical macrofossils	soil formation	AMS	Sieved at 250 & 125 µm
GrA-29535	3.3	2490 ± 40	2730-2360	541.504-4352.118/+13.22	840-850	0401.015	terrestrial botanical macrofossils	active Tagus	AMS	Sieved at 250 & 125 µm
GrA-29538	3.3	335 ± 35	490-300	540.649-4352.679/+15.68	610-620	0401.104	terrestrial botanical macrofossils	end sed.	AMS	Sieved at 250 µm
GrA-29539	3.5	1095 ± 35	1070-930	541.584-4352.084/+16.65	300-310	0401.106	terrestrial botanical macrofossils	soil formation	AMS	Sieved at 250 & 125 µm
GrA-29843	3.3	65 ± 40	270-0	541.504-4352.118/+13.22	540-550	0401.015	terrestrial botanical macrofossils	active Tagus	AMS	Sieved at 250 µm
GrA-30615	3.2	5790 ± 40	6680-6480	540.407-4359.849/+12	1024-1029	0501.029	terrestrial botanical macrofossils	start sed.	AMS	Sieved at 200 µm
GrA-30616	3.3	4485 ± 35	5300-4970	542.943-4350.667/+12.73	923-926	0401.302	terrestrial botanical macrofossils	top valley fill	AMS	Sieved at 125 µm
GrA-30961	3.3	6360 ± 45	7420-7170	542.943-4350.667/+12.73	1588-1590	0401.302	terrestrial botanical macrofossils	active channel	AMS	Sieved at 125 µm
GrA-31004	3.5	5900 ± 45	6860-6630	540.407-4359.849/+12	1046-1050	0501.029	terrestrial botanical macrofossils	end sed.	AMS	Sieved at 200 µm
GrA-31005	3.3	6500 ± 50	7510-7300	542.943-4350.667/+12.73	1491-1495	0401.302	terrestrial botanical macrofossils	active channel	AMS	Sieved at 125 µm
GrA-32584	3.4	8030 ± 40	9030-8750	531.088-4346.563/+11.38	2230-2240	0501.016	*Iris pseudacorus* seed	drowning	AMS	Sieved at 63 µm
GrA-32586	3.4	2440 ± 30	2710-2350	531.726-4345.914/+11.07	820-830	0501.013	terrestrial botanical macrofossils	marsh sed.	AMS	Sieved at 125 µm
GrA-32587	3.6	2625 ± 30	2785-2720	514.130-4322.014/+4	860-880	0501.050	seed/berry	start sed.	AMS	Sieved at 125 µm
GrA-32644	3.6	450 ± 30	540-470	512.824-4323.436/+3	360-370	0501.051	terrestrial botanical macrofossils	marsh sed.	AMS	Sieved at 63 µm
GrA-32645	3.6	2555 ± 30	2760-2500	514.940-4321.160/+4	1440-1450	0501.044	terrestrial botanical macrofossils	mouth bar	AMS	Sieved at 125 µm
GrA-32646	3.6	5010 ± 35	5900-5650	512.474-4323.832/+3	860-870	0501.052	terrestrial botanical macrofossils	marsh sed.	AMS	Sieved at 63 µm
GrA-32647	3.5	2480 ± 30	2720-2360	522.094-4335.448/+3.94	240-250	0501.042	non-rounded wood pieces	soil formation	AMS	Sieved at 125 µm
GrA-32650	3.5	600 ± 25	660-540	524.799-4333.804/+7.60	690-700	0501.030	twig with bud	active Tagus	AMS	Sieved at 125 µm
GrA-32651	3.5	6165 ± 35	7170-6950	526.038-4333.421/+7.42	770-780	0501.025	oxidized organic plant remains	marsh sed.	AMS	Sieved at 63 µm
GrA-32654	3.5	7440 ± 40	8360-8180	526.038-4333.421/+7.42	1260-1270	0501.025	terrestrial botanical macrofossils	start sed.	AMS	Sieved at 63 µm

Table 3.1 *(continued)*

Lab. Nr.	Figure	14C age yrs BP ± 1σ	Age cal. BP 2σ	Coordinates (x-y/z) (m)	Sample depth (cm)	Borehole nr.	Material	Significance	14C type	Remarks
GrA-32655	3.2	6265 ± 35	7270-7020	544.750-4358.375/+17.40	1967-1974	0401.304	undifferentiated plant remains	clay layer	AMS	Sieved at 63 µm
GrA-32656	3.7	1765 ± 30	1820-1570	504.812-4310.535/+2	440-480	0501.071	terrestrial botanical macrofossils	marsh sed.	AMS	Sieved at 63 µm
GrA-33636	3.6	101.91 ± 0.4%	0	512.474-4323.832/+3	1590-1610	0501.052	terrestrial botanical macrofossils	marsh sed.	AMS	Sieved at 63 µm
GrA-33637	3.5	5640 ± 45	6510-6300	522.373-4335.353/+4.30	1160-1170	0501.041	deciduous leaf remains	marsh sed.	AMS	Sieved at 63 µm
UtC-14744	3.5	1630 ± 35	1610-1410	526.420-4333.197/+5	140-150	0601.002	bulk clay	soil formation	AMS	-
UtC-14745	3.5	3849 ± 47	4420-4100	526.420-4333.197/+5	280-290	0601.002	bulk clay	soil formation	AMS	-
UtC-14747	3.2	3089 ± 38	3390-3210	540.407-4359.849/+12	604-607	0501.029	terrestrial botanical macrofossils	active sed.	AMS	Sieved at 125 µm
UtC-14748	3.2	4129 ± 42	4830-4520	540.407-4359.849/+12	711-712	0501.029	terrestrial botanical macrofossils	active sed.	AMS	Sieved at 125 µm
UtC-14749	3.2	1022 ± 37	1060-790	540.407-4359.849/+12	331-334	0501.029	total organic fraction < 125 µm	start sed.	AMS	Sieved at 125 µm
UtC-14750	3.2	1136 ± 38	1180-960	540.407-4359.849/+12	331-334	0501.029	roots of fraction > 125 µm	start sed.	AMS	Sieved at 125 µm
UtC-14904	3.7	3647 ± 41	4090-3850	505.439-4310.324/+2	1281	0601.302	terrestrial botanical macrofossils	start sed.	AMS	Sieved at 63 µm
UtC-14905	3.7	6247 ± 46	7270-7010	505.439-4310.324/+2	2192-2196	0601.302	terrestrial botanical macrofossils	start sed.	AMS	Sieved at 63 µm
UtC-14906	3.7	8900 ± 50	10 200-9780	505.439-4310.324/+2	2842-2848	0601.302	terrestrial bot. macrofossils + roots	marsh sed.	AMS	Sieved at 63 µm
UtC-14907	3.7	9990 ± 70	11 800-11 200	505.439-4310.324/+2	3710-3716	0601.302	terrestrial botanical macrofossils	marsh sed.	AMS	Sieved at 63 µm
UtC-14908	3.7	12160 ± 90	14 260-13 780	505.439-4310.324/+2	4919-4925	0601.302	root + small branch-like pieces	start floodplain	AMS	Sieved at 63 µm
UtC-14909	3.5	4145 ± 42	4830-4530	523.321-4334.600/+7	1004-1010	0601.301	terrestrial botanical macrofossils	active sed.	AMS	Sieved at 63 µm
UtC-14910	3.5	6860 ± 50	7800-7590	523.321-4334.600/+7	1898	0601.301	terrestrial botanical macrofossils	start sed.	AMS	Sieved at 63 µm
UtC-14911	3.5	8880 ± 60	10 190-9740	523.321-4334.600/+7	2748-2753	0601.301	terrestrial botanical macrofossils	start sed.	AMS	Sieved at 63 µm
UtC-1983	3.9	6040 ± 50	7010-6740	536.620-4342.720/+7.5	761-760	Alpiarça III	peat	end saltmarsh	bulk	unpublished
Beta-150352	3.5	3400 ± 40	3830-3480	522.980-4334.110/+7.40	740	Fonte Bela	unknown	active sed.	unknown	R. Pereira et al. (2002)
SEV	3.4	unknown	816	530.589-4347.131/+11.15	103-104	SEV	peat/wood	active sed.	unknown	Azevêdo et al. (2006a)
SEV	3.4	unknown	3086	530.589-4347.131/+11.15	454-455	SEV	peat/wood	active sed.	unknown	Azevêdo et al. (2006a)
SEV	3.4	unknown	3550	530.589-4347.131/+11.15	649-650	SEV	peat/wood	active sed.	unknown	Azevêdo et al. (2006a)
SEV	3.4	unknown	6960	530.589-4347.131/+11.15	1074-1075	SEV	peat/wood	active sed.	unknown	Azevêdo et al. (2006a)
SEV	3.4	unknown	8097	530.589-4347.131/+11.15	1230	SEV	peat/wood	active sed.	unknown	Azevêdo et al. (2006a)

Table 3.2 | Summary of Facies Units (FU) characteristics in the Lower Tagus Valley.

Facies Unit	Interpretation	Lithology	Details
1A	fluvial terrace deposits	very fine to coarse-grained sand, usually poorly sorted and with gravel	compact sediment, unit has flat top and slopes seaward, incised into Miocene-Pliocene deposits plant roots in top
1B	high-gradient fluvial channels	fine to coarse-grained, angular sand, poorly sorted, with increasing gravel to base	fining-upwards, unit has rather flat top morphology and slopes seaward, incised into Miocene-Pliocene deposits
2	aggrading fluvial overbank	clay, (silty) clay loam, loam and very fine to fine sand with parallel lamination	generally fining-upwards, dark-brown soil A-horizon in top with plant remains, roots and black/brown mottling. Many carbonate concretions (≤ 3cm), decreasing to top. In coring VAL in top of unit: marble-like appearance. Contains plant roots & plant remains
3A	brackish water marshes and tidal flats	generally structureless clay and silty clay with locally very fine sand lamination. In coring VFX at -29 and -31 m m.s.l. coarse sand layers	pyrite crystals and pyrite in diatoms, foraminifera and plant remains, bioturbation. Top 1.5-2 m + m.s.l.: very firm consistency, angular blocky structure, carbonized plant material, many carbonate concretions = pedogenesis. Underneath: soft, shell-like breaking, bioturbation = no ripening. Pedogenesis decreases southward
3B	intertidal and subtidal flats	plastic, soft clay and (silty) clay loam with laminae and lenses of very fine to coarse-grained sand with some gravel. Clay-sand contacts sharp. Generally rhythmic clay-sand alternations	shells, shell fragments and carbonate foraminifera are only present south of Azambuja. This unit often contains methane gas. Some sand layers disturbed and preserved as sand nests or spots = bioturbation
4	shallow-marine prodelta	plastic, soft slightly sandy, (silty) clay loam and silty clay with rare sand laminae, many sand spots = bioturbation + burrowing.	lower part of unit is fining-upwards series of ~6 m with shell-rich lag deposit overlain by medium sand, fining to very fine sand. Top has gradual but rapid transition to FU-5A. Valley-wide presence from Azambuja southwards Many shell fragments and shells in living position
5A	distributary mouth tidal bars with shells	medium to poorly sorted medium to coarse-grained sand. Coarse-grained intervals with gravel. Disturbed clay laminae in sand	coarsening-upwards, within unit: small, sharp erosive bounding surfaces with gravel, clay pebbles & shell fragments. Not present in Ponte Vasco da Gama and more downstream cross sections. Shells abundantly present
5B	fluvially influenced tidal channels without shells	poorly sorted very fine to coarse-grained sand with gravel, disturbed clay drapes	generally fining-upwards (coarsening-upwards in coring 0501.044). Shells & foraminifera are extremely rare horizontally layered freshwater plant remains
6A	condensed fluvial floodbasins	sandy loam, loam, silt loam and (silty) clay loam and humic clay, peaty clay and peat intervals	located on top of FU-1, tough consistency, small carbonate concretions, root traces, white & green spots, animal bioturbation, admixture of sand grains. Locally greenish, bluish colours. Alternating wet and dry conditions
6B	fluvial floodbasins	silt loam, (silty) clay loam and clay, very locally poorly sorted (loamy) coarse-grained sand with gravel deposited by small brook channels. Distal areas: gyttja, peat, peaty clay and humic clay layers	unit forms southwards thinning wedge. Ongoing sedimentation on active floodplain with shallow (ephemeral) flood-channels at surface. Contains iron-oxides, iron-concretions, manganese spots, carbonate concretions and is well oxygenated. More charcoal to top. A-horizons: ≤ 50 cm, dark brown-grey to dark brown, sometimes hard, dry and crumbly with white lines (no carbonate)
7	natural levees and crevasses	sandy loam, loam, silt loam and usually well sorted very fine to fine-grained sand in laminae	present on both sides along Tagus channel (FU-8), not present in A10 cross section and more downstream. Shallow (ephemeral) flood-channels at surface. Often much charcoal present. Locally medium to coarse-grained sands, some in channels or splays
8	fluvial channels	medium to coarse-grained sand, up to 100% gravel (in coring GOL) in channel lags. No large stones downstream of coring GOL.	fining-upwards, pebbles & cobbles dominated by quartz & quartzite (≥ 93%), up to 5% granite, sand has colourful, "clean" appearance, charcoal present. In coring GOL: several stacked fining-upwards sequences. Near Vila Franca de Xira and more downstream no sandy channel belt present. No significant downstream grainsize change
9	aeolian dunes	well sorted, angular medium sand (210-420 µm) with large scale, low-angle cross-bedding.	*Morro da Serra*: strongly bioturbated organic horizons often cut-off by erosion and present at base of cross-bedded slip faces. Concentrations of large mica's and charcoal within organic horizons. Low angle cross-bedding points to dominance of NW winds. *Cabeço da Bruxa*: no palaeosols or charcoal found, situated on FU-1

Borehole nr.	Coordinates (x-y/z) (m)	Depth (cm)	Artefact (all fragments)	Age cal BP	Facies Unit	Determination by
0401.027	544.076-4359.453/+17.17	310	possibly thin walled jar, 1st-5th Century AD	1950-1550	FU-7	prof. dr. D.G. Yntema
0401.101	543.832-4358.693/+16.8	430	possibly early *sigillata* pottery, Roman	2250-1650	FU-8	dr. A.C. Mientjes
0501.010	532.125-4345.496/+8.59	590	pottery, 4th-5th Century/Early Middle Ages	1650-1550	FU-8	dr. A.C. Mientjes
0501.012	532.750-4344.700/+14.32	875	possibly small amphora, Roman	2250-1650	FU-8	dr. A.C. Mientjes
0501.032	524.604-4333.900/+7.56	600	possibly early *sigillata* pottery, Roman	2250-1650	FU-8	dr. A.C. Mientjes
0501.055	516.605- 4319.334/+4	160-190	cooking pot, Bronze/Iron Age	3950-2250	FU-6B	dr. A.C. Mientjes
0601.301 (VAL)	523.321- 4334.600/+7	876	mortar fragment, Late-Roman	1950-1650	FU-5B	L.M. Kootker

Table 3.3 | Archaeological finds from the Lower Tagus Valley. The "Age cal BP" column shows calibrated radiocarbon-equivalent ages. Coordinates in European Datum 1950/UTM Zone 29N.

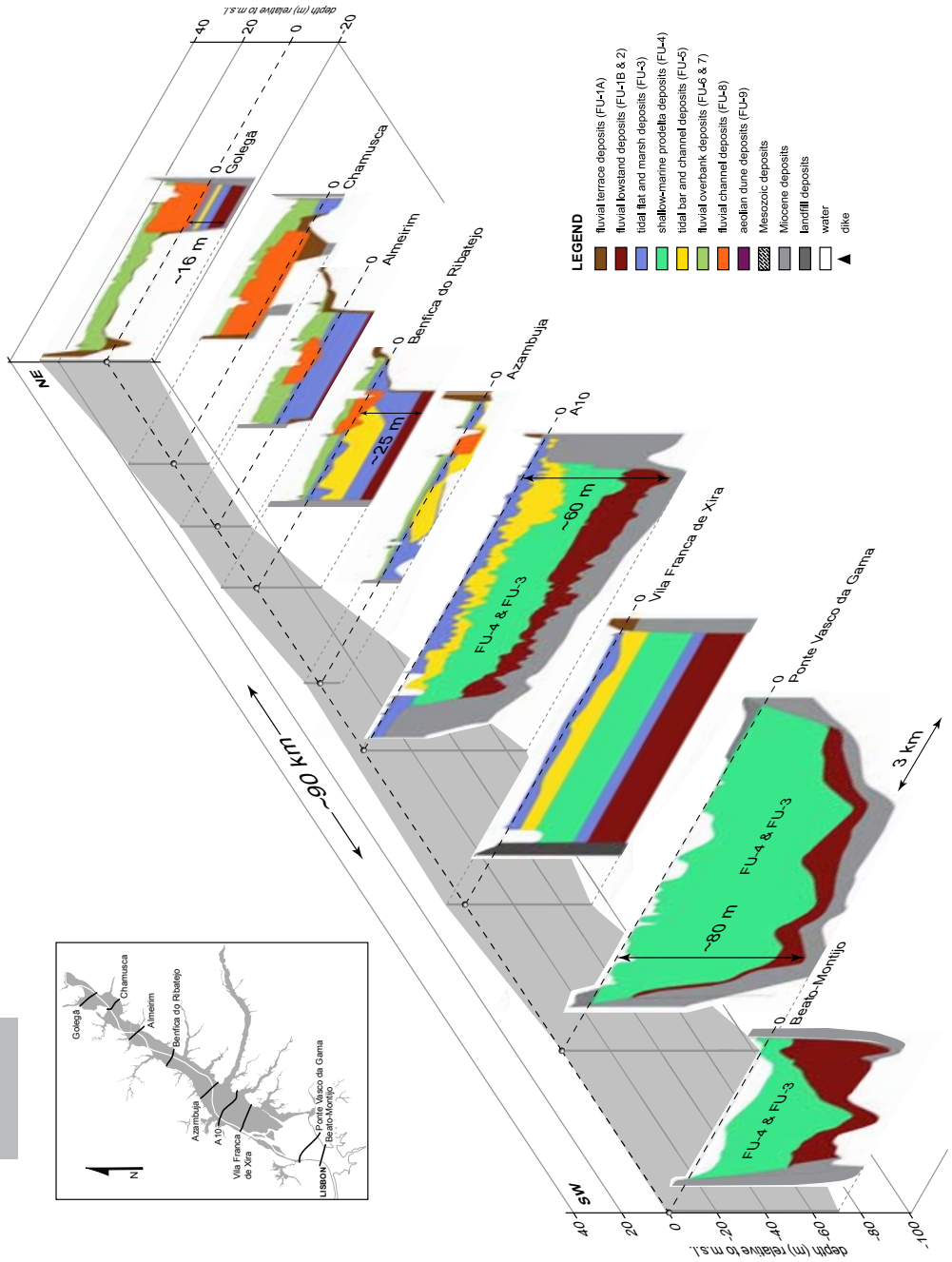

Figure 3.8 | 3D compilation of six manually cored cross sections (Figs. 3.2-3.7) and three cross sections based on geotechnical studies for bridge construction: A10 bridge (BRISA, 2005), Ponte Vasco da Gama bridge (LUSOPONTE, 1995), Beato-Montijo bridge (never built) (De Mendonça, 1933). Horizontal distance not to scale.

deposits. The coarse gravel indicates a high-energy environment. Combined with the steep seaward gradient (~60 cm/km), this unit is interpreted as fluvial sediment deposited as channel bars of a coarse-grained braided bedload river. This unit was deposited before or at the start of the Late Glacial period, based on a radiocarbon date of ~14,000 cal BP in the top of this unit in coring VFX (Fig. 3.7), indicating the start of floodbasin formation.

FU-2

FU-2 is an inland thinning unit overlying FU-1B. It consists of fine sand and clayey silt in a generally fining-upward sequence (Figs. 3.5, 3.7 and 3.8). The great thickness of this unit (~12 m in coring VFX, Fig. 3.7) and the many carbonate concretions, imply long-term deposition during the entire Late Glacial period. This unit was deposited in a floodbasin which locally (coring VFX) changed into a levee. The basal ~6 m of FU-2 in coring VFX (Fig. 3.7) was deposited by a single-channel river that developed as a result of less extreme discharge peaks and higher production of finer sediment due to increased temperatures, precipitation and vegetation cover after ~14,000 cal BP. Deposition of the upper ~6 m (Fig. 3.7, coring VFX), resulted from upstream migration of fluvial onlap (Chapter 2).

FU-3A

FU-3A is a widespread unit consisting mainly of soft clay. Foraminiferal and biological evidence (e.g. *Jadammina macrescens*, *Trochammina inflata*, Chenopodiaceae sp. pollen) indicate brackish conditions and a brackish water marsh or tidal flat environment. The substantial thickness of the marsh and tidal flat deposits suggests vertical aggradation rather than progradation during rapid sea-level rise before 7000 cal BP. Only in the upper 1.5-2 m pedogenesis has taken place due to subaerial exposure and soil ripening. This unit was found in all cross sections, except the most landward cross section (Fig. 3.2) and occurs between -35 m and +2 m m.s.l. (Figs. 3.3-3.7 and 3.8). This tidal unit was formed from ~11,500 cal BP up to the present day (Fig. 3.7).

FU-3B

Closely associated with FU-3A, a laminated unit (FU-3B) was found, consisting predominantly of clay with sand laminae. Based on the distinct lamination, burrows and the shell and foraminiferal content (e.g. *Hydrobia ulvae*, *Scrobicularia plana*, *Ammonia becarii* and *Elphidium* sp), this unit is interpreted to be deposited by intertidal and subtidal flats. FU-3B is locally present in the north (Figs. 3.2-3.4) and nearly valley-wide in the south (Figs. 3.5-3.7). Deposition started around 8000 cal BP and presently still continues in the central basin south of Vila Franca de Xira (Fig. 3.8).

FU-4

FU-4 mainly consists of strongly bioturbated (silty) clay loam and silty clay (Table 3.2), contains a variety of marine fauna (e.g. *Chlamys* sp., *Nucula* sp. and brittle star fragments) and was deposited in a shallow-marine prodelta environment. This unit was formed in the deepest parts of the drowned Lower Tagus Valley and was found in the southern cross sections (Figs. 3.7 and 3.8). The shallow-marine prodelta deposits probably grade laterally into tidal deposits (FU-3 and 5) near Azambuja, since they were not found near Benfica do Ribatejo (Fig. 3.5). According to the radiocarbon dates in coring VFX (UtC-14906 and UtC-14904), deposition of FU-4 started slightly before 10,000 cal BP and ended around 4000 cal BP.

FU-5A

Deposits of FU-5A consist of medium to coarse-grained sand with disturbed clay laminae in a coarsening-upward sequence, which is formed by coalesced distributary mouth tidal bars which are part of the prograding tidally influenced bayhead delta (Chapter 2). Although partly reworked, the shell content (e.g. *Scrobicularia plana*, *Hydrobia ulvae* and *Crassostrea angulata*) indicates that brackish water prevailed. This unit stratigraphically overlies shallow-marine prodelta deposits (FU-4) in the south (Figs. 3.7 and 3.8, A10) and tidal deposits (FU-3 and 5) in the north (Figs. 3.5 and 3.6). Progradational deposition of FU-5A moved from Benfica do Ribatejo (Fig. 3.5) southward as soon as sea level had reached its maximum (~7000 cal BP, Fig. 3.9).

FU-5B

FU-5A is overlain by deposits poor in shells (FU-5B). This extensive, generally fining-upward, sand-dominated unit with occasional clay drapes, is interpreted as pointbar-type deposit formed in fluvially influenced tidal channels. Strong salinity variations may explain the absence of fauna. This unit is narrow and thin in the north (~2m, Fig. 3.2) and wide and thick further south in the valley (~7 m, Fig. 3.6). The great width possibly resulted from meandering and lateral migration. FU-5B is closely related to FU-5A, because the tidal-fluvial channels prograded over their distributary mouth tidal bars. Deposition started before ~7000 cal BP near Golegã (Fig. 3.2) based on radiocarbon date GrA-32655 and subsequently moved southwards.

FU-6A

FU-6A is a clay-dominated unit with evidence of soil formation (e.g. firm consistency, carbonate concretions, root traces) and locally peaty intervals. Sedimentation rate was low, as testified by the pedogenesis in these relatively

consolidated fluvial floodbasin deposits. FU-6A was only found in the north of the study area and with a wide extension (Figs. 3.2 and 3.3). Deposition started shortly after 7000 cal BP (GrA-30615 and GrA-31004, Fig. 3.2) near Golegã and shortly before 5000 cal BP near Chamusca (GrA-30616, Fig. 3.3), indicating downstream fluvial progradation. On top of the higher areas (+8 to +10 m m.s.l.) of the terraces, sedimentation started shortly after 5000 cal BP (GrA-29216 and GrA-29218, Fig. 3.2; GrA-30616, Fig. 3.3).

FU-6B

FU-6B is a silt and clay-dominated, locally organic unit, containing several soil A-horizons (Figs. 3.2-3.5). This unit forms a southward thinning wedge of fluvial floodbasin deposits (Chapter 2). In the Almeirim cross section (Fig. 3.4), the top of FU-3A is dated at 6960 cal BP and the overlying floodbasin deposits of FU-6B at 3550 cal BP at ~2 m from the base. The transition from FU-3A to FU-6B and thus the start of deposition of this unit occurred between these dates and—taking the slower accumulation rate and soil formation in the upper part of FU-3A in account—is estimated at 4,500 cal BP. Further north (Figs. 3.2 and 3.3), sedimentation started 3000-2500 years later due to the incised position of the Tagus channel, which initially prevented sedimentation outside the incised valley. From Almeirim southward the valley was wider, thereby facilitating floodbasin sedimentation as soon as the fluvial system prograded over the tidal deposits which filled the valley.

FU-7

FU-7 consists of laminated loam, silt loam and well–sorted, fine sand which are interpreted as fluvial levee deposits. This unit was found northward from Azambuja, with a maximum thickness near Almeirim (Fig. 3.4). Within this unit, medium to coarse-grained sand in erosive small channels and splays is interpreted as crevasse-splays (Figs. 3.3 and 3.4). According to the genetic relationship with FU-6B, this unit was also deposited since ~4500 cal BP. The levee tops were found up to 5 m above the floodbasin. The levee deposits extend far into the Tagus floodplain where they overlie floodbasin deposits (FU-6B) and palaeosol levels, implying rather recent (<1000 y), stronger sedimentation on the levees (Figs. 3.2-3.5).

FU-8

FU-8 is gravel–rich, medium to coarse-grained sand in a fining-upwards sequence. It is interpreted as deposited in fluvial channel bars similar to the present-day channel bed situation. The fluvial channel originated after ~7000 cal BP near Golegã (GrA-32655, Fig. 3.2) and is progressively younger downstream (Figs. 3.2-3.5). Generally, both width and thickness decrease from

Golegã southward (Fig. 3.8), resulting from the younger age and limited time available for vertical aggradation and lateral migration. The channel deposits contain many archaeological remains (e.g. pottery, bricks, charcoal), indicating deposition and/or reworking from Roman times onwards, as supported by several young (< 600 years) radiocarbon ages (Table 3.3, Figs. 3.2, 3.4 and 3.5).

FU-9

The deposits of FU-9 comprise well-sorted, medium-grained sand with low-angle cross-bedding (Table 3.2) formed by aeolian deposition during the Holocene (Chapter 2). Morphologically this unit appears as local dunes rising above the surrounding plain.

Relative sea-level reconstruction

The relative sea-level curve was constructed using 20 radiocarbon dates from the Lower Tagus Valley (Fig. 3.9A and B). Due to the great depth of the incised lowstand valley, the first sedimentary registration of relative sea-level rise started already around 11,500 cal BP, making this reconstruction unique for Europe. We used seven basal samples (Table 3.4), at the base of the fine-grained sedimentary sequence (FU-3A), directly overlying lowstand sandy fluvial deposits which therefore are compaction-free points. Further, we used 13 samples from non-basal, not compaction-free levels (Table 3.5) higher in the Holocene valley-fill stratigraphy (mostly FU-3). However, we assume compaction of these samples was limited, since the samples were taken from points underlain by relatively thin clay beds. Although just seven data points with a wide error envelope are present after 7000 cal BP, the horizontal part of the curve seems to indicate no effects of compaction or tectonic subsidence after 7000 cal BP.

Most radiocarbon dates for relative sea-level reconstruction are based on freshwater terrestrial botanical macro remains because terrestrial plant material is not affected by hard-water or reservoir effects (Tables 3.4 and 3.5). The abundance of freshwater terrestrial plant material in marsh sediments of FU-3 is explained by three mechanisms: 1) Higher marshes at the margins of the central basin were only occasionally flooded and a transition zone between freshwater and brackish water environments existed; 2) Freshwater plant material was flushed into tidal environments during Tagus river floods; 3) High tidal marshes changed progressively into floodbasins with freshwater vegetation as a result of the southward prograding fluvial system. Although the dated organic material may have been reworked, the internal stratigraphic consistency of the dates indicates their reliability.

The time-depth data were plotted as points representing sampling depth. The horizontal error bars indicate the uncertainty range in time at the

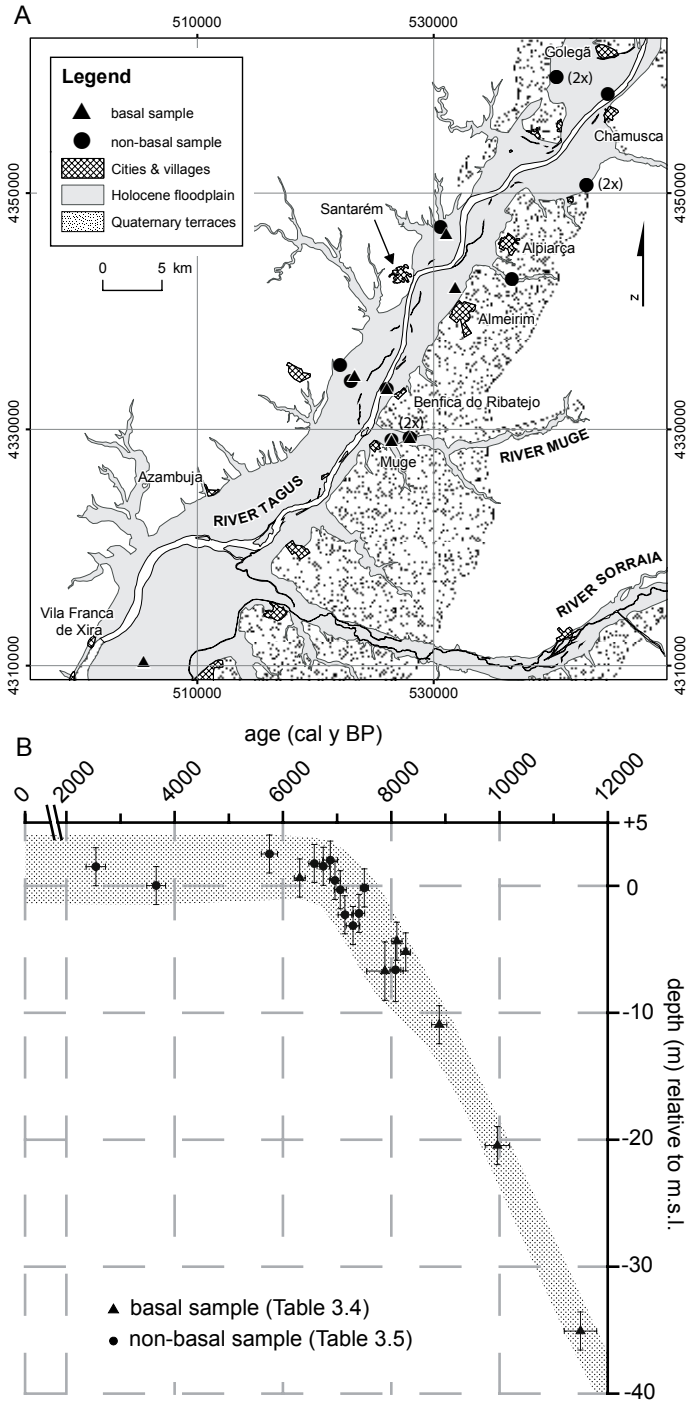

Figure 3.9 | Relative sea-level curve of the Lower Tagus Valley. Map (A) shows the location of the samples used for construction of the sea-level curve (B). Horizontal error bars indicate the uncertainty range in time at the 2σ-confidence interval. Vertical error bars represent the uncertainty in depth determination.

Lab. Nr.	14C age yrs BP ± 1σ	Age cal. BP 2σ m.s.l.	Mean cal. BP age to present m.s.l.	Sample depth (cm) relative	Material	Significance	Tidal reference	Source
GrA-27234	5530 +/- 45	6410-6210	6310	+59.5	peat	start of brackish-water influence as indicated by dinoflagellates & Chenopodiaceae pollen	HAT-MHW	this study
AA-48978	7318 +/-44	8200-8010	8105	-439.0	plant & wood fragments	start of brackish-water influence as indicated by foraminifera and Chenopodiaceae pollen	MHWST-MHW	Van der Schriek et al. (2007b)
GrA-32654	7440 +/- 40	8360-8180	8270	-523	freshwater terrestrial botanical macrofossils	start of brackish-water influence as indicated by agglutinating foraminifera, diatoms, dinoflagellates & Chenopodiaceae pollen	MHWST-MHW	this study
AA-49816	7668 +/- 49	8221-7548 (marine correction)	7885	-674.5	*Scrobicularia plana* shell fragments	start of brackish-water influence as indicated by estuarine shells and calcareous foraminifera	MHWNT-MTL	Van der Schriek et al. (2007b)
GrA-32584	8030 +/- 40	9030-8750	8890	-1097	*Iris pseudacorus* seed	start of brackish-water influence as indicated by agglutinating foraminifera & FeS_2	MHWST-MHW	this study
UtC-14911	8880 +/- 60	10 190-9740	9965	-2050.5	freshwater terrestrial botanical macrofossils	start of brackish-water influence as indicated by FeS_2	HAT-MHW	this study
UtC-14907	9990 +/- 70	11 800-11 200	11 500	-3513	freshwater terrestrial botanical macrofossils	start of brackish-water influence as indicated by diatoms & FeS_2	HAT-MHW	this study

Table 3.4 | Basal samples used for sea-level reconstruction in the Lower Tagus Valley. In the "Significance" column the environmental meaning of the samples is given. The "Tidal reference" column gives the reference of a sample with respect to sea level. HAT: Highest Astronomical Tide; MHW: Mean High Water; MHWST: Mean High Water Spring Tide; MHWNT: Mean High Water Neap Tide; MTL: Mean Tide Level.

Table 3.5 | Non-basal samples used for sea-level reconstruction in the Lower Tagus Valley. In the "Significance" column the environmental meaning of the samples is given. The "Tidal reference" column gives the reference of a sample with respect to sea-level. HAT: Highest Astronomical Tide; MHW: Mean High Water; MHWST: Mean High Water Spring Tide; MHWNT: Mean High Water Neap Tide; MTL: Mean Tide Level.

Lab. Nr.	14C age yrs BP ± 1σ	Age cal. BP 2σ	Mean cal. BP age	Sample depth (cm) relative to present m.s.l.	Material	Significance	Tidal reference	Source
AA-48980	4985 +/- 73	5900-5600	5750	+248.8	organic clayey silt	end of regional brackish-water indicators (Chenopodiaceae) in pollen diagram	HAT-MHW	Van der Schriek et al. (2007b)
UtC-1983	6040 +/- 50	6600-6320	6460	+200	peat	end of regional brackish-water indicators as indicated by disappearing Chenopodiaceae pollen	HAT-MHW	this study, Janssen & Van Leeuwaarden unpublished
GrA-30615	5790 +/- 40	6680-6480	6580	+173.5	freshwater terrestrial botanical macrofossils	end of brackish-water influence as indicated by agglutinating foraminifera, dinoflagellates & Chenopodiaceae pollen	HAT-MHW	this study
GrA-31004	5900 +/- 45	6860-6630	6745	+152	freshwater terrestrial botanical macrofossils	near end of brackish-water influence as indicated by agglutinating foraminifera, dinoflagellates & Chenopodiaceae pollen	HAT-MHW	this study
GrA-32647	2480 +/- 30	2720-2360	2540	+149	non-rounded wood fragments	end of brackish-water influence; no brackish-water indicators	HAT-MHW	this study
unknown	unknown	unknown	6960	+40	organic material	near end of brackish-water influence	HAT-MHW	Azevêdo et al. (2006a)
Beta-150352	3400 +/- 40	3830-3480	3655	0	organic material & Charcoal	continuing tidal marsh sedimentation	MHWNT-MTL	Ramos Pereira et al. (2002)
AA-48979	6626 +/- 44	7580-7430	7505	-19	plant fragments	maximum tidal influence as indicated by agglutinating foraminifera peak	MHWST-MHW	Van der Schriek et al. (2007b)
GrA-32651	6165 +/- 35	7170-6950	7060	-33	oxidized freshwater terrestrial botanical macrofossils	continuing tidal marsh sedimentation	MHWST-MHWNT	this study
GrA-31005	6500 +/- 50	7510-7300	7405	-220	freshwater terrestrial botanical macrofossils	continuing tidal flat sedimentation as indicated by dinoflagellates & Chenopodiaceae pollen	HAT-MHW	this study
GrA-32655	6265 +/- 35	7270-7020	7145	-230.5	undifferentiated plant remains	continuing tidal flat sedimentation as indicated by dinoflagellates & Chenopodiaceae pollen	HAT-MHW	this study
GrA-30961	6360 +/- 45	7420-7170	7295	-316	freshwater terrestrial botanical macrofossils	continuing tidal flat sedimentation as indicated by dinoflagellates & Chenopodiaceae pollen	HAT-MHW	this study
AA-48977	7263 +/- 46	8180-7980	8080	-665	plant fragments	continuing tidal marsh sedimentation as indicated by agglutinating and calcareous foraminifera	MHWST-MTL	Van der Schriek et al. (2007b)

2σ-confidence interval. The vertical error bars represent the uncertainty in depth determination, which consists of four components: 1) low-resolution elevation data of the Carta Militar de Portugal 1:25.000 topographic map (± 50 cm); 2) altitude determination of the sampling site (± 30 cm); 3) sampling method (± 10 cm); 4) determination of indicative meaning relative to mean tidal level (MTL) (± 60/140/160 cm), which was estimated using pollen and faunal content and the overview given by Van der Schriek *et al.* (2007b). Most samples were taken from marsh sediments, which according to Bettencourt and Ramos (2003) are formed in a 60 cm vertical range between Mean High Water Neap Tide (MHWNT) and Highest Astronomical Tide (HAT). Two samples with a faunal content that did not allow a precise environmental determination relative to MTL have vertical error bars of 140 cm (MTL-MHWNT; *Scrobicularia*) and 160 cm (MTL-MHW; agglutinated and calcareous foraminifera).

The basal dates (Table 3.4) represent the start of brackish-water influence and therefore yield the upper tidal limit. The non-basal dates (Table 3.5) from high marsh deposits (FU-3A) also yield the upper tidal limit. The present-day interval between MTL and highest astronomical tide (HAT) corresponds to 0 and +2 m relative to m.s.l. (Portela and Neves, 1994; Bettencourt and Ramos, 2003). All sea-level index points except one were found below +2 m m.s.l. which corresponds with the top of tidal marsh unit FU-3A. In many locations the +2 m level was dated at ~7000 cal BP, which implies that silting of the Tagus valley occurred simultaneously over large areas due to the abrupt decrease or even cessation of the rate of relative sea-level rise.

Generally, the envelope of the relative sea-level curve reflects the interval between MHW and HAT and therefore the curve represents the upper limit of sea level, although with an error envelope of ~5 m. The curve presented here is the first for SW Europe that covers the Late Glacial and Holocene periods.

3.4 PALAEOGEOGRAPHY

Full-colour versions of the palaeogeographic maps can be found in *Addendum 1*.

Last Glacial Maximum; ~20,000 cal BP (Fig. 3.10)

During the Late Pleistocene period, sea level lowered progressively until the Last Glacial Maximum (LGM; ~20,000 cal BP) to reach the lowest level of the last glacial (Hanebuth *et al.*, 2000). Consequently, the coastline was located around the present 120 m depth contour (Fig. 3.10). The dropping

base level caused a progressive incision of the Tagus into Miocene and Pliocene fluvial, estuarine and marine deposits and into the Pleistocene Tagus fluvial deposits resulting in terrace formation (Cunha *et al.*, 2005). The lowstand Tagus was a braided river with a steep gradient (~60 cm/km) and coarse sand and gravel deposits (FU-1B) (Fig. 3.8). A radiocarbon date of 14,260-13,780 cal BP (UtC-14908) (Table 3.1) in the top of lowstand unit FU-1B in coring VFX (Fig. 3.7), suggests that the lowstand Tagus was active around 20,000 cal BP.

The Tagus incision during the Late Pleistocene sea-level lowstand reached as far upstream as Abrantes (Martins, 1999; INETI, 2007), 20 km east

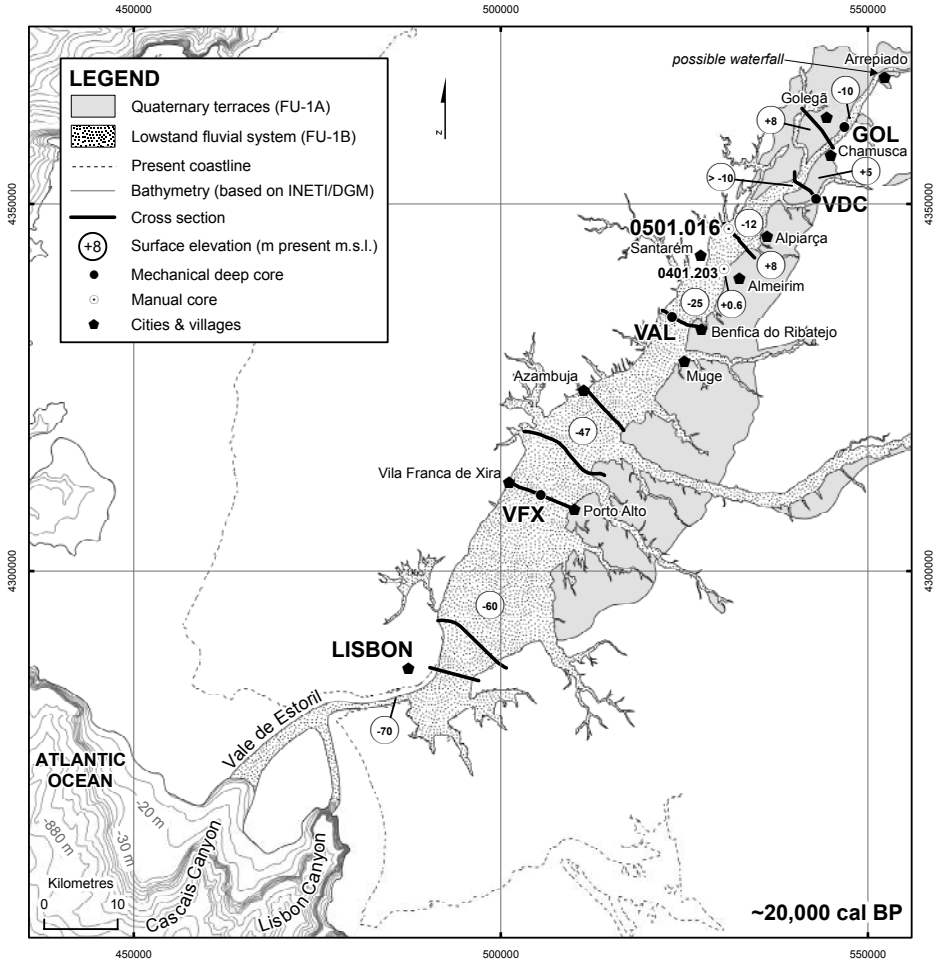

Figure 3.10 | Palaeogeography around 20,000 cal BP showing the braidplain of the incised fluvial lowstand surface and the extension of the Tagus onto the continental shelf. The location of the possible waterfall in the north is indicated. Bathymetry and coastline adjusted to 20,000 cal BP (120 m below present day sea level). A full-colour version of this palaeogeographic map can be found in *Addendum 1*.

of Arrepiado (Fig. 3.1) where a granite outcrop marks the northern limit of the Lower Tagus Valley. The Tagus incised a narrow and deep bedrock channel in the granite, currently being ~15 m deep with the base of the channel at +4 m m.s.l. (Rocha *et al.*, 2005). About 9 km downstream, near Golegã (Fig. 3.10), the top of the lowstand system (FU-1B) was found at about -10 m m.s.l. (Fig. 3.2). Assuming a constant gradient for the lowstand surface of 60 cm/km, the depth of that surface downstream of the granite outcrop is estimated at -5 m m.s.l. In that case a jump in the gradient of 9 m was present around 20,000 cal BP, implying the presence of a waterfall near Arrepiado where the Tagus leaves the Palaeozoic Hesperian Massif (Fig. 3.10).

Based on the Golegã, Chamusca and Almeirim cross sections (Figs. 3.2-3.4) and data from INETI reports 1977 and 4946 (INETI, 2007), it is concluded that the narrow and deep lowstand valley widens about 5 km upstream of Alpiarça (Fig. 3.10). Downstream of Alpiarça, the width increases to about 10 km (Figs. 3.4, 3.5 and 3.8). The greater width of the lowstand system in the downstream area of the Lower Tagus Valley is interpreted as resulting from lateral shifting of the main channel course across the floodplain.

Within the incised valley—now covered by Holocene deposits—terraces are found, which represent floodplain levels created during the Late Pleistocene incision. Between Arrepiado and Alpiarça in the north (Figs. 3.2 and 3.3), these terraces are the largest. Further downstream, smaller terrace remnants were found along the eastern and western valley margin just north of Santarém (Fig. 3.4 and coring 0401.203 in Fig. 3.10) and along the eastern margin near Benfica do Ribatejo (Fig. 3.5). The terrace surfaces in the north have similar elevations of about +8 to +5 m m.s.l. The other terrace surfaces have elevations between 0 (coring 0401.203) and -6 m m.s.l. (Fig. 3.5) and were probably formed during different periods. The three geotechnical cross sections in the south (Fig. 3.8) show an undulating gravel surface, suggesting the presence of terraces in the lowstand unit (FU-1B).

The lowstand system of the Lower Tagus Valley flowed through a narrow bedrock-confined channel near Lisbon (Fig. 3.10). West of Lisbon, the Tagus continued its main course through the Vale de Estoril and the partly exposed Cascais Canyon as suggested by Vanney and Mougenot (1981). Possibly a subordinate Tagus channel entered the Atlantic Ocean through the Lisbon Canyon, because its upstream end is located close to the Vale de Estoril (Fig. 3.10). According to Vanney and Mougenot (1981), the Vale de Estoril was used for (fluvial) transport of Tagus sediment. This implies a direct Tagus-to-deep sea connection causing rapid discharge of Tagus sediment into the (deeper) ocean. The narrow shelf, and therefore direct land-ocean connection was also responsible for the strong effect of sea-level lowering on upstream valley incision.

20,000-12,000 cal BP (Fig. 3.11)

After the LGM, sea-level rise started and around 14,000 cal BP had reached -80 m m.s.l. (Hanebuth *et al.*, 2000). Shortly after ~14,000 cal BP, the low-stand braided Tagus (FU-1B) changed into a single-channel river as suggested by the onset of floodbasin/levee sedimentation (FU-2) near Vila Franca de Xira (Fig. 3.7, coring VFX). The basal 6 m of FU-2 contains many large carbonate concretions due to soil formation indicating rather slow accumulation. The change to a single-channel fluvial system cannot be explained by sea-level rise, since sea level was still 33 m below the Vila Franca de Xira site. More likely, the fluvial-style change was caused by climate change and related rapid expansion of *Pinus* and deciduous and evergreen *Quercus* and other Mediterranean vegetation since the LGM (Roucoux *et al.*, 2005; Naughton *et*

al., 2007b). The generally colder and drier Heinrich event 1 was followed by the temperate Bölling-Allerød period (Naughton *et al.*, 2007b). An increased vegetation cover and more evapotranspiration, less extreme discharge peaks and the production of more fine-grained sediment, resulted in a single-channel river. The slow accumulation is interpreted as due to limited sediment supply and limited accommodation space due to low sea level.

Around 12,000 cal BP, relative sea level reached about -40 m m.s.l. (Fig. 3.9B). The overbank environment in coring VFX (Fig. 3.7, FU-2) became wetter and more dynamic at that time, as testified by the intercalated fine sand layers, the decreased amount and size of carbonate concretions and the increase of humic levels (Fig. 3.7). The change to wetter circumstances in FU-2 is the possible effect of a rising groundwater table due to the sea-level rise. It controlled the inland migration of fluvial onlap (Cohen, 2005; Vis and Kasse, submitted). The coupled rise of channel base elevation and floodplain surface resulted in upstream migration of the long profile crossover, creating more accommodation space (Blum and Törnqvist, 2000; Cohen, 2005). The rising sea level pushed the single-channel fluvial system upstream. Based on cores for the A10 bridge construction (BRISA, 2005), the single-channel system was also present between Azambuja and Vila Franca de Xira. Therefore, the palaeogeographic map of ~12,000 cal BP (Fig. 3.11) shows a wide plain with a straight to meandering Tagus channel belt and levees and floodbasins in that area.

Shortly after ~11,500 cal BP the first tidal environments developed near Vila Franca de Xira (Fig. 3.7, coring VFX at -35 m). Therefore, they most likely were present further southward around 12,000 cal BP, as indicated on the palaeogeographic map (Fig. 3.11). In the study area, brackish water marshes and tidal flats (FU-3A) were often found directly on top of the lowstand fluvial sediments, indicating rapid drowning (Chapter 2). The tidal deposits document a change from a freshwater floodbasin to a brackish water tidal marsh as the tides started flooding the lower floodplain reaches.

12,000-7000 cal BP (Fig. 3.12)

This period is characterized by the final stage of sea-level rise from -40 m m.s.l. around 12,000 cal BP to the present level at 7000 cal BP (Fig. 3.9B). As a result, the lowstand valley was transgressed by tidal and marine environments and around 7000 cal BP the Lower Tagus Valley was completely drowned (Fig. 3.12). Due to the rising sea level, a transgressive tidal environment was formed. The oldest tidal deposits were dated near Vila Franca de Xira shortly after 11,800-11,200 cal BP (-35.13 m, UtC-14907) (Fig. 3.7, coring VFX), near Benfica do Ribatejo at 10,190-9740 cal BP (-20.50 m, UtC-14911) (Fig. 3.5, coring VAL) and north of Santarém at 9030-8750 cal BP (-10.97 m, GrA-32584) (Fig. 3.4, coring 0501.016). The transgression and associated tidal and

marsh deposition (FU-3) near Vila Franca de Xira was followed in less than ~1500 years by the onset of shallow-marine conditions (Fig. 3.7, FU-4).

In the north, the incised lowstand valley between Arrepiado and Alpiarça was situated below sea level, offering accommodation space for the development of tidal environments as far upstream as Arrepiado (Fig. 3.12). In the narrow valley, little space existed for tidal marshes and flats; instead a tidal flat to tidal channel environment dominated here until around 7270-7020 cal BP (GrA-32655) (Fig. 3.2, FU-3B & 5B). Further downstream near Almeirim (Fig. 3.4), the data suggest a narrow zone with intertidal channels and flats (FU-3B) flanked by extensive brackish water marshes and tidal flats (FU-3A).

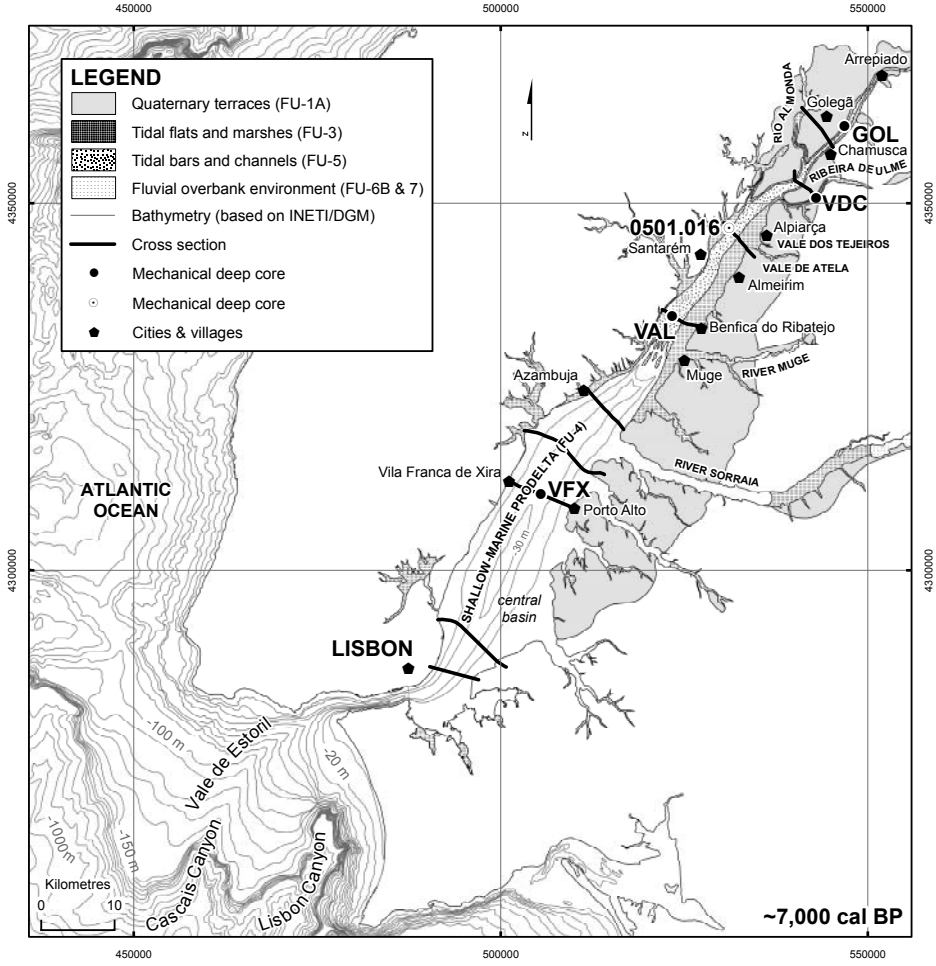

Figure 3.12 | Palaeogeography around 7000 cal BP showing the situation at the end of sea-level rise. Tidal environments reach as far upstream as Arrepiado in the north and a large basin exists between Muge and Lisbon. Bathymetry adjusted to 7000 cal BP, coastline conform the present-day. A full-colour version of this palaeogeographic map can be found in *Addendum 1*.

The transition from the narrow zone with tidal channels and flats north of Alpiarça to the distributary mouth tidal bars (FU-5A) near Benfica do Ribatejo occurred near Almeirim (Fig. 3.12). Around 7800-7590 cal BP (UtC-14910) the distributary mouth tidal bars were formed near Benfica do Ribatejo on top of brackish water marsh and tidal flat deposits (Fig. 3.5). The distributary mouth tidal bars were the transition between the tidal environments upstream and the central basin with prodelta environment (FU-4) downstream of Benfica do Ribatejo. This basin resulted from the rapid sea-level rise in combination with insufficient sediment input from upstream. The small and sheltered inland basin was up to 30 m deep (Fig. 3.12). Since 10,200-9780 cal BP (UtC-14906) the shallow-marine prodelta was established as recorded in coring VFX (Fig. 3.7).

Similar to the Tagus valley, all tributary valleys were drowned and experienced tidal conditions at least in their lower reaches. Both the Rio Almonda (Fig. 3.2, coring 0501.029) and the Ribeira de Ulme tributaries (Fig. 3.3, coring VDC)—which were incised into Pleistocene Tagus terraces (FU-1A)—contained brackish water marshes and tidal and intertidal flats (FU-3A&B). Further downstream in the deeper incised southern tributaries, tidal environments reached up to 15 kilometres upstream (e.g. Daveau and Gonçalves, 1985; Van der Schriek *et al.*, 2007b).

7000-4000 cal BP (Fig. 3.13)

A prograding tidally influenced bayhead delta existed in the Lower Tagus Valley since ~7000 cal BP, resulting from the end of sea-level rise and the continued input of sediment from the large Tagus catchment (Fig. 3.13). The Tagus channel belt (FU-8) originated in the narrow valley near Golegã (Fig. 3.2) after 7270-7020 cal BP (GrA-32655). This corroborates with deposition of organic-rich fluvial clay (FU-6A) since 6860-6630 cal BP (GrA-31004) on top of tidal marsh clay (FU-3A) in the Rio Almonda depression (Figs. 3.2 and 3.13, coring 0501.029). The channel belt south of Chamusca originated before 5300-4970 cal BP (GrA-30616), because floodbasin sedimentation (FU-6A) occurred at that time in the Ribeira de Ulme depression (Fig. 3.3, coring VDC).

North of Santarém, the first floodbasin sedimentation (FU-6B) covered a brackish water marsh (FU-3A) around 4500 cal BP (Fig. 3.4). This resulted from downstream fluvial progradation, leading to the formation of a fluvial wedge in the north. Around 4500 cal BP, fluvial aggradation could overtop the higher elevated terraces (FU-1A) along the narrow valley north of Alpiarça (Figs. 3.2, 3.3 and 3.13). This resulted in an up to one meter thick firm, organic-rich clay layer with traces of soil formation (FU-6A) (Figs. 3.2 and 3.3).

Contemporaneously with the fluvial deposition in the northern Tagus

valley, the tributary valleys were filled with organic-rich clay and peat. In the Vale dos Tejeiros and the Vale de Atela just south of Alpiarça (Fig. 3.13), peat growth and deposition of organic-rich clay started around 6000 cal BP (Van Leeuwaarden and Janssen, 1985). At the same time, fluvial overbank deposition started in the Muge valley (Van der Schriek *et al.*, 2007b). The main factor determining the formation of organic-rich clay and peat in the tributary valleys is the downstream prograding fluvial wedge of the Tagus, blocking the tributaries progressively in time. The thickening of the Tagus fluvial wedge to the north, on top of estuarine deposits at +2 m (FU-3A) is expressed by thicker

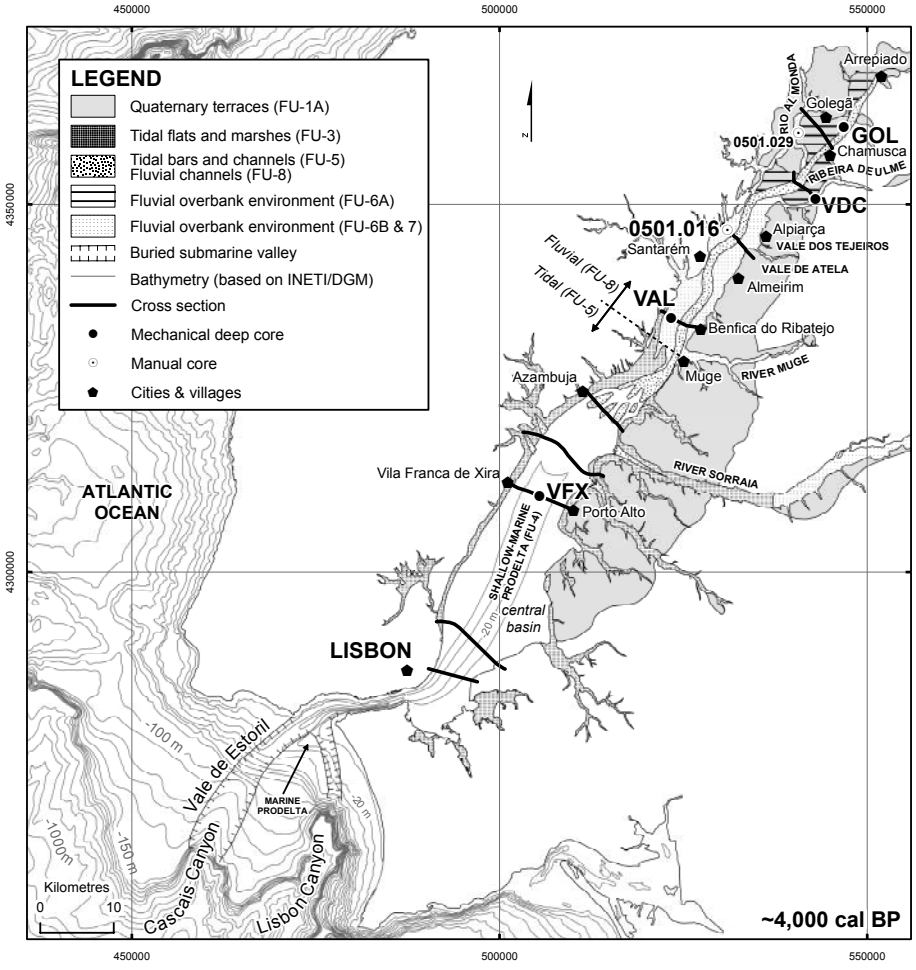

Figure 3.13 | Palaeogeography around 4000 cal BP showing the gradual infilling of the valley due to bayhead delta progradation. The central basin is shallowing and the offshore marine canyons west of Lisbon start to be filled; a marine prodelta develops across the marine canyons. Bathymetry adjusted to 4000 cal BP, coastline conform the present-day. A full-colour version of this palaeogeographic map can be found in *Addendum 1*.

deposits of organic-rich clay and freshwater peat in the tributaries.

The prograding Tagus fluvial wedge pushed the tidal environments downstream (Fig. 3.13). Near Benfica do Ribatejo (Fig. 3.5) this caused a shift from distributary mouth tidal bars (FU-5A) to fluvially influenced tidal channels (FU-5B) and intertidal and subtidal flats (FU-3B) around 4830-4530 cal BP (UtC-14909). Between 4420-4100 cal BP (UtC-14745) and 2720-2360 cal BP (GrA-32647) the tidal deposition ended here and fluvial overbank sedimentation (FU-7) started (Fig. 3.13).

From ~7000 cal BP onwards, the central basin south of Azambuja was filled with shallow-marine prodelta deposits (FU-4) as indicated by the strongly bioturbated marine deposits which formed near Vila Franca de Xira at 7270-7010 cal BP (UtC-14906) (Figs. 3.7 and 3.13). Since ~4090-3850 cal BP (UtC-14904), distributary mouth tidal bars (FU-5A) migrated over the prodelta deposits near Vila Franca de Xira (Fig. 3.7, coring VFX). Therefore, before ~4000 cal BP these bars were present further upstream (Azambuja and A10 cross sections; Figs. 3.6 and 3.8), as indicated on the palaeogeographic map (Fig. 3.13). Initial distributary mouth tidal bar deposition near Vila Franca de Xira started at a water depth of about 10 m, since sea level at that time was similar to the present day (Fig. 3.9B).

As the Tagus central basin was progressively filled, more sediment was transferred from the Tagus valley onto the shelf. The exported sediments were not transferred through the Vale de Estoril and Cascais Canyon to the Tagus abyssal plain since sea level was at its present-day level. Instead, they were deposited in a marine prodelta on the continental shelf southwest of Lisbon (Vanney and Mougenot, 1981) (Fig. 3.13).

4000-1000 cal BP (Fig. 3.14)

During this period, the environmental changes in the Lower Tagus Valley were dominated by Tagus River sediment delivery, since sea-level rise had ended (Fig. 3.9B). Consequently, further downstream progradation of the bayhead delta characterizes this period (Fig. 3.14). The vertically aggrading Tagus channel belt—previously confined to the incised lowstand valley—stepped out of the incised valley (Figs. 3.2 and 3.3) and the adjacent terraces were flooded more regularly. Near Chamusca (Fig. 3.3) the Tagus migrated laterally, as deduced from the wide channel belt (FU-8) and the levee deposits (FU-7) extending close to the valley margin. The two wedges of levee deposits also indicate lateral movement of the Tagus (Fig. 3.3, coring 0401.105). Possibly the gravely terrace deposits underneath the channel belt facilitated lateral erosion.

Since ~4000 cal BP, the Tagus channel belt prograded further downstream until the area between Muge and Azambuja was reached around 1500-1000 cal BP (Fig. 3.14). Floodbasins and levees (FU-6B and 7) were

formed over the tidal deposits (FU-3) (Fig. 3.6). From Azambuja the distributary mouth tidal bars (FU-5A) gradually prograded downstream, shallowing the central basin (Fig. 3.14). They were replaced by fluvially influenced tidal channels without shells (FU-5B). The strong daily and seasonal fluctuations in salinity may explain the scarcity of brackish fauna in these deposits.

Besides southward progradation, the Tagus floodplain also extended upstream up to Abrantes (20 km east of Arrepiado) (Fig. 3.14). The present gradient of the Tagus floodplain shows a knickpoint with a gradient change from ~85 cm/km upstream to ~30 cm/km downstream of Abrantes. This knickpoint illustrates the landward position of the Holocene fluvial onlap related to Holocene sea-level rise and floodplain aggradation.

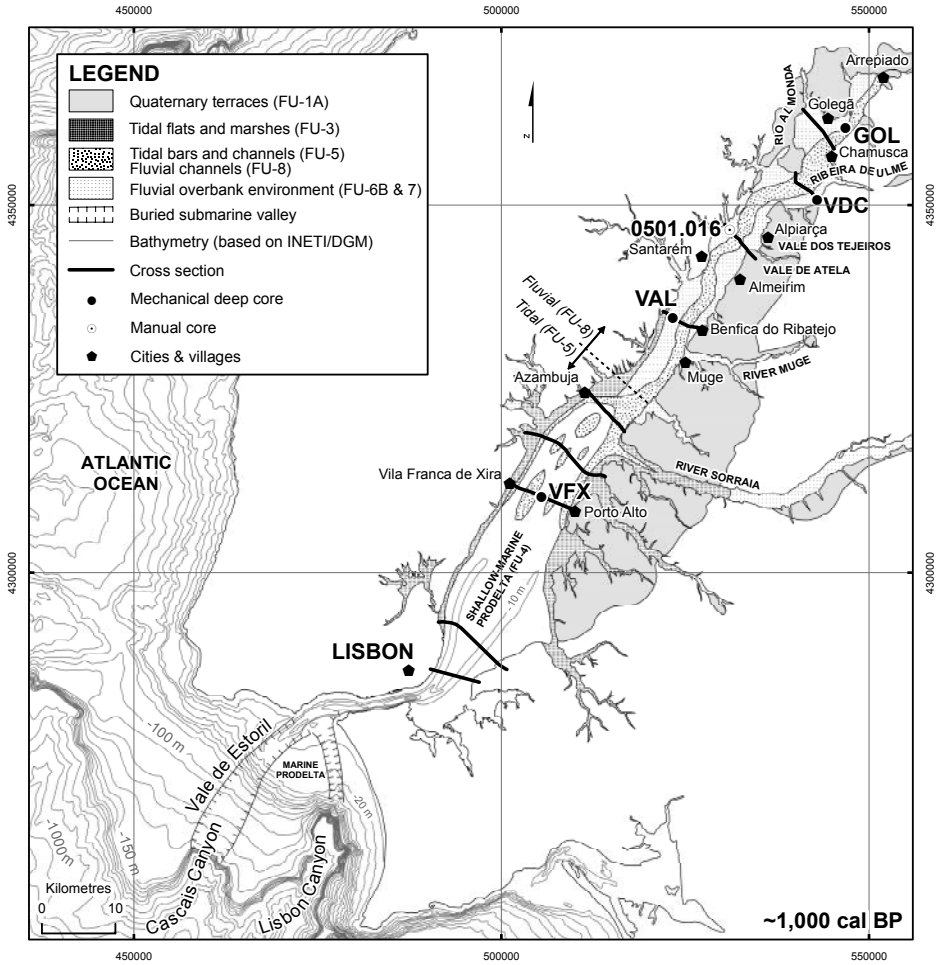

Figure 3.14 | Palaeogeography around 1000 cal BP showing a nearly filled Lower Tagus Valley and shallow central basin due to delta progradation. The offshore marine prodelta is near to its present size. Bathymetry and coastline conform the present-day. A full-colour version of this palaeogeographic map can be found in *Addendum 1.*

1000 cal BP-present (Figs. 3.1 and 3.14)

This period is dominated by increased fluvial activity, which is expressed in the rapid lateral reworking of the Tagus channel belt (FU-8) as indicated by many young (< ~1000 years) radiocarbon dates (Figs. 3.2-3.4) and the presence of charcoal, brick and pottery in channel lag deposits (Table 3.3). Increased floodbasin and levee sedimentation (FU-6B and 7) started at circa 1000 cal BP, covering a black floodplain soil in the area between Golegã and Benfica do Ribatejo (Figs. 3.2-3.5). Similarly, deposition of organic clay and peat formation in tributary valleys abruptly ended around 1000 cal BP (coring 0501.029, Golegã cross section) (Van Leeuwaarden and Janssen, 1985; Van der Schriek *et al.*, 2007b). In less than 1000 years the area south of Azambuja accumulated up to ~2 m above m.s.l. (compare Figs. 3.14 and 3.1). Most of the central basin silted up and is presently less than 5 m deep, with the exception of some deeper tidal channels which reach 10 m depth. Consequently, the sediment transfer through the central basin has increased and the offshore prodelta southwest of the narrow tidal inlet near Lisbon is receiving more sediment (Fig. 3.1).

3.5 DISCUSSION

The palaeogeography of the Lower Tagus Valley reflects the interplay of various forcing factors. Their relative contribution to the valley development changed since ~20,000 cal BP.

Climate & vegetation change

Climate and vegetation changes determine river discharge and sediment supply and hence changes in river style and aggradation versus incision (Blum and Törnqvist, 2000). Over the past 20,000 years climate has been extremely variable over the Iberian Peninsula. The gradually moister and warmer climate since ~20,000 cal BP caused the rapid expansion of *Pinus*, deciduous and evergreen *Quercus* and other Mediterranean vegetation over Portugal (Roucoux *et al.*, 2005; Naughton *et al.*, 2007b). This led to more evapotranspiration, less extreme discharge peaks and the production of more fine-grained sediment, resulting in the Late Pleistocene change from a braiding to a single-channel Tagus river at 14,000 cal BP (Figs. 3.10 and 3.11). Simultaneously, other European river systems changed from braiding to meandering: for instance the Maas and Rhine in The Netherlands and Germany (Pons and Schelling, 1951; Kasse *et al.*, 1995; Makaske and Nap, 1995; Van Huissteden and Kasse, 2001; Kasse *et al.*, 2005), rivers in southern and central Poland (Van Huissteden and Kasse, 2001; Starkel *et al.*, 2007) and rivers in northern France (Antoine, 1997; Antoine *et al.*, 2003). The Tagus slowly aggraded ~6 m of fine-grained

fluvial overbank deposits between ~14,000 cal BP and ~12,000 cal BP, possibly due to its downstream position close to the long profile crossover point and the coast, while more upstream the river was still incising (Fig. 3.11).

The Late Pleistocene Younger Dryas dry and cold event (~13,000-11,700 cal BP), was marked by a temporal small decrease of deciduous *Quercus* along with the increase of pioneer species (*Betula*) and the expansion of semi-desert and herbaceous plants (Roucoux *et al.*, 2005; Fletcher *et al.*, 2007; Naughton *et al.*, 2007b). It did not lead to detectable changes in the Tagus fluvial system and fine-grained overbank deposition steadily continued during the Younger Dryas period (Fig. 3.7, FU-2). This is comparable to some rivers in northwest Europe (e.g. Vandenberghe *et al.*, 1994; Mol *et al.*, 2000; Antoine *et al.*, 2003; Kasse *et al.*, 2005), although other rivers did temporarily change to braiding (Pons and Schelling, 1951; Berendsen *et al.*, 1995; Kasse *et al.*, 1995; Starkel *et al.*, 2007). The Tagus River probably did not respond by a channel-pattern change because the effect of the Younger Dryas climate was too small to cause important changes in vegetation cover, discharge and sediment supply (Vandenberghe and Woo, 2002).

According to Dias *et al.* (2000) the extensive coarse-grained sediment bodies on the north Portuguese continental shelf can be attributed to fluvial erosion of estuarine valley fills in response to a Younger Dryas sea-level lowering. However, our study does not support an erosional phase during the Younger Dryas. Furthermore, valley fills of estuaries due to sea-level rise are generally fine-grained, so renewed erosion would not lead to coarse-grained deposition on the shelf. Moreover, recent sea-level studies do not show a drop in sea level during the Younger Dryas (Hanebuth *et al.*, 2000; Waelbroeck *et al.*, 2002; Peltier and Fairbanks, 2006).

Around 5000 cal BP a major climate change occurred from a humid to a drier climate (e.g. Fletcher *et al.*, 2007; Naughton *et al.*, 2007b). This major change, recorded widely in the Mediterranean and Northern Africa (e.g. DeMenocal *et al.*, 2000; Renssen *et al.*, 2006), is not registered clearly in the Lower Tagus Valley sedimentary basin. Although the increased aridity and vegetation change may have led to increased sediment supply to the Lower Tagus Valley, this effect cannot be separated from the impact of sea-level rise decline that also occurred around that same period (Fig. 3.9B).

Sea-level change

Sea-level change is the most important forcing factor for the palaeogeography of the Lower Tagus Valley. The Late Pleistocene sea-level lowstand forced a very strong incision of the valley as far upstream as Abrantes, 20 km east of Arrepiado (Martins, 1999; INETI, 2007) (Fig. 3.1). South of Lisbon the valley was incised to at least -70 m m.s.l. (Fig. 3.10) and was directly con-

nected to the ocean via the Vale de Estoril and Cascais Canyon, bypassing the exposed continental shelf (≤ -100 m m.s.l.). The rising sea level since ~20,000 cal BP rapidly drowned the lowstand valley, creating a transgressive system until ~7000 cal BP (Fig. 3.12). The complete drowning of the valley created an inland sheltered sea in the downstream part and tidal environments as far upstream as Arrepiado. Since ~7000 cal BP sea-level rise ended (Fig. 3.9B) and the palaeogeography of the valley was dominated by fluvial sediment input from the hinterland (Fig. 3.13). High sea level and sediment supply caused inland migration of the point of fluvial onlap, resulting in upstream migration of the long profile crossover east of Arrepiado and vertical aggradation of the highstand floodplain (Blum and Törnqvist, 2000; Cohen, 2005).

Van der Schriek *et al.* (2007a) suggested that sea-level change was only of importance to the river system during interglacials and by erosion of coastal highstand prisms at the beginning of interglacial periods. Fluvial incision only occurred during warming phases of climate transitions. However, our study clearly shows that strong fluvial incision occurred during the glacial sea-level lowstand. The drowning of the valley during sea-level rise resulted in the formation of a highstand prism in the valley. The downstream Lower Tagus Valley has had a different evolution than more upstream reaches, since they are affected by distinctly different forcing factors.

Pleistocene topography

Inherited morphology of the Pleistocene surface partly determines the palaeogeographic development during the Holocene. The morphology of the Lower Tagus Valley with its narrow exit near Lisbon created a sheltered inland basin upstream of Lisbon as soon as the sea flooded the valley. The narrow exit strongly reduced the effect of storms and storm surges in the drowned valley, creating a relatively quiet environment on a wave-dominated Atlantic Coast. This quiet environment together with the depth of the incision facilitated deposition of fine-grained prodelta deposits and prohibited the import of coastal sand.

The width and depth of the Late Pleistocene incised Lower Tagus Valley (Fig. 3.10) are governed by a combination of a large catchment (upstream control), a low sea level and narrow (~30 km) continental shelf (downstream controls). According to Mattheus *et al.* (2007) incised-valley dimensions equilibrate with catchment size; the larger the catchment, the larger the width and cross-sectional area of the incised valley. In their study the shelf is at least 100 km wide, resulting in relatively shallow incised valleys. Our study shows that besides catchment size as upstream control and sea level as downstream control, the width of the shelf is another downstream control, determining the incision depth through the fluvial gradient and the landward extent of regres-

sive erosion of the lowstand valley. A narrow shelf combined with a lowstand shoreline seawards of the shelf break promotes cross-shelf valley formation (Törnqvist *et al.*, 2006). The Lower Tagus Valley was directly linked with the submarine canyons southwest of Lisbon (Vale de Estoril and Cascais Canyon), which resulted in deep Late Pleistocene incision due to glacial sea-level lowering and a steep valley gradient of 60 cm/km (Fig. 3.10). The Pleistocene sea-level fluctuations combined with tectonic uplift, resulted in partial removal of older Pleistocene deposits in the lowstand valley and therefore the lowstand fluvial deposits in the Lower Tagus Valley are relatively thin (Fig. 3.8). A similar situation was found at the base of the Odiel-Tinto and Guadalete valley fills in south Portugal (Dabrio *et al.*, 2000). Because of the deep erosion and high-gradient of the lowstand valley, the succeeding up to 50 m thick sedimentary sequence contains a unique record of Late Glacial and Holocene fluvial and marine environmental change (Figs. 3.7 and 3.8).

The transgression over a high-gradient Pleistocene surface (like the Lower Tagus Valley) in comparison to a broad and gently sloping surface will result in different facies distributions and coastal plain architecture. In contrast to the Rhine-Meuse delta and other European coastal plains (Jelgersma, 1961; Van de Plassche, 1981; Van der Woude, 1981; Denys and Baeteman, 1995; Weerts and Berendsen, 1995; Törnqvist *et al.*, 1998; Behre, 2004; Cohen, 2005), basal peat was not found at the base of the Late Glacial and Holocene sedimentary sequence. The steep gradient of the sandy and gravely fluvial lowstand surface and the rapid sea-level rise since ~20 000 cal BP, excluded groundwater-rise driven basal peat formation. Moreover, the combination of dry Mediterranean summers and a dense vegetation cover during the early Holocene period (Roucoux *et al.*, 2005; Naughton *et al.*, 2007b) prevented permanent high groundwater tables in the lowstand surface.

In the Holocene valley-fill only one channel belt was found and, except for some lateral migration (Fig. 3.3), no avulsions occurred during the Holocene period, in contrast to previous suggestions by Azevêdo *et al.* (2006b). The absence of avulsions is partly explained by the fact that the first stages of Holocene fluvial aggradation occurred within a narrow incised lowstand valley (Fig. 3.2). Despite the fact that the present-day Tagus levees reach up to 5 m above the floodbasins (superelevation), the normalized superelevation (ratio between superelevation and bankfull channel depth) ranges between 0.3-0.6, whereas normalized superelevation values of 0.6-1.1 are required for channels to avulse (Bryant *et al.*, 1995; Heller and Paola, 1996; Mohrig *et al.*, 2000). This implies that at least in the present situation, the large bankfull channel depth reduces the chances for avulsion, despite the high levees (Mohrig *et al.*, 2000). Another approach to estimate the possibilities for avulsion is the "gradient-advantage concept", which is based on the

ratio between cross-valley slope and down-valley slope (slope ratio) (Mackey and Bridge, 1995; Slingerland and Smith, 1998; Törnqvist and Bridge, 2002; Slingerland and Smith, 2004). This value is ~7 for the present day Tagus River, which is smaller than the slope ratio of more than 8 suggested by Slingerland and Smith (1998) but larger than the slope ratio of 3-5 as proposed by Törnqvist and Bridge (2002) as threshold values for the initiation of avulsion. Avulsion chances in the Lower Tagus Valley were probably even smaller in the past, when the levees were not as high as in the present situation. Finally, the narrow confined nature of the valley bordered by Tertiary deposits in the west and Quaternary terraces in the east was a limiting factor for full avulsions, since the Tagus River was forced to leave the valley through the narrow exit south of Lisbon (Fig. 3.1).

Neotectonic and isostatic movement

The end of sea-level rise at 7000 cal BP (Fig. 3.9B) occurred earlier in the study area than in most sea-level studies (e.g. Toscano and Macintyre, 2003; Camoin *et al.*, 2004; Peltier and Fairbanks, 2006). However, other studies—some from southern Spain—found a similar timing for the end of sea-level rise (Zazo *et al.*, 1994; Goy *et al.*, 1996; Rodríguez-Ramírez *et al.*, 1996; Dabrio *et al.*, 1999; Fernández-Salas *et al.*, 2003). The main factors influencing relative sea level are glacio- and hydro-isostacy and neotectonics. Since Portugal is located more than 2000 km south of the Fennoscandian ice sheet, glacio-isostatic effects are assumed to be negligible (Peltier and Fairbanks, 2006). The hydro-isostatic effect due to unloading and loading of the continental shelf is unknown but taken into account that the shelf along the Portuguese coast is narrow, hydro-isostatic movements must have been gentle. Despite the historic strong tectonic activity in the area, long-term tectonic uplift is estimated to be less than 0.1 mm/y, based on uplift of Early Pleistocene deposits to about 200 m in 2.5 Ma (Cabral, 1995). Along the northern Portuguese coast, coastal deposits were uplifted up to 16 m during the last 6000 years (~2.7 mm/y) (Granja and De Groot, 1996; Granja, 1998). However, the horizontal sea-level curve since 7000 cal BP (Fig. 3.9B) suggests that no detectable uplift or subsidence occurred, since otherwise the tidal marsh data points younger than ~7000 years would be located either above (in case of uplift since deposition) or below the + 2 m m.s.l. line (in case of subsidence since deposition).

Human influence

Between 6000 and 5000 cal BP (the Neolithic) the first agricultural activities started in the Iberian landscape (Savory, 1968; Múgica *et al.*, 1998; Jorge, 1999). From about 2000 cal BP onwards, the extent of montane forest in the central Spanish Tagus catchment decreased gradually and in central Spain,

signs of landscape degradation were detected from ~2000 cal BP onwards (Andrade *et al.*, 1990; Andrade *et al.*, 1996; Franco *et al.*, 1997; Múgica *et al.*, 1998). From the Middle Ages and mainly from ~1000 cal BP onwards, natural vegetation virtually disappeared and grazing, burning, agriculture and deforestation increased dramatically, leading to the disappearance of forests and strong erosion of soils (Klein, 1920; Slicher van Bath, 1960; Van den Brink and Janssen, 1985; Janssen, 1994; Van der Knaap and Van Leeuwen, 1995; Allen *et al.*, 1996; Carrión, 2002).

The loss of vegetation cover and the resulting erosion of catchment slopes have had a pronounced effect on the Tagus floodplain. This is testified by up to three times faster vertical aggradation of natural levees and floodbasins and the increased lateral extent of levees over the floodbasin (Figs. 3.2-3.5). Increased overbank sedimentation rates since ~1000 cal BP, and rapid lateral migration and aggradation of the fluvial channel belt are attributed to the increased human impact. Simultaneously, organic clay deposition and peat formation in tributary valleys abruptly ended by increased clastic deposition. The tidal flat area south of Azambuja extended rapidly to the south and silted up to ~2 m above m.s.l. (Freire, 1985) (Fig. 3.14).

3.6 CONCLUSIONS

The infilling of the Lower Tagus Valley was dominated by relative sea-level rise and fluvial sediment supply. Relative sea level rose rapidly since the Last Glacial Maximum and reached the present-day level around 7000 cal BP, thereby drowning the Lower Tagus Valley. Relative sea-level stability since 7000 cal BP resulted in the increased relative importance of fluvial sediment supply. The palaeogeographic evolution of the Lower Tagus incised valley-fill reveals five major phases:

1. Around 20,000 cal BP (Last Glacial Maximum): the Late Pleistocene sea-level lowstand and narrow continental shelf forced a strong incision of the valley up to ~100 km upstream from the present coastline. Around ~20,000 cal BP a direct connection existed between the Lower Tagus Valley and the ocean, causing efficient sediment bypassing across the shelf. A braided high-gradient river was present in the incised valley;
2. 20,000-12,000 cal BP: the gradually moister and warmer climate since ~20,000 cal BP led to the change from a braiding to a single-channel Tagus river at 14,000 cal BP. The Younger Dryas event did not lead to detectable changes in the Tagus palaeogeography and deposition steadily continued;

3. 12,000-7000 cal BP: rapid sea-level rise caused transgression and drowning of the incised Lower Tagus Valley. Shallow-marine and tidal environments established up to ~80 km upstream of the present coastline around ~7000 cal BP. The deeply incised, lowstand-valley facilitated accommodation for an up to 50 m thick Late Glacial and Holocene sedimentary record;
4. 7000-1000 cal BP: since ~7000 cal BP relative sea-level rise ended and the valley-fill evolution was dominated by fluvial sediment input from the Tagus catchment. The bayhead delta prograded southward and the fluvial wedge covered tidal and shallow-marine deposits. Channel belt avulsions did not occur. The Tagus valley was progressively filled and an offshore marine prodelta was formed. The horizontal relative sea-level curve since ~7000 cal BP proves that neotectonic uplift or subsidence were limited;
5. 1000 cal BP-present: floodbasin sedimentation increased up to three-fold from the Middle Ages onwards, levees silted up ~5 m above the floodbasins and extended far into the floodplain and the channel belt was completely reworked. Peat formation in tributary valleys stopped due to large clastic input. Widespread silting up of tidal flats occurred. The increased sediment supply is attributed to deforestation, agriculture and soil erosion.